

Quantitative MRI as a biomarker in Spinal Muscular Atrophy

MAPPING OF MUSCLE AND NERVE PROPERTIES
WITH MRI FOR DISEASE PROGRESSION AND
TREATMENT EFFECTS IN SMA

UMC Utrecht Brain Center

LOUISE OTTO



Quantitative MRI as a biomarker in Spinal Muscular Atrophy

Mapping of muscle and nerve properties with MRI for
disease progression and treatment effects in SMA

Louise A.M. Otto

© Louise A.M. Otto, 2022

All rights reserved. No parts of thesis may be reproduced, stored or transmitted in any way or form or by any means, without the prior written permission of the author or, when applicable, of the publishers of the scientific journals in which the papers have been published.

ISBN 978-94-6458-075-4

Cover Peter Otto, *Zonder titel* 2012, *Zonder titel*, 2011, aquarel

Lay-out Publiss | www.publiss.nl

Print Ridderprint | www.ridderprint.nl

The Prinses Beatrix Spierfonds and Spierziekten Nederland provided financial support for the studies in this thesis. The financial support of the Prinses Beatrix Spierfonds and UMC Utrecht Brain Center for the publication of this thesis is gratefully acknowledged.

Quantitative MRI as a biomarker in Spinal Muscular Atrophy

Mapping of muscle and nerve properties with MRI for disease progression and treatment effects in SMA

**De toepassing van kwantitatieve MRI
als biomarker bij spinale spieratrofie**

In kaart brengen van spier- en zenuweigenschappen met behulp van MRI voor ziekteprogressie en effect van behandeling bij spinale musculaire atrofie (met een samenvatting in het Nederlands)

PROEFSCHRIFT

ter verkrijging van de graad van doctor aan de
Universiteit Utrecht
op gezag van de
rector magnificus, prof.dr. H.R.B.M. Kummeling,
ingevolge het besluit van het college voor promoties
in het openbaar te verdedigen op

dinsdag 22 maart 2022 des middags te 4.15 uur

door

Louise Adrienne Maria Otto

geboren op 31 juli 1992
te Arnhem

PROMOTOREN:

Prof. dr. W.L. van der Pol

Prof. dr. J. Hendrikse

COPROMOTOR:

Dr. M. Froeling

Dit proefschrift werd (mede) mogelijk gemaakt met financiële steun van het Prinses Beatrix Spierfonds.

Voor pappa & mamma

CONTENT

Chapter I	General introduction	9
Chapter II	Quantitative MRI of skeletal muscle in a cross-sectional cohort of patients with spinal muscular atrophy types 2 and 3	27
Chapter III	Quantification of disease progression in spinal muscular atrophy with muscle MRI—a pilot study	57
Chapter IV	Monitoring nusinersen treatment effects in children with spinal muscular atrophy with quantitative muscle MRI	79
Chapter V	Quantitative MR neurography of the sciatic nerve in patients with spinal muscular atrophy: a longitudinal study during nusinersen treatment	99
Chapter VI	Can quantitative MRI detect pre-symptomatic abnormalities in SMA? A case-report	117
Chapter VII	General discussion	127
Appendices	Thesis assessment committee	152
	Nederlandse samenvatting	154
	Dankwoord	160
	Curriculum vitae	164
	List of publications	166



CHAPTER I

General introduction

SPINAL MUSCULAR ATROPHY – CLINICAL CHARACTERISTICS AND GENETIC BACKGROUND

Hereditary spinal muscular atrophy (SMA) is a monogenetic neuromuscular disease characterized by progressive muscle weakness and is the leading genetic cause of infant death and disability in childhood. The incidence of SMA is 1:6.000 to 13.000.(1) This implies that in the Netherlands every year approximately 15-25 children are born who will develop SMA later in life. Prevalence was until recently unknown, due to limited information on life expectancy of the more chronic forms of the disease, which may be better than previously thought.(2) Estimates in the Netherlands now range between 400-500 patients.

The clinical diagnosis of spinal muscular atrophy is based on a combination of symptoms, i.e. hypotonia or other signs of muscle weakness such as stalled gross motor development, areflexia, tongue fasciculations and tremor. Before genetic testing became available, diagnostic strategies depended on techniques that could confirm a neurogenic cause of weakness, i.e. EMG and muscle biopsies. Genetic testing for a homozygous deletion of the *SMN1* gene has been the gold standard to confirm the diagnosis after 1995. Genetic techniques have high sensitivity and specificity. Heterozygous deletion in combination with another loss of function mutation occurs in less than 5% of patients.(3) Parents are carriers and have no symptoms of muscle weakness. Carriership frequencies vary somewhat between ethnicities. In the Netherlands, the most accurate estimate is 1 in 42.(1)

As of 2017, SMA is one of the first hereditary disorders for which genetic therapies are available. This has dramatically altered treatment approaches that were previously mainly supportive.(4,5) Although there are reasons for optimism, SMA remains a severe disorder that cannot be cured. The fact that SMA has been added to the national newborn screening program in 2019 is probably the biggest step forward, although this still awaits implementation. An important challenge is to design treatment strategies that balance effectiveness, treatment burden and societal costs.

Historical context

The first description of a SMA phenotype dates back to the end of the 19th century by dr. Werdnig and consecutively by dr. Hoffman.(6,7) They reported case histories of several children with early onset muscle weakness combined with autopsy reports of the spinal cord and muscle. Autopsy showed degeneration of the anterior horn cells of the spinal cord in combination with muscle atrophy. This combination of findings is reflected in the name of the disease (spinal refers to the spinal cord) that is still used today. The use of the eponym Werdnig-Hoffman disease to describe the most severe presentation of SMA (i.e. type 1 SMA) is rightly in decline. As discussed in detail by Dubowitz,(8) the patients described by Werdnig and Hoffmann would nowadays be classified as a variant of early childhood (intermediate) SMA, i.e. SMA type 2, rather than infantile onset or SMA type 1. A second eponym, Kugelberg-Welander disease, was previously used for ambulant patients with SMA, following the report on juvenile muscular atrophy by these authors in 1956.(9) We now refer to this group of patients as SMA type 3.

The short historic outline in the previous paragraph already points out the strikingly wide range of SMA severity. The genetic background of SMA was elucidated in 1995. Since then, we know that all patients with SMA carry the same genetic defect despite the variation in severity. Several years after 1995, we learnt about the reason for the existence of a spectrum of SMA severity, ranging from prenatal cases of weakness, through the hypotonic, or 'floppy' infant and various degrees of stalled gross motor development to patients who remain ambulant throughout life. Humans are unique among animals as carriers of a highly homologous *SMN2* gene, of which the copy number is inversely correlated with disease severity.(10,11)

Spinal muscular atrophy causes weakness that is most apparent in proximal and axial muscles.(12,13) This pattern is remarkably similar in all SMA types. Strength of flexors, such as neck flexors, biceps, finger flexors and hamstrings, is relatively preserved compared to their extensors (neck extensors, triceps, quadriceps and finger extensors).(12,14) Intercostal respiratory muscles are weak, while the diaphragm is spared.(15) Bulbar involvement is pronounced with impairment in swallowing, biting, speech and mouth opening.(16–18) Complications of progressive muscle weakness include scoliosis, sputum clearance and respiratory problems and severe contractures.(19–21)

The variation in severity was already acknowledged in the 60's of the previous century, as the severe infantile, intermediate and mild forms of SMA. In the 1990's this distinction was formalized into a classification system based on acquired motor milestones

and age of symptom onset (Table 1). This system was subsequently extended to cover the range from pre-natal onset (type 0), to onset at adult age (type 4).(22) This classification system has been further amended to specify variation within types, e.g. type 1.1-1.9(23) or type 1a, 1b, 1c; 2a and 2b; 3a and 3b(24) , but is still used today.

Table 1 Classification of SMA types(24,25)

	Type 0	Type 1	Type 2	Type 3	Type 4
% of patient population	1-5%	50%	25-30%	15%	5%
Age of onset	Pre- and neonatal	0-6 months; 0-2 weeks (1a); <3 months (1b) or >3 months (1c)	6-18 months	1.5-3 years; (type 3a) or >3 years (3b)	>18 years*
Highest acquired motor milestone	None	Never learn to sit. Head control in prone position sometimes acquired (type 1c)	Sitting without support; additional standing/walking with support (2b), if not (2a)	Walking independently	Walking independently
Survival (without treatment)(2)	Extremely short; intra-uterine death or within first days	Severely shortened; depending on mechanical ventilation	2a: shortened, depending on mechanical ventilation 2b: probably close to normal life expectancy	Normal life expectancy	Normal life expectancy
SMN copy number(3)	1	(1)-2-3	(2)-3-(4)	3-4	4-5

* some favor an onset after 21 years or 30 years.(26,27)

Sometimes the classification is simplified by referring to acquired motor milestones only; i.e. type 1 patients as 'non-sitters', type 2 patients as 'sitters' and type 3 as 'walkers'. An advantage is that this simplification can also be used for older patients and considers the progressive nature of SMA that causes loss of previously acquired motor skills. For example, 'sitters' can be used to refer to both patients with type 2 who still have the ability to sit independently and patients with type 3 who lost the ability to walk. With the introduction of genetic therapies, infants are now showing improvement in motor function unprecedented in the history of SMA. These new phenotypes will require us to reevaluate the SMA classification system. Children with severe SMA treated with genetic therapies

may obtain hybrid characteristics, for example facial weakness and tongue fasciculations of type 1, axial weakness previously seen in type 2, while still achieving the ability to walk (type 3).

Genetics

As shortly mentioned above, in 1995 the group of professor Judith Melki published that SMA is caused by the homozygous deletion of the '*survival motor neuron 1*' (*SMN1*) gene.(28) Only a minority of patients carried a heterozygous deletion combined with a missense/nonsense point mutation of the *SMN1* gene (1-5% of the cases(3)). The locus of the *SMN1* gene had been previously mapped to the 5q13 locus.(29) This explains why SMA is sometimes still referred to as 5q-SMA, to distinguish it from other genetic neurogenic causes of muscle weakness for which spinal muscular atrophy is also used as a descriptive term for motor neuron loss (e.g. distal SMA, SMA-LED).

The *SMN* locus contains a second gene, which is unique to humans. This *SMN2* gene differs by five nucleotides from the *SMN1* gene, but only the critical conversion from a C to a T in exon 7 of *SMN2* explains differences in function, because it leads to the frequent skipping of exon 7 in the mRNA transcript and the production of a shortened, probably unstable protein that is rapidly degraded.(30) Full-length *SMN* protein is therefore produced only at residual levels by the remaining *SMN2* gene, which is insufficient to prevent eventual motor neuron degradation. The variation in severity is explained by interindividual differences in *SMN2* copy number and thereby the severity of *SMN* protein deficiency. SMA severity correlates inversely with *SMN2* copy number, i.e. a higher copy number is associated with a milder disease phenotype. *SMN2* copy number is the first known and remains the most important disease severity modifier, although high expression of other gene products (PLS3, NCALD) may rescue the cellular defects caused by *SMN* protein deficiency.(3,31-34) The number of *SMN2* genes varies in healthy individuals, from 0 to more than 5 copies; in patients with SMA *SMN2* copy number ranges from 1 to over 5.(35)

SMN protein

SMN protein is ubiquitously expressed and is as subunit of protein complexes involved in many cell-regulatory processes.(36) How the loss of *SMN* exactly causes disease is therefore not exactly known. *SMN* is important for mRNA splicing, axonal transport, endocytosis, ubiquitination and ribosomal function. *SMN* involvement in specific ribosomal functions may be a promising unifying mechanism to explain the underlying pathophysiology. It was shown that *SMN* protein is important for the function of a specific subset of ribosomes that

are active in motor neurons, but also a number of other tissues.(37) This could explain the particular vulnerability of motor neurons to SMN protein deficiency and should predict which other tissues and organs are vulnerable in SMA.(38) It has been shown in humans with SMA and in animal models that structural and functional defects occur in multiple organs such as heart, kidney, spleen, gastrointestinal and vascular system and skeletal muscle.(39–41)

Tissues may differ in the SMN protein concentrations they require to function properly. All constituents of the motor unit, i.e. motor neurons, nerves, the neuromuscular junction and muscle, suffer from SMN depletion and show anatomical and functional alterations.(42–45) Moreover, in addition to tissue-specific requirements, the SMN threshold hypothesis proposes different SMN concentration requirements at distinct *timepoints* during embryonal development.(46) For example, SMN expression in the central nervous system and skeletal muscle is highest prenatally, indicating its pivotal developmental role.(47,48) The exact SMN requirements of tissues in the course of the disease are not known. Restoring SMN levels to the lower limit of normal at the timepoint of highest demand in vulnerable tissues could be an important next step in 'tailoring' treatment strategies for optimal outcome.

In this context, skeletal muscle is particularly interesting as it is not only affected by denervation that ultimately causes muscles to waste but may be also primarily dependent on sufficient levels of SMN protein. From mice studies we learned that SMN protein levels in skeletal muscle are significantly lower in SMA compared to controls and that SMN expression in muscle is also lower than in other tissues, such as brain and spinal cord.(46) SMN deficiency in muscle, even though requirements are lower than in neurons, is probably linked with the structural alterations to the sarcomere and dysregulated muscle maturation and growth observed in SMA.(49–53) The SMN requirements of other tissues and in particular muscle demonstrate the high potential of systemic SMN-augmenting or additional targeted treatment. For example, muscle pathology could be reversed in mice with systemic SMN repletion. Animal data even suggest that non-motor SMN rescue could be sufficient or beneficial for motor neuron function and survival, although not all research is equivocal(54–56)

Treatment strategies

Within 20 years after the discovery of the SMA determining genes, therapies aimed at *SMN1* and *SMN2* have emerged. This development has had exceptional speed. The current treatments are primarily based on increasing cellular SMN levels, by improving

SMN2 splicing (nusinersen/Spinraza and risdiplam/Evrysdi) or introducing the missing *SMN1* gene via a viral vector (onasemnogene abeparvovec/Zolgensma). Other treatment strategies target the neuromuscular junction or muscle.

The first FDA-approved treatment for SMA was nusinersen (Spinraza) in 2016. Nusinersen is an antisense oligonucleotide that is delivered intrathecally via lumbar puncture.(57) In young patients this on average results in progress on motor function scales(58,59), although slightly less than half of patients may not respond to therapy. Data in adult patients suggest that treatment effects may still be observed after long disease duration in subgroups.(60)

Risdiplam is a second *SMN2* splicing modifier that is administered orally.(61,62) Early results indicate that risdiplam had favorable impact on motor function scores in a cohort that encompassed a broad clinical spectrum of SMA (0-25 years).(63,64) European market authorization has been granted at the beginning of 2021.

Zolgensma is an adeno-associated virus (AAV-9)-based form of gene therapy. It is administered via venous injection and has specific (although not exclusive) tissue tropism for motor neurons.(65,66) In one phase I trial, infants with SMA type 1 demonstrated progress on motor scales with the acquisition of new milestones (i.e. 11 out of 12 learned to sit independently).(67) Its use in clinical trials has been limited to type 1 and pre-symptomatically diagnosed children, although EMA has granted a broader label.

Gene therapy and splicing modifiers are extremely costly, varying from 80.000€ per injection of nusinersen to €1.9 million for gene therapy, whilst the costs for risdiplam are estimated at 250.000€ per year.(68) This has led to ethical and policy discussions on cost-effectiveness and large variation in reimbursement within the European Union. In the Netherlands, reimbursement of nusinersen went stepwise. Treatment of children <5 years was possible from January 2018. Treatment when the first dose is administered before the age of 9.5 years in children with 3 *SMN2* copies or less is reimbursed from August 2018. In January 2020, a nationwide open-label study started to assess efficacy of nusinersen in patients with SMA who start treatment at an older age or when they have higher *SMN2* copy numbers.

In the meantime, a second line of therapies is under development. Novel treatment strategies target the motor unit at other sites than the motor neuron, i.e. muscle or the neuromuscular junction. Pyridostigmine inhibits the breakdown of acetylcholine in the synapse and enhances neuromuscular transmission. Although it does not improve

motor function, we found that it has a positive impact on endurance and patient-reported stamina. It is a low-cost treatment option that could be useful as add-on to SMN augmenting therapies.(69) Several pharmaceutical companies are interested in targeting muscle tissue directly. The muscle-specific myostatin-inhibitor SRK-015 is currently under investigation in phase 2 studies in patients. Myostatin plays a key role in the negative regulation of muscle mass via various signaling pathways. Myostatin upregulation is found in conditions characterized by muscle-wasting such as cachexia, cancer and heart failure. (70) Inhibition of myostatin could increase muscle mass in SMA even it does not target the primary cause of SMA.(54,71) Interim analysis demonstrated improvement on motor scale scores after 6 months as monotherapy in a phase 2 study. Treatment results were more pronounced in combination with SMA augmenting therapies.(72)

The future for patients with SMA is, due to the emergence of multiple treatment options, more hopeful than it has ever been. However, SMA is a problem far from being solved. For policy makers and physicians, market authorization of new drugs for rare diseases poses an enormous challenge to balance patient interests, burden of treatment and cost-effectiveness. None of these novel treatments will resolve irreversible damage to motor units. It is unclear whether new treatments will fulfill hopes for stabilization after a lifetime of disease progression. We will probably only learn about long-term effects after a decade of use. This indicates that we are still far away from tailored use of SMA drugs. Moreover, it is highly unlikely that we will see new trials to assess outcomes of combined therapies. The question therefore is how we proceed to define the best (combination of) treatment for individual patients. Biomarkers may represent an alternative approach to assess treatment effects

Biomarkers in SMA

Clinical markers such as motor function and muscle strength assessment are and have been widely used as (primary) endpoints in clinical trials. Although these tools have served their purpose, they have clear limitations. First, clinical scales can't be used for the whole spectrum of SMA. Second, most scales have limited sensitivity and changes in strength and motor scores due to disease progression beyond day-to-day variation can only be observed after several years of follow-up.(14,73,74) Therefore, we need additional outcome measures that detect early changes in anatomy or function that predict clinical improvement. In other words, there is a need for novel biomarkers in SMA.

SMN mRNA and protein levels have been the first biomarkers that were explored. (75-77) SMN expression levels vary between cell types, between tissue and with age, and

do not consistently show correlations with disease severity.(31,46,78,79) Studies on other biomarkers in blood or plasma include neurofilaments as a measure for axonal damage/ degeneration, or other plasma proteins.(80–84) Importantly, SMN or plasma protein levels do not reflect restoration of tissue functions. Electrophysiological assessment has been explored as a biomarker for motor neuron/unit function. Motor unit status can be monitored by a range of techniques, such as the compound action muscle potential (CMAP) and motor unit number estimation (MUNE). Although the CMAP amplitude and MUNE are lowered in SMA and correlate with *SMN2* copy number, doubts remain regarding usefulness in trials and clinical practice.(43) The CMAP-scan is an example of a next-generation technique that may be better to detect changes in the motor unit make-up.(85) Monitoring nerve function nevertheless remains technically challenging.

In other neuromuscular disorders such as Duchenne Muscular Dystrophy, Charcot-Marie Tooth, inclusion body myositis and limb-girdle muscular dystrophy, magnetic resonance imaging (MRI) of muscle has emerged as biomarker.(86–89) MR imaging is a non-invasive and versatile method to study anatomy of tissue *in vivo*. In contrast to CT imaging, MR imaging does not expose patients to radiation and is superior in depicting early fat infiltration and anatomical rendering.(90,91) MRI allows to examine muscles individually, whereas clinical evaluation and testing objectifies involvement per functional muscle group.(92–94) Muscle pathology in SMA is characterized by atrophy, sometimes in combination with occasional muscle fiber hypertrophy in muscle biopsies. At the macroscopic level, there is also clear fatty replacement of muscle tissue. Quantifying the degree of muscle abnormalities could potentially serve as a marker for disease progression and possibly for treatment effects. Mercuri et al. proposed a grading system(95) for qualitative and semi-quantitative evaluation of muscle. However, quantitative imaging can assess the degree of muscle degeneration more precisely compared to visual rating scales. Quantitative imaging is therefore considered a candidate biomarker in neuromuscular disease for disease progression and for therapeutic effects. (96)

MRI as biomarker in SMA: aims of this thesis

There are few studies available that explored muscle imaging in SMA. Most of the earlier work concerns case-reports or small studies.(97–102) At the start of the work described in this thesis, there were few cross-sectional studies that provided insight in muscle specific changes in different SMA types. Importantly, the available reports at the time lacked quantitative analysis of fat infiltration or diffusion tensor imaging (DTI) that would allow

assessments of the ratio of muscle and fat and the microstructural (ab)normality of the remaining muscle tissue.

Previous studies had shown that some muscles are particularly vulnerable to changes, while others seem to be left relatively spared throughout the disease course, i.e. the adductor longus, muscles from the posterior compartment and the gracilis and sartorius muscles.(98,99,102–104) Some studies addressed correlations with specific disease characteristics. For example, Sproule et al. reported a strong correlation between muscle volume measured with MRI and clinical function and strength measures.(105) while Durmus et al. showed a significant correlation between disease duration and severity of MRI involvement in the gluteus maximus and triceps brachii muscles.(106) Bonati et al. revealed negative correlations between some quantitative MRI measures and motor scales.(107) These studies suggested a relation of (semi-)quantitative MR measures of remaining muscle with strength and function and that muscle imaging could be a surrogate marker for disease activity. Quantitative MRI in larger patient groups would allow to study features of muscle pathology; i.e. fat infiltration, muscle atrophy and inflammation, in more detail. These quantitative markers are the core of the data presented in this thesis. Since there were no follow-up studies that would allow assessments of quantitative changes in muscle composition or its quality over time, we also focused on the natural disease course to provide a reference if MRI were to be employed to monitor effects of novel treatments. After all, as more patients are starting therapies, there are fewer opportunities to obtain such natural history data. Because follow-up imaging studies are notoriously complicated by the challenge of a correct alignment of datasets to ensure measuring at the exact same location between time-points, this was a methodological issue needed fixing at the start of this project. We also wanted to establish feasibility and value of qMRI in tissue other than muscle in SMA. There are qMRI reports of the cervical spinal cord, one of which was performed by our team.(108,109) We wanted to establish whether qMRI of peripheral nerve would have added value.

The aims of this thesis were therefore the following:

1. To map properties of muscle and peripheral nerve in SMA with quantitative MRI.
2. To explore quantitative MRI of muscle and peripheral nerve as a biomarker for disease progression and treatment effects.

In **Chapter 2** we summarize qMRI changes in thigh muscle in 31 patients with SMA type 2 and type 3 of various ages, disease duration and severity.

Chapter 3 is a follow-up study after one year of the cohort described in chapter 2. It summarizes changes in qMRI parameters associated with disease progression in treatment-naïve, adult patients. This study also tackles the methodological issue of correct alignment of imaging datasets.

In **Chapter 4**, we used quantitative analysis of thigh muscles in a cohort of young children during their first year of treatment with nusinersen.

In **chapter 5**, we zoom in to quantitative imaging of the sciatic nerve in a cross-sectional cohort study of treatment-naïve patients. We also describe follow-up during treatment with nusinersen.

In **chapter 6** we explore the feasibility of quantitative MRI at the individual level by describing findings in an individual with a homozygous *SMN1* deletion but without clinical signs of weakness.

Chapter 7 provides the discussion of our findings.

REFERENCES

1. Pearn J. Incidence, prevalence, and gene frequency studies of chronic childhood spinal muscular atrophy. *J Med Genet.* 1978;15(6):409–413. doi:10.1136/jmg.15.6.409.
2. Wijngaarde CA, Stam M, Otto LAM, et al. Population-based analysis of survival in spinal muscular atrophy. *Neurology.* 2020;doi:10.1212/WNL.0000000000009248.
3. Wadman RI, Jansen MD, Stam M, et al. Intragenic and structural variation in the SMN locus and clinical variability in spinal muscular atrophy. *Brain Commun.* 2020;doi:10.1093/braincomms/fcaa075.
4. Mercuri E, Finkel RS, Muntoni F, et al. Diagnosis and management of spinal muscular atrophy: Part 1: Recommendations for diagnosis, rehabilitation, orthopedic and nutritional care. *Neuromuscul Disord.* 2018;doi:10.1016/j.nmd.2017.11.005.
5. Finkel RS, Mercuri E, Meyer OH, et al. Diagnosis and management of spinal muscular atrophy: Part 2: Pulmonary and acute care; medications, supplements and immunizations; other organ systems; and ethics. *Neuromuscul Disord.* 2018;doi:10.1016/j.nmd.2017.11.004.
6. Werdnig G. Zwei frühinfantile hereditäre Fälle von progressiver Muskelatrophie unter dem Bilde der Dystrophie, aber anf neurotischer Grundlage. *Arch Psychiatr Nervenkr.* 1891;doi:10.1007/BF01776636.
7. Hoffmann J. Ueber chronische spinale Muskelatrophie im Kindesalter, auf familiärer Basis. *Dtsch Z Nervenheilkd.* 1893;doi:10.1007/BF01668496.
8. Dubowitz V. Ramblings in the history of spinal muscular atrophy. *Neuromuscul Disord.* 2009;doi:10.1016/j.nmd.2008.10.004.
9. Kugelberg E, Welander L. Heredofamilial Juvenile muscular Atrophy Simulating muscular Dystrophy. *Arch Neurol Psychiatry.* 1956;doi:10.1001/archneurpsyc.1956.02330230050005.
10. Feldkötter M, Schwarzer V, Wirth R, Wienker TF, Wirth B. Quantitative analyses of SMN1 and SMN2 based on real-time lightcycler PCR: Fast and highly reliable carrier testing and prediction of severity of spinal muscular atrophy. *Am J Hum Genet.* 2002;doi:10.1086/338627.
11. Taylor JE, Thomas NH, Lewis CM, et al. Correlation of SMNt and SMNc gene copy number with age of onset and survival in spinal muscular atrophy. *Eur J Hum Genet.* 1998;6(5);doi:10.1038/sj.ejhg.5200210.
12. Wadman RI, Wijngaarde CA, Stam M, et al. Muscle strength and motor function throughout life in a cross-sectional cohort of 180 patients with spinal muscular atrophy types 1c–4. *Eur J Neurol.* 2018;25(3):512–518. doi:10.1111/ene.13534.
13. Deymeer F, Serdaroglu P, Poda M, Gülşen-Parman Y, Özçelik T, Özdemir C. Segmental distribution of muscle weakness in SMA III: Implications for deterioration in muscle strength with time. *Neuromuscul Disord.* 1997;doi:10.1016/S0960-8966(97)00113-2.
14. Wijngaarde CA, Stam M, Otto LAM, et al. Muscle strength and motor function in adolescents and adults with spinal muscular atrophy. *Neurology.* 2020;95(14):e1988–e1998. doi:10.1212/WNL.0000000000010540.
15. Wang CH, Finkel RS, Bertini ES, et al. Consensus statement for standard of care in spinal muscular atrophy. *J Child Neurol.* 2007;doi:10.1177/0883073807305788.
16. Van Der Heul AMB, Wijngaarde CA, Wadman RI, et al. Bulbar Problems Self-Reported by Children and Adults with Spinal Muscular Atrophy. *J Neuromuscul Dis.* 2019;doi:10.3233/JND-190379.
17. Wijngaarde CA, Stam M, De Kort FAS, Wadman RI, Van Der Pol WL. Limited maximal mouth opening in patients with spinal muscular atrophy complicates endotracheal intubation. *Eur. J. Anaesthesiol.* 2018;doi:10.1097/EJA.0000000000000838.

18. Van Bruggen HW, Wadman RI, Bronkhorst EM, et al. Mandibular dysfunction as a reflection of bulbar involvement in SMA type 2 and 3. *Neurology*. 2016;doi:10.1212/WNL.0000000000002348.
19. Fujak A, Kopschina C, Gras F, Forst R, Forst J. Contractures of the lower extremities in spinal muscular atrophy type II. Descriptive clinical study with retrospective data collection. *Ortop Traumatol Rehabil*. 2011;doi:10.5604/15093492.933792.
20. Wijngaarde CA, Brink RC, de Kort FAS, et al. Natural course of scoliosis and lifetime risk of scoliosis surgery in spinal muscular atrophy. *Neurology*. 2019;doi:10.1212/wnl.00000000000007742.
21. Wijngaarde CA, Veldhoen ES, Van Eijk RPA, et al. Natural history of lung function in spinal muscular atrophy. *Orphanet J Rare Dis*. 2020;doi:10.1186/s13023-020-01367-y.
22. Mercuri E, Bertini E, Iannaccone ST. Childhood spinal muscular atrophy: Controversies and challenges. *Lancet Neurol*. 2012. p. 443–452;doi:10.1016/S1474-4422(12)70061-3.
23. Dubowitz V. Chaos in the classification of SMA: A possible resolution. *Neuromuscul Disord*. 1995;5(1);doi:10.1016/0960-8966(94)00075-K.
24. Zerres K, Schöneborn SR. Natural History in Proximal Spinal Muscular Atrophy: Clinical Analysis of 445 Patients and Suggestions for a Modification of Existing Classifications. *Arch Neurol*. 1995;doi:10.1001/archneur.1995.00540290108025.
25. Munsat TL, Davies KE. International SMA Consortium Meeting (26–28 June 1992, Bonn, Germany). *Neuromuscul Disord*. 1992. p. 423–428;doi:10.1016/S0960-8966(06)80015-5.
26. Oskoui M, Darras BT, De Vivo DC. Spinal Muscular Atrophy: 125 Years Later and on the Verge of a Cure. *Spinal Muscular Atrophy Dis Mech Ther*. 2017;doi:10.1016/B978-0-12-803685-3.00001-X.
27. Boulis N, O'Connor DM, Donsante A. Molecular and Cellular Therapies for Motor Neuron Diseases. *Mol. Cell. Ther. Mot. Neuron Dis*. 2017.
28. Lefebvre S, Bürglen L, Reboullet S, et al. Identification and characterization of a spinal muscular atrophy-determining gene. *Cell*. 1995;80(1):155–165. doi:10.1016/0092-8674(95)90460-3.
29. Melki J, Abdelhak S, Sheth P, et al. Gene for chronic proximal spinal muscular atrophies maps to chromosome 5q. *Nature*. 1990;doi:10.1038/344767a0.
30. Monani UR, Lorson CL, Parsons DW, et al. A single nucleotide difference that alters splicing patterns distinguishes the SMA gene SMN1 from the copy gene SMN2. *Hum Mol Genet*. 1999;doi:10.1093/hmg/8.7.1177.
31. Crawford TO, Paushkin S V., Kobayashi DT, et al. Evaluation of SMN protein, transcript, and copy number in the biomarkers for spinal muscular atrophy (BforSMA) clinical study. *PLoS One*. 2012;doi:10.1371/journal.pone.0033572.
32. Wadman RI, Stam M, Gijzen M, et al. Association of motor milestones, SMN2 copy and outcome in spinal muscular atrophy types 0–4. *J Neurol Neurosurg Psychiatry*. 2017;88:364–367. doi:10.1136/jnnp-2016-314292.
33. Oprea GE, Kröber S, McWhorter ML, et al. Plastin 3 is a protective modifier of autosomal recessive spinal muscular atrophy. *Science* (80-). 2008;doi:10.1126/science.1155085.
34. Riessland M, Kaczmarek A, Schneider S, et al. Neurocalcin Delta Suppression Protects against Spinal Muscular Atrophy in Humans and across Species by Restoring Impaired Endocytosis. *Am J Hum Genet*. 2017;100(2);doi:10.1016/j.ajhg.2017.01.005.
35. Wirth B, Brichta L, Schrank B, et al. Mildly affected patients with spinal muscular atrophy are partially protected by an increased SMN2 copy number. *Hum Genet*. 2006;119:422–428. doi:10.1007/s00439-006-0156-7.
36. Singh RN, Howell MD, Ottesen EW, Singh NN. Diverse role of survival motor neuron protein. *Biochim. Biophys. Acta - Gene Regul. Mech*. 2017;doi:10.1016/j.bbagr.2016.12.008.

37. Lauria F, Bernabò P, Tebaldi T, et al. SMN-primed ribosomes modulate the translation of transcripts related to spinal muscular atrophy. *Nat Cell Biol.* 2020;doi:10.1038/s41556-020-00577-7.
38. Shababi M, Lorson CL, Rudnik-Schöneborn SS. Spinal muscular atrophy: A motor neuron disorder or a multi-organ disease? *J Anat.* 2014;224:15–28. doi:10.1111/joa.12083.
39. Jing Yeo CJ, Darras BT. Overturning the Paradigm of Spinal Muscular Atrophy as just a Motor Neuron Disease. *Pediatr Neurol.* 2020;doi:10.1016/j.pediatrneurol.2020.01.003.
40. Hamilton G, Gillingwater TH. Spinal muscular atrophy: Going beyond the motor neuron. *Trends Mol Med.* 2013;19:40–50. doi:10.1016/j.molmed.2012.11.002.
41. Wijngaarde CA, Blank AC, Stam M, Wadman RI, Van Den Berg LH, Van Der Pol WL. Cardiac pathology in spinal muscular atrophy: a systematic review. *Orphanet J Rare Dis.* 2017;12(1) doi:10.1186/s13023-017-0613-5.
42. Fan L, Simard LR. Survival motor neuron (SMN) protein: Role in neurite outgrowth and neuromuscular maturation during neuronal differentiation and development. *Hum Mol Genet.* 2002;doi:10.1093/hmg/11.14.1605.
43. Swoboda KJ, Prior TW, Scott CB, et al. Natural history of denervation in SMA: Relation to age, SMN2 copy number, and function. *Ann Neurol.* 2005;57:704–712. doi:10.1002/ana.20473.
44. Mishra VN, Kalita J, Kesari A, Mittal B, Shankar SK, Misra UK. A clinical and genetic study of spinal muscular atrophy. *Electromyogr Clin Neurophysiol.* 2004;
45. Wadman RI, Vrancken AFJE, Van Den Berg LH, Van Der Pol WL. Dysfunction of the neuromuscular junction in spinal muscular atrophy types 2 and 3. *Neurology.* 2012;doi:10.1212/WNL.0b013e3182749eca.
46. Groen EJM, Perenthaler E, Courtney NL, et al. Temporal and tissue-specific variability of SMN protein levels in mouse models of spinal muscular atrophy. *Hum Mol Genet.* 2018;27:2851–2862. doi:10.1093/hmg/ddy195.
47. Burtlet P, Huber C, Bertrand S, et al. The distribution of SMN protein complex in human fetal tissues and its alteration in spinal muscular atrophy. *Hum Mol Genet.* 1998;doi:10.1093/hmg/7.12.1927.
48. Ramos DM, d'Ydewalle C, Gabbeta V, et al. Age-dependent SMN expression in disease-relevant tissue and implications for SMA treatment. *J Clin Invest.* 2019;doi:10.1172/JCI124120.
49. Berciano MT, Castillo-Iglesias MS, Val-Bernal JF, et al. Mislocalization of SMN from the I-band and M-band in human skeletal myofibers in spinal muscular atrophy associates with primary structural alterations of the sarcomere. *Cell Tissue Res.* 2020;doi:10.1007/s00441-020-03236-3.
50. Martínez-Hernández R, Soler-Botija C, Also E, et al. The developmental pattern of myotubes in spinal muscular atrophy indicates prenatal delay of muscle maturation. *J Neuropathol Exp Neurol.* 2009;68(5):474–481. doi:10.1097/NEN.0b013e3181a10ea1.
51. Arnold AS, Gueye M, Guettier-Sigrist S, et al. Reduced expression of nicotinic AChRs in myotubes from spinal muscular atrophy I patients. *Lab Invest.* 2004;doi:10.1038/labinvest.3700163.
52. Ripolone M, Ronchi D, Violano R, et al. Impaired muscle mitochondrial biogenesis and myogenesis in spinal muscular atrophy. *JAMA Neurol.* 2015;doi:10.1001/jamaneurol.2015.0178.
53. Ando S, Tanaka M, Chinen N, Nakamura S, Shimazawa M, Hara H. SMN Protein Contributes to Skeletal Muscle Cell Maturation Via Caspase-3 and Akt Activation. *In Vivo (Brooklyn).* 2020;34(6) doi:10.21873/invivo.12161.
54. Long KK, O'Shea KM, Khairallah RJ, et al. Specific inhibition of myostatin activation is beneficial in mouse models of SMA therapy. *Hum Mol Genet.* 2019;doi:10.1093/hmg/ddy382.
55. Gavrilina TO, McGovern VL, Workman E, et al. Neuronal SMN expression corrects spinal muscular atrophy in severe SMA mice while muscle-specific SMN expression has no phenotypic effect. *Hum Mol Genet.* 2008;doi:10.1093/hmg/ddm379.

56. Hua Y, Sahashi K, Rigo F, et al. Peripheral SMN restoration is essential for long-term rescue of a severe spinal muscular atrophy mouse model. *Nature*. 2011;doi:10.1038/nature10485.
57. Hua Y, Vickers TA, Okunola HL, Bennett CF, Krainer AR. Antisense Masking of an hnRNP A1/A2 Intronic Splicing Silencer Corrects SMN2 Splicing in Transgenic Mice. *Am J Hum Genet*. 2008;doi:10.1016/j.ajhg.2008.01.014.
58. Finkel RS, Mercuri E, Darras BT, et al. Nusinersen versus sham control in infantile-onset spinal muscular atrophy. *N Engl J Med*. 2017;377:1723–1732. doi:10.1056/NEJMoa1702752.
59. Mercuri E, Darras BT, Chiriboga CA, et al. Nusinersen versus sham control in later-onset spinal muscular atrophy. *N Engl J Med*. 2018;378(7):625–635. doi:10.1056/NEJMoa1710504.
60. Hagenacker T, Wurster CD, Günther R, et al. Nusinersen in adults with 5q spinal muscular atrophy: a non-interventional, multicentre, observational cohort study. *Lancet Neurol*. 2020;doi:10.1016/S1474-4422(20)30037-5.
61. Sivaramakrishnan M, McCarthy KD, Campagne S, et al. Binding to SMN2 pre-mRNA-protein complex elicits specificity for small molecule splicing modifiers. *Nat Commun*. 2017;doi:10.1038/s41467-017-01559-4.
62. Poirier A, Weetall M, Heinig K, et al. Risdiplam distributes and increases SMN protein in both the central nervous system and peripheral organs. *Pharmacol Res Perspect*. 2018;doi:10.1002/prp2.447.
63. Messina S, Sframeli M. New Treatments in Spinal Muscular Atrophy: Positive Results and New Challenges. *J Clin Med*. 2020;9(7):2222. doi:10.3390/jcm9072222.
64. Mercuri E, G. B, Kirschner J, et al. SUNFISH part 1: Safety, tolerability, PK/ PD, and exploratory efficacy data in patients with Type 2 or 3 spinal muscular atrophy (SMA). *Eur J Neurol*. 2019;
65. Dominguez E, Marais T, Chatauret N, et al. Intravenous scAAVg delivery of a codon-optimized SMN1 sequence rescues SMA mice. *Hum Mol Genet*. 2011;doi:10.1093/hmg/ddq514.
66. Duque S, Joussemet B, Riviere C, et al. Intravenous administration of self-complementary AAVg enables transgene delivery to adult motor neurons. *Mol Ther*. 2009;doi:10.1038/mt.2009.71.
67. Mendell JR, Al-Zaidy S, Shell R, et al. Single-Dose Gene-Replacement Therapy for Spinal Muscular Atrophy. *N Engl J Med*. 2017;doi:10.1056/NEJMoa1706198.
68. Zorginstituut Nederland. 2020. .
69. Stam M, Wadman RI, Wijngaarde CA, et al. Protocol for a phase II, monocentre, double-blind, placebo-controlled, cross-over trial to assess efficacy of pyridostigmine in patients with spinal muscular atrophy types 2-4 (SPACE trial). *BMJ Open*. 2018;doi:10.1136/bmjopen-2017-019932.
70. Elkina Y, von Haehling S, Anker SD, Springer J. The role of myostatin in muscle wasting: An overview. *J Cachexia. Sarcopenia Muscle*. 2011;doi:10.1007/s13539-011-0035-5.
71. Zhou H, Meng J, Malerba A, et al. Myostatin inhibition in combination with antisense oligonucleotide therapy improves outcomes in spinal muscular atrophy. *J Cachexia Sarcopenia Muscle*. 2020;doi:10.1002/jcsm.12542.
72. Scholar Rock Announces Positive Proof-of-Concept Data from TOPAZ Phase 2 Trial Interim Analysis of SRK-015 in Patients with Type 2 and Type 3 Spinal Muscular Atrophy. 2020.
73. Kaufmann P, McDermott MP, Darras BT, et al. Observational study of spinal muscular atrophy type 2 and 3: Functional outcomes over 1 year. *Arch Neurol*. 2011;68(6):779–786. doi:10.1001/archneurol.2010.373.
74. Kaufmann P, McDermott MP, Darras BT, et al. Prospective cohort study of spinal muscular atrophy types 2 and 3. *Neurology*. 2012;79(18):1889–1897. doi:10.1212/WNL.ob013e318271f7e4.
75. Chiriboga CA, Swoboda KJ, Darras BT, et al. Results from a phase 1 study of nusinersen (ISIS-SMN Rx) in children with spinal muscular atrophy. *Neurology*. 2016;doi:10.1212/WNL.0000000000002445.

76. Sumner CJ, Huynh TN, Markowitz JA, et al. Valproic Acid Increases SMN Levels in Spinal Muscular Atrophy Patient Cells. *Ann Neurol*. 2003;doi:10.1002/ana.10743.
77. Tiziano FD, Lomastro R, Pinto AM, et al. Salbutamol increases survival motor neuron (SMN) transcript levels in leucocytes of spinal muscular atrophy (SMA) patients: Relevance for clinical trial design. *J Med Genet*. 2010;doi:10.1136/jmg.2010.080366.
78. Wadman RI, Stam M, Jansen MD, et al. A comparative study of SMN protein and mRNA in blood and fibroblasts in patients with spinal muscular atrophy and healthy controls. *PLoS One*. 2016;doi:10.1371/journal.pone.0167087.
79. Sumner CJ, Kolb SJ, Harmison GG, et al. SMN mRNA and protein levels in peripheral blood: Biomarkers for SMA clinical trials. *Neurology*. 2006;doi:10.1212/01.wnl.0000201929.56928.13.
80. Darras BT, Crawford TO, Finkel RS, et al. Neurofilament as a potential biomarker for spinal muscular atrophy. *Ann Clin Transl Neurol*. 2019;doi:10.1002/acn3.779.
81. Wurster CD, Günther R, Steinacker P, et al. Neurochemical markers in CSF of adolescent and adult SMA patients undergoing nusinersen treatment. *Ther Adv Neurol Disord*. 2019;doi:10.1177/1756286419846058.
82. Wurster CD, Steinacker P, Günther R, et al. Neurofilament light chain in serum of adolescent and adult SMA patients under treatment with nusinersen. *J Neurol*. 2020;doi:10.1007/s00415-019-09547-y.
83. Kolb SJ, Coffey CS, Yankey JW, et al. Baseline results of the NeuroNEXT spinal muscular atrophy infant biomarker study. *Ann Clin Transl Neurol*. 2016;doi:10.1002/acn3.283.
84. Fuller HR, Gillingwater TH, Wishart TM. Commonality amid diversity: Multi-study proteomic identification of conserved disease mechanisms in spinal muscular atrophy. *Neuromuscul Disord*. 2016;doi:10.1016/j.nmd.2016.06.004.
85. Sleutjes BTHM, Wijngaarde CA, Wadman RI, et al. Assessment of motor unit loss in patients with spinal muscular atrophy. *Clin Neurophysiol*. 2020;doi:10.1016/j.clinph.2020.01.018.
86. Morrow JM, Sinclair CDJ, Fischmann A, et al. MRI biomarker assessment of neuromuscular disease progression: A prospective observational cohort study. *Lancet Neurol*. 2016;15(1):65–77. doi:10.1016/S1474-4422(15)00242-2.
87. Godi C, Ambrosi A, Nicastro F, et al. Longitudinal MRI quantification of muscle degeneration in Duchenne muscular dystrophy. *Ann Clin Transl Neurol*. 2016;doi:10.1002/acn3.319.
88. Hogrel JY, Wary C, Moraux A, et al. Longitudinal functional and NMR assessment of upper limbs in Duchenne muscular dystrophy. *Neurology*. 2016;doi:10.1212/WNL.0000000000002464.
89. Willis TA, Hollingsworth KG, Coombs A, et al. Quantitative Muscle MRI as an Assessment Tool for Monitoring Disease Progression in LGMD2f: A Multicentre Longitudinal Study. *PLoS One*. 2013;8(8) doi:10.1371/journal.pone.0070993.
90. Özsarlak Ö, Schepens E, Parizel PM, et al. Hereditary neuromuscular diseases. *Eur J Radiol*. 2001. doi:10.1016/S0720-048X(01)00399-0.
91. Schedel H, Reimers CD, Nägele M, Witt TN, Pongratz DE, Vogl T. Imaging techniques in myotonic dystrophy. A comparative study of ultrasound, computed tomography and magnetic resonance imaging of skeletal muscles. *Eur J Radiol*. 1992;doi:10.1016/0720-048X(92)90113-N.
92. Bonati U, Hafner P, Schädelin S, et al. Quantitative muscle MRI: A powerful surrogate outcome measure in Duchenne muscular dystrophy. *Neuromuscul Disord*. 2015;25(9):679–685. doi:10.1016/j.nmd.2015.05.006.
93. Ponrartana S, Ramos-Platt L, Wren TAL, et al. Effectiveness of diffusion tensor imaging in assessing disease severity in Duchenne muscular dystrophy: preliminary study. *Pediatr Radiol*. 2015;45(4):582–589. doi:10.1007/s00247-014-3187-6.

94. Kinali M, Arechavala-Gomez V, Cirak S, et al. Muscle histology vs MRI in Duchenne muscular dystrophy. *Neurology*. 2011;76(4):346–353. doi:10.1212/WNL.0b013e318208811f.
95. Mercuri E, Pichiecchio A, Counsell S, et al. A short protocol for muscle MRI in children with muscular dystrophies. *Eur J Paediatr Neurol*. 2002;doi:10.1016/S1090-3798(02)90617-3.
96. Strijkers GJ, Araujo ECA, Azzabou N, et al. Exploration of new contrasts, targets, and MR imaging and spectroscopy techniques for neuromuscular disease—A workshop report of working group 3 of the biomedicine and molecular biosciences COST action BM1304 MYO-MRI. *J Neuromuscul Dis*. 2019;6(1):1–30. doi:10.3233/JND-180333.
97. Leroy-Willig A, Willig TN, Henry-Feugeas MC, et al. Body composition determined with MR in patients with Duchenne muscular dystrophy, spinal muscular atrophy, and normal subjects. *Magn Reson Imaging*. 1997;15(7):737–744. doi:10.1016/S0730-725X(97)00046-5.
98. Chan WP, Liu GC. MR imaging of primary skeletal muscle diseases in children. *Am J Roentgenol*. 2002;179(4):989–997. doi:10.2214/ajr.179.4.1790989.
99. Ueno T, Yoshioka H, Iwasaki N, Tanaka R, Saida Y. MR findings of spinal muscular atrophy Type II: sibling cases. *Magn Reson Med Sci MRMS an Off J Japan Soc Magn Reson Med*. 2003;2(4):195–198. doi:10.2463/mrms.2.195.
100. Mercuri E, Pichiecchio A, Allsop J, Messina S, Pane M, Muntoni F. Muscle MRI in inherited neuromuscular disorders: Past, present, and future. *J Magn Reson Imaging*. 2007;25(2):433–440. doi:10.1002/jmri.20804.
101. Oh J, Kim SM, Shim DS, Sunwoo IN. Neurogenic muscle hypertrophy in Type III spinal muscular atrophy. *J Neurol Sci*. Elsevier B.V.; 2011;308(1–2):147–148. doi:10.1016/j.jns.2011.06.023.
102. Quijano-Roy S, Avila-Smirnow D, Carlier RY, et al. Whole body muscle MRI protocol: Pattern recognition in early onset NM disorders. *Neuromuscul Disord*. 2012;22(SUPPL. 2)doi:10.1016/j.nmd.2012.08.003.
103. Brogna C, Cristiano L, Verdolotti T, et al. MRI patterns of muscle involvement in type 2 and 3 spinal muscular atrophy patients. *J Neurol*. 2019;doi:10.1007/s00415-019-09646-w.
104. Inoue M, Ishiyama A, Komaki H, et al. Type-specific selectivity pattern of skeletal muscle images in spinal muscular atrophy. *Neuromuscul Disord*. 2015;25:S194. doi:10.1016/j.nmd.2015.06.042.
105. Sproule DM, Punyanitya M, Shen W, et al. Muscle volume estimation by magnetic resonance imaging in spinal muscular atrophy. *J Child Neurol*. 2011;26(3):309–317. doi:10.1177/0883073810380457.
106. Durmus H, Yilmaz R, Gulsen-Parman Y, et al. Muscle magnetic resonance imaging in spinal muscular atrophy type 3: Selective and progressive involvement. *Muscle and Nerve*. 2017;55(5):651–656. doi:10.1002/mus.25385.
107. Bonati U, Holiga Š, Hellbach N, et al. Longitudinal characterization of biomarkers for spinal muscular atrophy. *Ann Clin Transl Neurol*. 2017;4(5):292–304. doi:10.1002/acn3.406.
108. Stam M, Haakma W, Kuster L, et al. Magnetic resonance imaging of the cervical spinal cord in spinal muscular atrophy. *NeuroImage Clin*. 2019;doi:10.1016/j.nicl.2019.102002.
109. El Mendili MM, Lenglet T, Stojkovic T, et al. Cervical spinal cord atrophy profile in adult SMN1-linked SMA. *PLoS One*. 2016;doi:10.1371/journal.pone.0152439.



CHAPTER II

Quantitative MRI of skeletal muscle in a cross-sectional cohort of patients with spinal muscular atrophy types 2 and 3

Louise A.M. Otto¹, W-Ludo van der Pol¹, Lara Schlaffke², Camiel A. Wijngaarde¹,
Marloes Stam¹, Renske I. Wadman¹, Inge Cuppen³, Ruben P.A. van Eijk^{1,4},
Fay-Lynn Asselman¹, Bart Bartels⁵, Danny van der Woude⁵, Jeroen Hendrikse⁶,
Martijn Froeling⁶

¹Department of Neurology, UMC Utrecht Brain Center, University Medical Center
Utrecht, Utrecht University, the Netherlands

²Department of Neurology, BG-University Hospital Bergmannsheil, Ruhr-University
Bochum, Bochum, Germany

³Department of Neurology and Child Neurology, UMC Utrecht Brain Center,
University Medical Center Utrecht, Utrecht University, the Netherlands

⁴Biostatistics & Research Support, Julius Center for Health Sciences and Primary Care,
University Medical Center Utrecht, Utrecht University, Utrecht, The Netherlands

⁵Department of Child Development and Exercise Center, University Medical Center
Utrecht, Utrecht University, the Netherlands

⁶Department of Radiology, University Medical Center Utrecht, Utrecht University, the
Netherlands

ABSTRACT

Objective The aim of this study was to document upper leg involvement in spinal muscular atrophy (SMA) with quantitative MRI (qMRI) in a cross-sectional cohort of patients of varying type, disease severity and age.

Methods 31 patients with SMA types 2 and 3 (29.6 years; 7.6-73.9) and 20 healthy controls (37.9 years; 17.7-71.6) were evaluated in a 3T MRI with a protocol consisting of DIXON, T2 mapping and diffusion tensor imaging (DTI). qMRI measures were compared with clinical scores of motor function (Hammersmith Functional Motor Scale Expanded, HFMSSE) and muscle strength.

Results Patients exhibited an increased fat fraction and fractional anisotropy (FA), and decreased mean diffusivity (MD) and T2 as compared to controls (all $p < 0.001$). DTI parameters FA and MD manifest stronger effects than can be accounted for the effect of fatty replacement. Fat fraction, FA and MD show moderate correlation with muscle strength and motor function: FA is negatively associated with HFMSSE and MRC sum score ($\tau = -0.56$ and -0.59 ; both $p < 0.001$) whereas for fat fraction values are $\tau = -0.50$ and -0.58 , respectively (both $p < 0.001$).

Conclusions This study shows that DTI parameters correlate with muscle strength and motor function. DTI findings indirectly indicate cell atrophy and act as a measure independently of fat fraction. Combined these data suggest the potential of muscle DTI in monitoring disease progression and to study SMA pathogenesis in muscle.

Keywords spinal muscular atrophy, magnetic resonance imaging, diffusion tensor imaging, quantitative imaging, skeletal muscle

ABBREVIATIONS

DMD Duchenne Muscular Dystrophy; DTI diffusion tensor imaging; FA fractional anisotropy; HFMSE Hammersmith Functional Motor Scale, Expanded; LGMD Limb Girdle Muscular Dystrophies; MD mean diffusivity; SMA Spinal Muscular Atrophy; qMRI quantitative MRI

INTRODUCTION

Hereditary proximal Spinal Muscular Atrophy (SMA) is caused by Survival Motor Neuron (SMN) protein deficiency due to homozygous loss of function of the *SMN1* gene.(1) The presence of the nearly identical *SMN2* gene in the human genome ensures production of residual levels of full length SMN protein and the *SMN2* copy number inversely correlates with disease severity.(2) Treatment strategies that aim to increase SMN protein levels have been shown effective, in particular in infants and younger children with SMA.(3) Treatment of patients with the antisense oligonucleotide Spinraza that skews splicing of *SMN2* towards full length transcripts improves survival and motor milestone achievement in children with infantile onset SMA (i.e. type 1) and motor function in SMA type 2.(4) Additional data are needed to judge efficacy of SMN-augmenting strategies in older children and adults.

Levels of SMN protein are most critical in alpha-motor neurons, but other tissues, including muscle, probably also require specific threshold levels for proper development and function.(5,6) Clinical studies have documented that the natural history of SMA is characterized by decline in muscle strength and motor function over time after an initial phase of stalled gross motor development in early childhood.(7) Less is known of the natural history of anatomy and function of the tissues constituting the motor unit, i.e. the motor neuron, neuromuscular junction and muscle. Degeneration of alpha-motor neurons, which is the classical pathological hallmark of SMA, can be monitored *in vivo* by nerve conduction study techniques, in particular compound muscle action potential (CMAP) amplitude.(8) Fewer studies have addressed anatomy and function of muscle over time. Magnetic Resonance Imaging (MRI) is a powerful and non-invasive tool to study anatomy and tissue characteristics of skeletal muscle *in vivo*.(9) Most imaging studies in SMA have focused on a qualitative appreciation of muscle, grading fat infiltration visually.(10–20) Quantitative MRI (qMRI) can complement qualitative evaluation of muscles and has shown promising results in other neuromuscular disorders, such as Duchenne muscular dystrophy (DMD) and limb girdle muscular dystrophies (LGMD).(21,22) Quantitative MRI in SMA has not been studied in detail.(18,23,24) The application of qMRI in diseased muscle

proposes some technical challenges, as T2 signal and DTI parameters can be influenced or are confounded by fat present in the muscle.(22,25,26)

This study aims to document qMRI properties of muscle tissue in SMA. To this end, we explore the feasibility of a scan protocol of the upper leg that includes DIXON, T2 mapping and diffusion tensor imaging (DTI) in a cross-sectional cohort of 31 patients with SMA types 2 and 3, encompassing a broad range of disease severity and disease duration. We present the distinctive patterns of fatty infiltration and the associations of qMRI measurements with clinical parameters. We also assessed bias of fat infiltration for the interpretation of MR metrics in the presence of severe fat infiltration that is a hallmark of neuromuscular pathology.

METHODS

Study population

We recruited patients through the Dutch SMA database. Patients who agreed to participate were asked to recruit an age and gender-matched control. The diagnosis SMA was genetically confirmed in all patients. We used the clinical classification system for SMA typing(2); highest acquired milestone 'independent sitting' for type 2, 'walk independently at any stage in life' for type 3 and symptom onset before (3a) or after 36 months (3b), yet before adulthood. In case of discrepancy between the age at onset or highest acquired motor milestone, the latter defined the SMA type.

Exclusion criteria were tracheostomy, tracheostomal or any type of invasive ventilation; Forced Vital Capacity (FVC) >15% postural change between sitting and supine or symptoms of nocturnal hypoventilation; presence of pronounced swallowing disorders; orthopneu; contra-indication for 3T MR or non-MR compatible material in the body; pregnancy; claustrophobia.

The study protocol was approved by the local ethics committee (no.17-226/NL61066.041.17). All participants, and/or their parents in case of minors, had to be capable of understanding the study information and had to give oral and written informed consent.

Clinical evaluation

All subjects underwent a clinical evaluation of muscle strength of forty-two muscle groups using the Medical Research Council (MRC) score, which is a widely used scoring system to

document muscle strength of separate muscles.(27) Motor function was assessed with the expanded Hammersmith Functional Motor Scale Expanded (HF MSE) (range 0-66). A lower score on the HF MSE indicates poorer motor ability and function. Testing was performed by two trained evaluators (LO and DvdW), on the same day, either prior to MR with one hour of non-straining exercise before scanning, or followed after MR examination. Lung function in patients was measured by Forced Vital Capacity (FVC) in sitting and lying position prior to the magnetic resonance (MR) examination.

MR acquisition

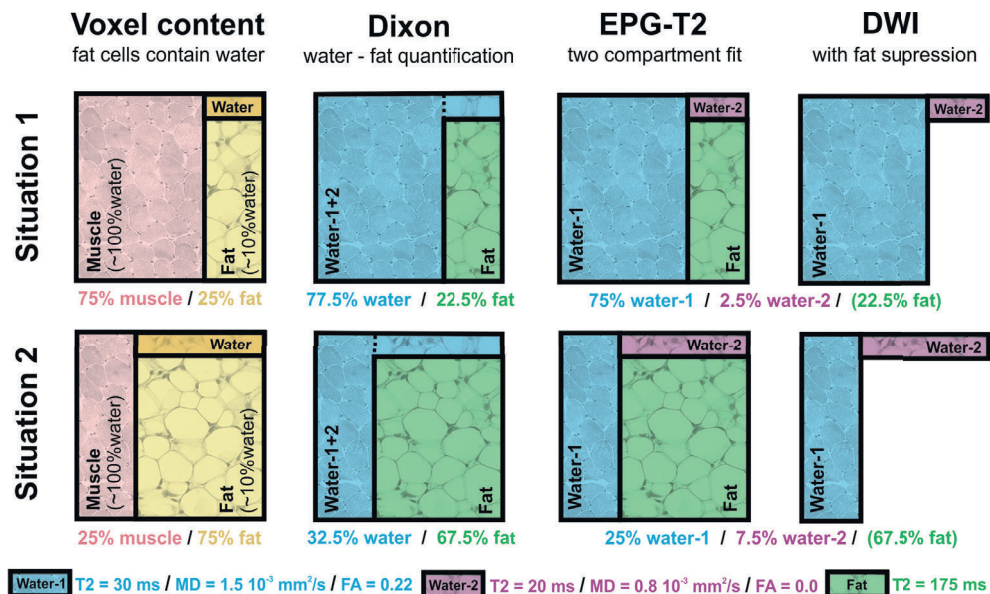
All MR examinations were performed on a 3T MR scanner (Philips Ingenia, Philips Medical Systems, the Netherlands). Subjects were scanned in supine position, feet-first with a 12-channel posterior and 16 channel anterior body coil, field of view set at 17,5 cm distance from the upper limit of the femoral head stretching 15 cm towards the knee. In children and subjects of smaller stature and/or hindered by severe contractures, the image stack was centered mid-femoral. Both legs were scanned.

Total scanning time was ~10 minutes including the survey and comprised 3 exams, i.e. a DIXON acquisition for measuring fat infiltration, T2 mapping to determine the water T2 relaxation time and DTI scans to measure the hindered diffusion of water molecules in tissue. For each voxel, the rate of diffusion and a preferred direction oriented in a three-dimensional space can be obtained. Fractional anisotropy (FA) describes the anisotropic organization of tissue, approaching 1 when the diffusion is mainly aimed in one direction. Mean diffusivity (MD) is the average diffusion in all directions. MD combined with FA gives insight in the microstructure of tissue.(28) Acquisition parameters of the MR protocol are listed in table 1. The acquisition methods are further explained in figure 1. and fat, and slightly underestimates the fat quantity because of attributing its water content to the water/muscle compartment. EPG-T2 uses a two-compartment fit accounting for the fat compartment. However, the estimated T2 of the water compartment is a combination of water in

muscle and water in fat. The diffusion-weighted imaging (DWI) acquisition has fat suppression and therefore only measures the water signal. Therefore, the measured diffusion properties are a combination of water in muscle and water in fat

Table 1. Acquisition parameters of MR protocol. Specifications per sequence at a field strength of 3T.

Sequence	4-point DIXON	T2 mapping	DWI
Sequence	Multi acquisition gradient echo	multi echo spin echo	spin echo-EPI
Repetition time (ms)	210	4598	5000
Echo time (ms)	2.6/3.36/4.12/4.88	17x 7.6	57
Flip angle (degrees)	10	90/180	90/180
Acquisition Matrix	320x320		160x92
FOV	480x480		480x276
Resolution (mm ²)	1.5x1.5	3x3	3x3
Slices	25	13	25
Slice thickness (mm)	6	6	6
Slice gap (mm)	0	6	0
b-values (nr of images) (mm ² /s ²)		0	0 (1), 1 (6), 10 (3), 25 (3), 100 (3), 200 (6), 400 (8), 600 (12)
Fat suppression			Gradient inversion + SPAIR (main fat signal) + SPIR (olefinic fat signal)
SENSE / Partial Fourier	2 / 1	2 / 1	1.9 / 0.75
Acquisition time (min:s)	1:20	3:05	3:30

**FIGURE 1** Methods of DIXON, EPG-T2 and DWI explained. A schematic representation of the water-fat partial volume effect in each of the used acquisition methods. Situation 1 (top row) represents a voxel with low fat infiltration and situation 2 (bottom row) one with high fat infiltration. The pink quadrant in the first column represents muscle tissue, which is assumed to contain only water. The

yellow quadrant represents fat tissue, which is assumed to contain 10% of water that is rendered dark yellow. The DIXON method distinguishes between water and fat, and slightly underestimates the fat quantity because of attributing its water content to the water/muscle compartment. EPG-T2 uses a two-compartment fit accounting for the fat compartment. However, the estimated T2 of the water compartment is a combination of water in muscle and water in fat. The diffusion-weighted imaging (DWI) acquisition has fat suppression and therefore only measures the water signal. Therefore, the measured diffusion properties are a combination of water in muscle and water in fat.

MR processing

All MR data were processed using QMRITools for Mathematica (mfroeling.github.io/QMRITools).⁽²⁹⁾ The processing steps for each method are summarized in figure 2. Before processing all data was visually inspected for artefacts and data quality. The Dixon data was processed using an iterative decomposition of water and fat with echo asymmetry and least squares estimation (IDEAL)⁽³⁰⁾ with B_0 and T_2^* estimation. The T2-mapping data were processed using an extended phase graph (EPG) fitting approach considering inhomogeneous B_1^+ .⁽³¹⁾ This method accounts for different T2 relaxation times for the water and fat component with the T2 of the fat component fixed to a value calibrated on the subcutaneous fat. The diffusion data was processed using an fitting method (iWLLS) with REKINDLE outlier detection⁽³²⁾, taking intravoxel incoherent motion (IVIM) into account.⁽³³⁾ Before tensor estimation the data was denoised using a principal component analysis (PCA) method ⁽³⁴⁾ after which data was corrected for subject motion and eddy current distortion using affine registration. A detailed overview of all processing steps and the multicenter reproducibility of the methods can be found in Schlauffke et al.⁽³⁵⁾

Since the T2 and the DTI parameters have a bias with increasing fat contribution, ^(22,25) simulations were performed to estimate this effect.^(22,26) The simulations were performed using multi-compartment extensions of the used models with each compartment simulated as shown in figure 1. For a detailed description of all simulations we refer to the supplemental file (S1). For estimation of the bias in T2 due to fat infiltration, fat fractions were simulated from 0 to 100% fat with a fixed known value for the T2 of fat of 180ms and a T2 of water in fat (10%) of 20ms.^(36,37) T2 of fat was based on the calibration values of our data, T2 of water in fat on literature; and EPG T2 fitting of subcutaneous fat on spectroscopy experiments.^(37–39) With increasing fat fraction, the water component for fat creates a bias in the estimated T2 of muscle, since water T2 is modeled as a single T2 water value see (figure 1). Similarly, in the estimation of tensor parameters the water component of fat creates a bias in MD and FA. Here, this compartment is assumed to have isotropic diffusion (FA=0) with an MD of $0.8 \text{ mm}^2/\text{s}$. With an increasing fat fraction the water signal decreases causing a decrease in SNR as well as a stronger contribution of the water component of fat.^(22,25)

Muscle segmentation

The in-phase or out-phase images and fat images of the 4-point DIXON sequence were used for manual segmentation of individual muscles in the image stack. Open-source software (ITK-SNAP version 3.6)(40) was used for segmentation on the 25 slices per image stack. Where the integrity of the muscle was still clear, muscles were annotated every third slice and then interpolated to fill in the missing slices. However, in more affected subjects with significant fat infiltration and atrophy, muscles had to be discriminated slice per slice. In case of incongruency because of deviating anatomy in severely affected subjects, two authors (LO and MF) segmented the slices individually and reached consensus. In total, 12 muscles per leg were partially apparent in the image stack. The demarcated regions of interest (ROI) were then used to retrieve the quantitative information from the other related sequences. To transfer the DIXON based segmentations to the T2 and DTI data a combined rigid and b-spline image registration was used (Elastix)(41). Muscles with volume smaller than 10 voxels ($\approx 67.5\text{mm}^3$) were omitted from analyses.

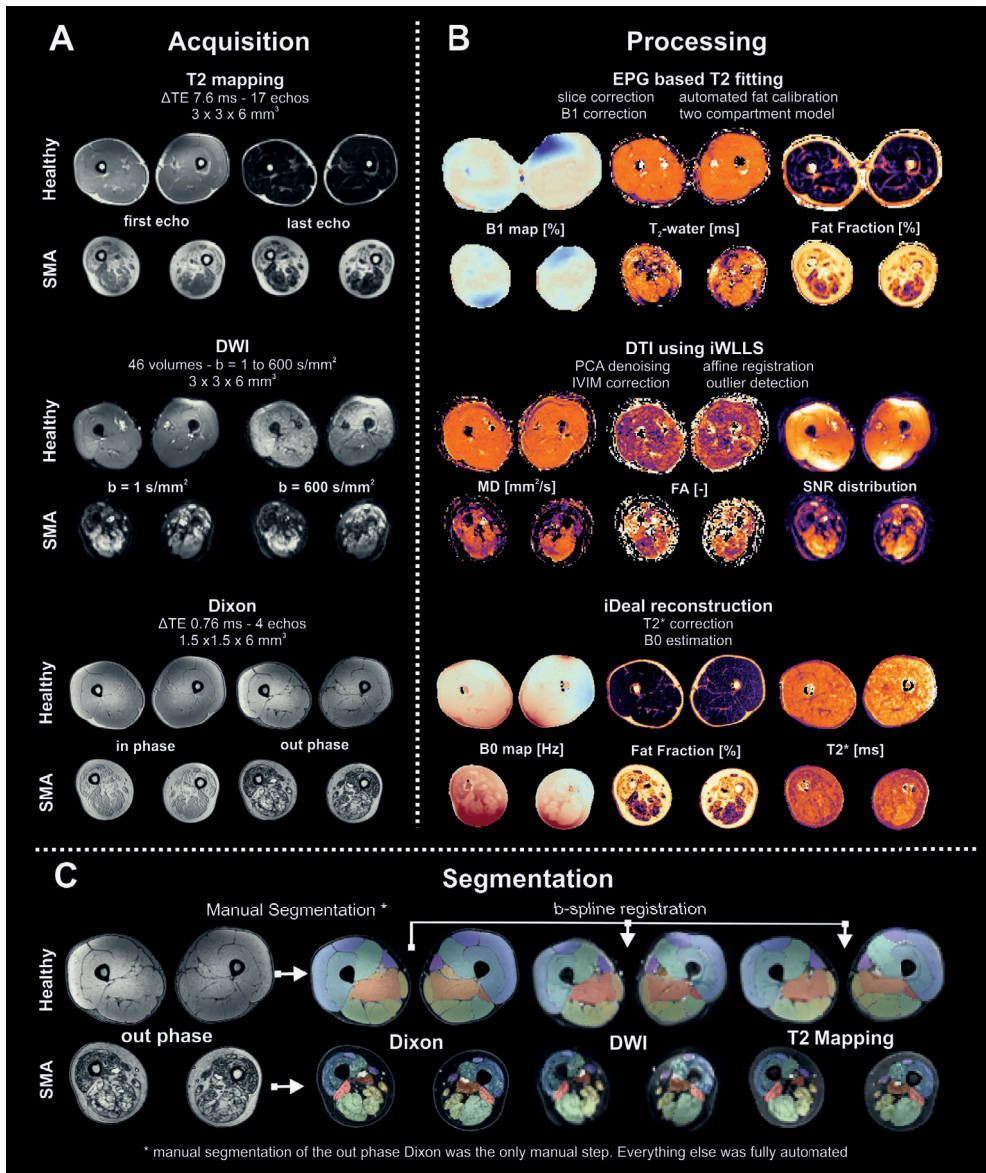


FIGURE 2 Data processing. Overview of the various steps involved in the acquisition and processing pipeline. (A) Example data for a healthy volunteer and a SMA patient for all three qMRI methods. (B) A summary of the processing steps and example parameters obtained for each of the qMRI methods. (C) Overview of the muscle segmentation. Muscle are manually segmented using the out-phase Dixon image. Then segmentation is transferred to the DTI and T2 mapping data using b-spline registration. DTI, diffusion tensor imaging; DWI, diffusion-weighted imaging; FA, fraction anisotropy; MD, mean diffusivity; SMA, spinal muscular atrophy; TE, echo time

Statistical analysis

Statistical analysis was performed using SPSS version 25 for Windows (SPSS Inc. Chicago). Differences between patients and controls were assessed by means of an independent Student's t-test with Welch's correction. MR parameters were averaged across muscles per subject. Subjects were classified as either 'case' for patients or 'control'. The mean difference between cases and controls was converted into a standardized mean difference according to Hedge's g in order to compare effect sizes across qMRI parameters. For multiple group comparisons (i.e. controls, SMA type 2 and SMA type 3), we used a one-way ANOVA. Due to non-normality of the data, associations between clinical and imaging parameters were evaluated using Kendall's tau correlation coefficient and associations were further explored with multiple linear regression. Results were considered significant when $p < 0.05$; we did not correct for multiplicity due to the exploratory nature of the analysis. Codes and data are available upon request by any qualified investigator.

RESULTS

Study population

We obtained datasets of 31 patients with SMA with a mean age of 29.6 years (range 7.6-73.9) and of 20 controls with a mean age of 37.9 years (range 17.7-71.6). Minors could not be matched to controls. 15 patients had SMA type 2, 7 type 3a and 9 type 3b. Mean HMFSE score was 5 points for type 2 and 34 points for type 3. Patients characteristics, muscle strength and motor function mean values are reported in table 2.

Table 2. Baseline demographics and characteristics. Clinical characteristics of study participants.

	Type 2	Type 3a	Type 3b	Controls
n	15	7	9	20
Sex (M:F)	6:9	3:4	6:3	8:12
Age in years (range)	24.9 (7-73)	23.5 (7-49)	42.0 (18-55)	37.9 (17-71)
Mean disease duration in months (SD; range)	276 (172; 82-661)	265 (202; 69-581)	362 (180; 77-661)	-
<u>Ambulatory status</u>				
Ambulatory, n (%)	-	3 (43%)	8 (89%)	20 (100%)
Nonambulatory, n (%)	15 (100%)	4 (57%)	1 (11%)	-

Clinical measurements				
Mean MRC sum score, (SD)	110 (34.4)	151 (43.7)	177 (38.8)	229 (2)
Mean MRC score lower extremities (SD)	11 (4.8)	15 (6.4)	17 (6.8)	30 (-)
Mean HFMSE score (SD; range)	5.9 (10; 0-36)	28.4 (22.8; 0-53)	40.0 (18.0; 2-63)	-

N= number, M=male, F=female, SD= standard deviation, MRC = Medical Research Council.

MR acquisition and processing

Two datasets of patients were excluded from final data analysis because image quality was insufficient resulting in 49 datasets. All muscle groups in controls and 58% of muscles in patients were successfully segmented (total 430 muscles; 34 rectus femoris, 29 vastus medialis, 23 vastus lateralis and 15 vastus intermedius muscle; 44 m. semimembranosus, 44 m. semitendinosus, m. biceps femoris long and short head 43 and 38, respectively; m. adductor magnus 38, the adductor longus muscle 44, and gracilis 41 and sartorius muscle 37).

Fat infiltration across age categories

Figure 3 summarizes patterns of fatty infiltration stratified for SMA type. Patients with SMA type 2 show generalized atrophy and fatty infiltration starting at a young age, underlined here by images of patients from 7 years and on, and thickening of the subcutaneous fat layer. The pattern in type 3a and 3b appears more gradual, as fat infiltration of individual muscle groups was more pronounced from the age of 10 and increasing with age. Fat infiltration showed a characteristic pattern with predominant involvement of the anterior compartment, in particular the vasti muscles whereas the m. rectus femoris remained identifiable when the vasti had already perished. The pattern of fat infiltration of the posterior compartment showed more heterogeneity. The short head of the biceps femoris, m. semimembranosus, m. gracilis and m. sartorius are the last muscles involved in the process of fatty replacement. The adductor magnus is affected at a relatively early stage while the m. adductor longus is relatively spared. From the start of puberty muscle images of patients with SMA type 3a resemble type 2 more than type 3b. Complete fatty replacement with an intact fascia occurs in types 2 and 3a before the age of 30, but only after the age of 45 in type 3b.

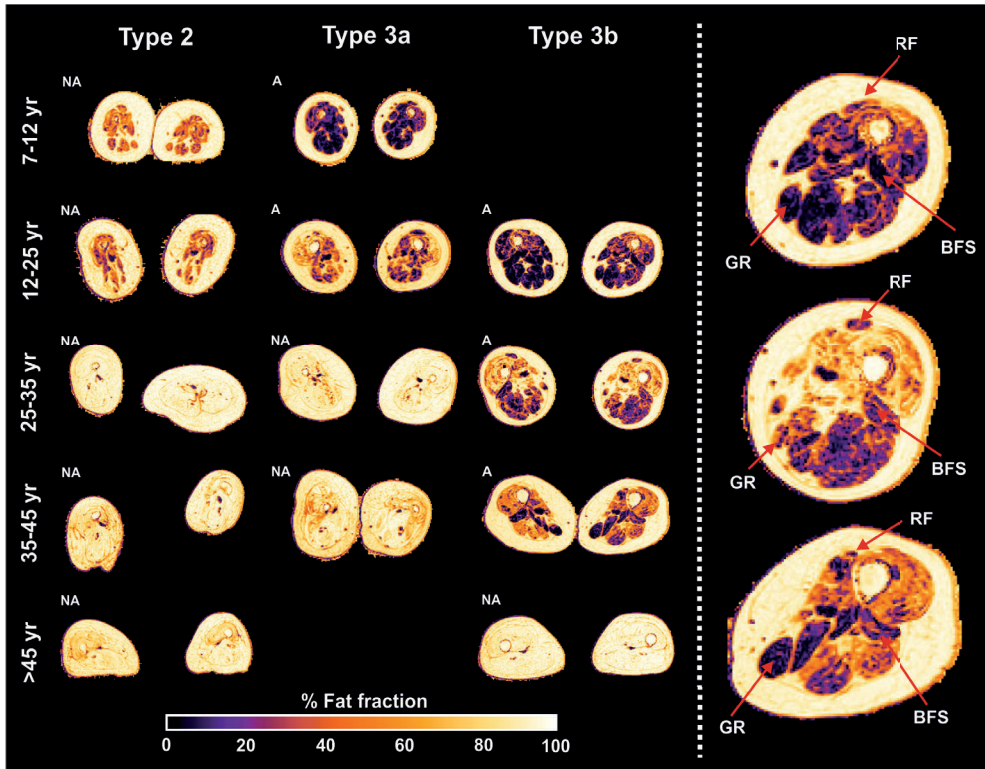


FIGURE 3 Overview of fat infiltration stratified for SMA type and age. Images of the thigh in the transversal plane of the middle section of the image stack. The images are categorized into age category for distinct SMA types. The heat bar beneath indicates a scale from 0% to 100%. The right column presents a magnification of the left leg of type 3b patients. The red arrows point at the annotated muscles, which seem relatively spared. A, ambulant; BFS, biceps femoris, short head; GR, gracilis; NA, nonambulant; RF, rectus femoris

Comparison of groups

The mean values per qMRI parameter for patients and controls are given in table 3. The individual muscles are now allocated to a specific muscle group; either quadriceps, hamstrings or adductors, with the exception of the m. sartorius and m. gracilis. Figure 4 (left column) depicts each qMRI measure for the distinct muscle groups for type 2 and type 3 patients versus controls. The comparison of type 2 and type 3 is based on measurements of 7 patients type 2 and 12 patients with type 3 in which one or more muscles of the quadriceps could be identified, and of the hamstrings in 23 patients (of which 11 type 2 and 12 type 3) and adductor group in 25 patients (12 type 2 and 13 patients type 3).

Table 3. Descriptive statistics of the dataset. Cross-sectional statistics of differences in qMRI outcomes between the SMA and control cohort. All reported values are in mean \pm standard deviation.

QMRI	SMA	CONTROLS	
FF-DIXON (%)	47.6 \pm 17.4	7.6 \pm 1.5	mean difference: -40.0; 95% CI [-47.0 to -33.0] standardized mean difference: 3.06 p-value <0.001
T2 (ms)	27.3 \pm 1.5	28.9 \pm 0.4	mean difference: 1.54; 95% CI [0.9 to 2.2] standardized mean difference: -1.38 p-value <0.001
DTI - FA	0.41 \pm 0.09	0.24 \pm 0.03	mean difference: -0.17; 95% CI [-0.2 to -0.1] standardized mean difference: 2.41 p-value <0.001
DTI - MD (mm ² /s)	1.13 \pm 0.28	1.47 \pm 0.10	mean difference: 0.34; 95% CI [0.2 to 0.5] standardized mean difference: -1.54 p-value <0.001

qMRI = quantitative magnetic resonance imaging, SMA = spinal muscular atrophy, FF=fat fraction, DTI = diffusion tensor imaging, FA = fractional anisotropy, MD = mean diffusivity, CI= confidence interval. Standardized mean difference according to Hedge's g.

Differences in fat fraction between groups

Mean fat fraction of all upper leg muscles was 7.6 \pm 1.5% in controls and 47.6 \pm 17.4% in patients (p <0.001). Overall, fat fraction is higher in type 2 than in type 3 (51.5 \pm 15.1 vs 36.7 \pm 20.5%, p <0.001). Type 2 exhibits higher averages of fat fraction over all three muscle groups, yet only the hamstrings demonstrate a significantly lower fat fraction for type 3 (p =0.012). The anterior compartment is most conspicuously fat infiltrated in all patients, with a mean fat fraction of 57.4 \pm 10.1% in type 2 and 46.1 \pm 20.3% in type 3 (p =0.12). The adductor group has the lowest mean fat fraction in type 2 with 41.8 \pm 14.9%. The posterior compartment and middle compartment exhibit a comparable average fat fraction in type 3 (36.4 \pm 20.0% and 36.9 \pm 22.3%). On the level of individual muscles, the m. adductor longus has the lowest fat fraction in SMA. This contrast is most apparent in type 2 (29.1 \pm 16.1%) where the fat fraction of all other muscles exceeds 50%. In type 3, the m. semimembranosus was least affected (30.3 \pm 14.5%).

Differences in T2 between groups

Mean T2, averaged over all muscles, is in close range for patients (27.3 ± 1.5) versus controls (28.9 ± 0.4) yet significantly different ($p < 0.001$). For the distinct muscle groups, T2 does not show uniform differences for type 2 and 3 across muscle groups (hamstrings: $p = 0.14$, quadriceps: $p = 0.26$, adductors: $p = 0.56$).

Differences in DTI parameters between groups

MD is lowered in patients ($1.13 \pm .28$) versus controls ($1.47 \pm .10$, $p < 0.001$). When we compare patients, MD is significantly lower in type 2 versus type 3 for quadriceps and hamstrings (both $p = 0.001$), but not different for the adductors ($p = 0.093$). FA is higher ($0.41 \pm .09$) in patients compared to controls ($0.24 \pm .03$, $p < 0.001$). FA is increased in type 3 and highest in type 2 for all muscle groups (all $p < 0.05$).

The effect of fat fraction on T2 and DTI parameters

An increasing fat fraction introduces a bias in T2 and diffusion parameters as we outlined in the Methods section. Consequently, we compared our measured data to simulations of this effect as is shown in figure 4 (right two columns). Theoretically, the effect of an increasing fat fraction would result in a gradual decrease of the T2 signal, a decrease in MD and an increase in FA. Our data shows that T2 of fat infiltrated muscles follow the predicted T2 decrease. A decrease of MD is seen together with an increase of FA, both of greater magnitude than the predicted effect of partial volume effects of fat. Overall, we observed that the estimated EPG fat fraction is different from estimated DIXON fat fraction. against fat fraction. In the middle column, each data point represents a measurement of individual muscles of all subjects with SMA (gray) and control subjects (green). In the right column, the data points are reduced to an average using local regression and 95% CI (shaded area). The red line represents the association based on simulations of increasing fat fraction, theoretically ranging to 100. The gray and green lines depict the data of this study. CI, confidence interval; FA, fractional anisotropy; MD, mean diffusivity

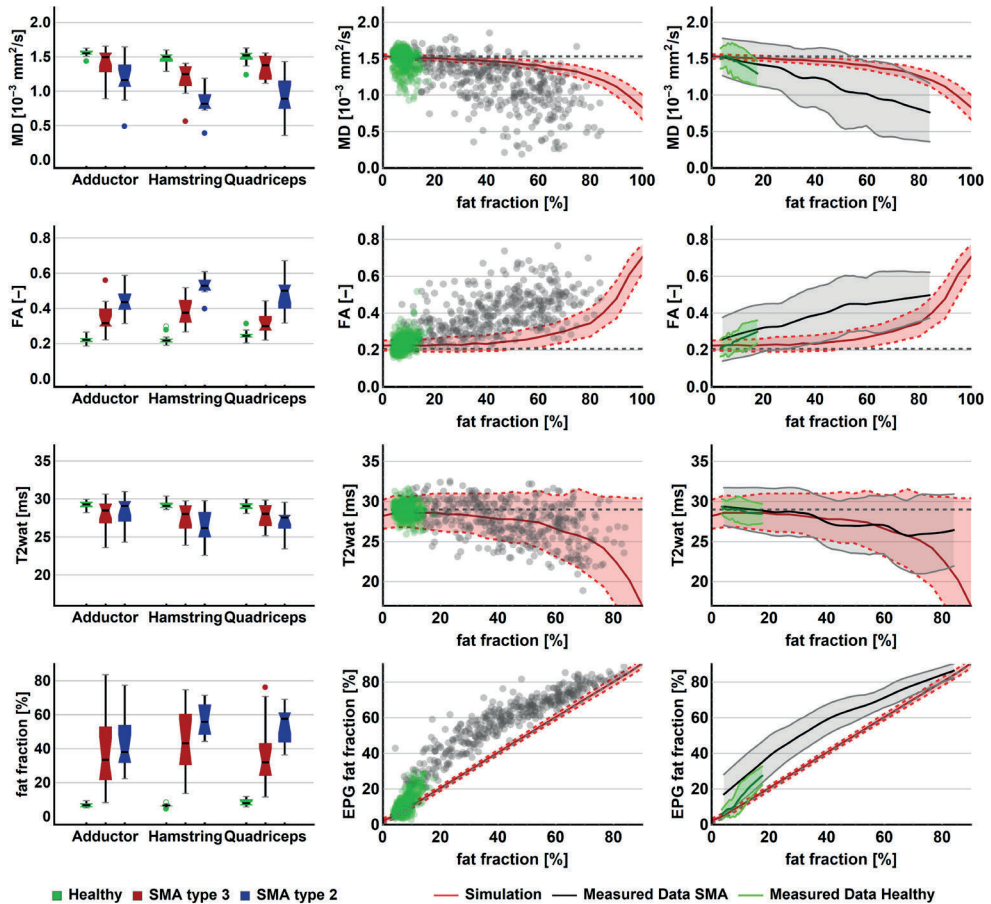


FIGURE 4 qMRI per muscle group and relations between qMRI parameters. The left panel shows boxplots for the qMRI parameters for the distinct muscle groups for healthy controls, SMA type 2 and SMA type 3. In the middle and right panels, each of the qMRI parameters is plotted

Association of qMRI with clinical measurements

We explored each of the qMRI in relation to clinical measures (figure 5). Disease duration is not a direct reflection of disease severity but given the progressive nature of SMA is a determinant. We found a significant moderate correlation of disease duration with fat fraction ($\tau = -0.34$, $p = 0.016$) and MD ($\tau = -0.33$, $p = 0.018$), but not with FA ($\tau = 0.02$, $p = 0.982$) nor with T2 ($\tau = -0.18$, $p = 0.193$). Motor function measured by the HFMSE scale showed a negative, moderate correlation with FA ($\tau = -0.56$, $p < 0.001$) and fat fraction ($\tau = -0.5$, $p < 0.001$). We observed a positive moderate correlation of MD ($\tau = 0.52$, $p < 0.001$) and HFMSE but not of T2 ($\tau = 0.2$, $p = 0.156$) with HFMSE. There was a moderate significant correlation of muscle strength represented by

the MRC sum score with FA ($\tau = -0.59$, $p < 0.001$), with fat fraction ($\tau = 0.58$, $p < 0.001$) and MD ($\tau = 0.55$, $p < 0.001$). We did not find a significant correlation with T2 ($\tau = 0.23$, $p = 0.103$). When we plotted the MRC sum score of the hamstrings, adductor and quadriceps muscles against the qMRI parameters, we observed similar trends (see figure 5 right column) with the strongest relationship with fat fraction ($\tau = 0.7$, $p < 0.001$). This correlation was similar to the correlation of contractile muscle CSA. For a detailed overview of CSA and volume of thigh muscle, and correlation with strength we refer to supplementary file S2. FA changes are partly driven by fat infiltration, but nonetheless FA has a significant contribution to the prediction on thigh muscle strength independent of fat fraction. Multiple linear regression analysis showed a significant contribution of fat fraction to the MRC sum score of upper leg with an R^2 of 0.76, whereas the R^2 of only MD or FA is 0.50 or 0.34 respectively. Adding both FA and fat fraction to the model increased the R^2 to 0.80, while the addition of MD did not contribute significantly.

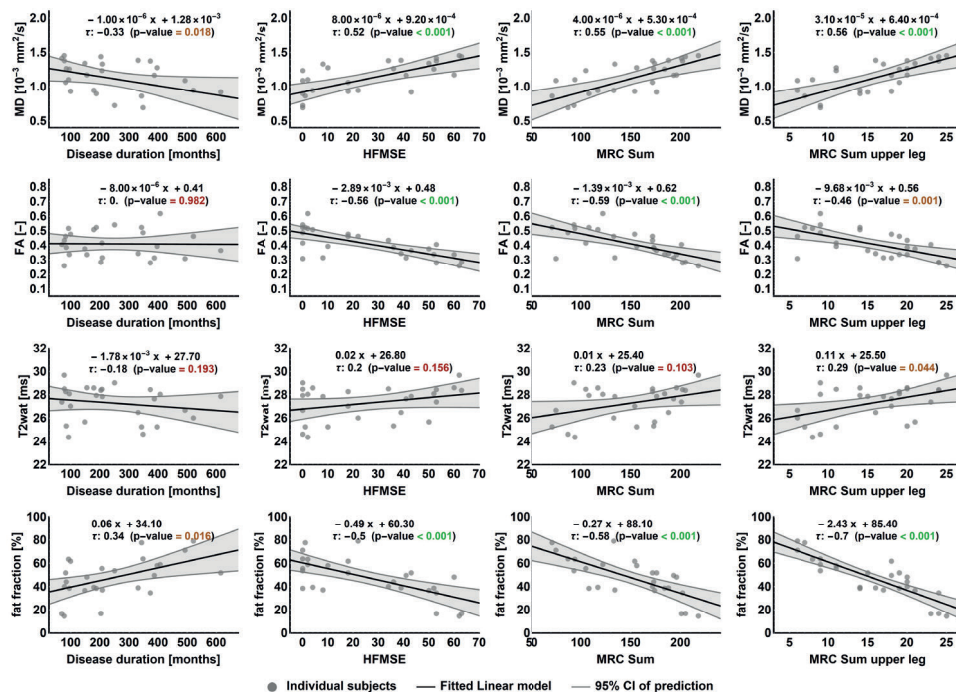


FIGURE 5 qMRI and relation with clinical measures. Each of the qMRI parameters (rows) is plotted against the following clinical outcome measures (columns); disease duration (in months), HFMSSE score, MRC sum score and MRC sum score of the upper leg. Data points represent the average value of all muscles per patient per qMRI parameter plotted against patient's clinical score. The correlation formula, Kendall's tau correlation coefficient and the P-value (significance level set at < 0.05) are shown per correlation plot. HFMSSE, Hammersmith Motor Function Scale Expanded, MRC, Medical Research Council

DISCUSSION

This study on a relatively large number of patients of different ages and disease severities outlines leg muscle involvement across the clinical spectrum of SMA and adds to accumulating experience with qMRI measures in neuromuscular diseases. DTI further elucidates distinct properties of skeletal muscle in SMA. The correlation of qMRI and clinical parameters suggest a potential as a biomarker for disease progression or treatment effect. Here, we extend the previous descriptions of muscle involvement in SMA with a diverse cohort, mounting from 7 up to 73 years of age. The patterns of muscle involvement and relative muscle sparing were comparable to previous reports; such as the m. adductor longus, m. gracilis, m. sartorius, and the short head of the m. biceps femoris and m. semimembranosus.(11,12,15,20,42) Strikingly, the severe involvement of the quadriceps did not impede some patients with type 3 to walk. Selective vulnerability of muscle is a hallmark of SMA but whether this is explained by anatomical or biochemical (i.e. related to SMN deficiency)(43,44) differences between muscle groups remains to be established. The progressive nature of SMA at muscle level is reflected by the more severe fatty infiltration of muscles in older patients. Similarly, patients with type 2 had earlier onset of fatty infiltration and therefore a higher fat fraction in all muscle groups than patients with type 3 at a similar age. The inclusion of older and severely affected patients allowed a cross-sectional description of qMRI across the full spectrum of SMA, which has not been described before. However, end-stage fatty infiltration resulted in the exclusion of these muscles from quantitative analysis because muscle was either no longer present, impossible to segment, unidentifiable, or under a volume of 10 voxels. Nonetheless, our data included muscles up to 80% of fat infiltration. Albeit little muscle was present, we could still establish a correlation between properties of remaining muscle and functional data. The use for longitudinal purposes, i.e. to study natural history of the quality of muscle tissue or the effects of treatment, seems therefore limited to young children with SMA type 2 and adolescents and young adults with SMA type 3.

Elevated T2 signal has been reported in neuromuscular disorders that trigger inflammatory processes in muscles, such as in DMD. Since the leukocyte infiltrates observed in DMD are not a hallmark of SMA, we did not expect similar changes in SMA. A previous study nevertheless reported an increased T2 in the upper leg in SMA patients, ranging from 34.3ms to 41.3ms, but this cannot be directly compared to our data as they used a multi-exponential signal model that does not account for EPG effects.(24) Moreover, Bonati et al. found a strong increased T2 in SMA patients in comparison to controls, exceeding 60ms whereas our data ranged to 31ms at most.(23) We think that these differences are explained

by methodological issues. In contrast to previous studies, we applied a two-compartment fit for T₂ mapping, which allowed a better estimation of water T₂ in the muscle, taking into account the partial volume effects of fat and the fat-independent behavior of muscle water T₂.⁽⁴⁵⁾ After correction for the increase of T₂ caused by fatty infiltration,⁽⁴⁶⁾ we found a decrease in T₂ that near-exactly follows the simulation of T₂ against an increasing fat fraction, similar to a previous study.⁽⁴⁷⁾ Therefore, we conclude that a decrease of T₂ as we perceived is solely related to partial volume effects caused by the amount of fat infiltration and that the T₂ signal increase in itself does not indicate any pathological process. However, if the T₂ relaxation of water in fat would have a higher value of ~ 30 ms instead of the assumed 20 ms, part of the decreased T₂ could potentially be attributed to pathological processes.

DTI analysis showed lowered MD and increased FA values in patients with SMA. As fat fraction is also a confounder on DTI, we repeated the simulation experiment in which we plotted MD and FA against an increasing fat fraction.^(22,25) After correction, our data illustrates stronger effects, i.e. a further decrease of MD and increase of FA, than could be explained based on partial volume effects alone. If the model would have wrongfully contributed the water component of fat to the muscle compartment, the results would be an underestimation of the situation and this would have led to even stronger effects. This suggests that we are indeed measuring disease-specific processes and that MD/FA measures behave independently of an increasing fat fraction. The latter also becomes apparent when we look at the relation of qMRI measures and clinical scores. Fat fraction strongly and FA and MD moderately correlate with thigh muscle strength. However, FA and fat fraction together improve the prediction of muscle strength, and despite its modest contribution suggest that FA adds to the prediction of MRC sum score independently of fat infiltration. This shows that although FA is strongly correlated with fat infiltration the diffusion parameters do provide additional information on muscle status.

An association of strength or function with DTI parameters has not been consistently found in DMD or LGMD.^(48,49) This may be explained by differences in muscular pathology but could also be due to methodological differences, including improved processing or segmentation of individual muscles rather than of muscle groups that could also potentially have benefited determining the relation between clinical parameters and image. The decrease of MD could indicate that the cellular compartment is subject to shrinkage, which is supported by the elevation of FA. This may be explained by atrophy of muscle fibers. The alternative explanation, in which the decrease of MD reflects changes in viscosity of the extracellular space due to fibrosis⁽⁴⁷⁾ is less likely, since it would be accompanied by

an invariable FA, as the cellular dimension would not change. Therefore, we hypothesize that our DTI findings indicate ongoing muscular atrophy, fitting the histopathological characteristics of muscle tissue rather than fibrosis. In muscles biopsies from patients with SMA round atrophic fibers are encountered in combination with large hypertrophic fibers,⁽⁵⁰⁾ which is compatible with an increased FA. Our data show that the changes in MD and FA precede fat infiltration. As fat infiltration is considered as an end-stage effect, the chances in restoring muscle function lie in the phase prior to fatty degeneration. A tool that is able to capture this transition zone, as we hereby demonstrate with MD/FA measures, may be very useful to monitor treatment effects in individual patients. Determining whether FA and MD are markers of alterations in muscle that precede fat infiltration should be a topic of future research. Follow-up data of patients will provide more insight in its potential in capturing disease. The use of qMRI measures in patients undergoing treatment would provide additional information its sensitivity monitoring early therapy effects.

Our study had several limitations. First, the variation in ages and disease severity is in itself an impeding factor for general statements. Furthermore, longitudinal data needs to confirm or counterfeit the cross-sectional results from this study. A bigger sample size would obviously benefit statistical power, yet the number of patients is acceptable for a rare disease. To allow the inclusion of young children we kept scan time minimal which compromises resolution and SNR, yet no data had to be excluded due to motion artifacts. Furthermore, the high-end of fat infiltration is pushing the limits of fat-suppression techniques and its reliability. However, each of the methods includes visual and quantitative quality-checks of the data; i.e. the b-0 map for DIXON, b-1 for T2 mapping, and SNR for DTI. Unfortunately, we were not able to find corresponding control subjects for matching to the very young patients. Albeit we developed a fully automated pipeline for processing the MRI data uniformly and reproducibly, manual segmentation was still needed, which is prone to error and time-consuming. Lastly, there was a notable difference between the fat fraction estimated by DIXON and by EPG which needs further investigation as a clear explanation for this is currently lacking.

In conclusion, we have provided qMRI measurements of skeletal muscle in a large cohort of SMA patients widely ranging in age and disease severity. This study depicts the natural disease course of muscle tissue. The MRI protocol we used has demonstrated high temporal stability and multicenter reproducibility and proved tolerable even by very young children. This study shows that DTI parameters complement existing MR protocols that have focused on T2 signal and fat fraction, and manifest good correlation with clinical

measures. We disclose abnormal DTI properties of skeletal muscle in SMA that have not been described before. DTI serves as a distinct parameter that can be monitored alongside and independent to the process of fat infiltration. This demonstrates the potential of quantitative MRI markers to study SMA pathogenesis and to monitor disease progression and treatment effects in muscle.

Acknowledgements

We thank all SMA patients, their families and control subjects for their participation and Christa van Ekris for her assistance.

Funding

This work was supported by the Prinses Beatrix Spierfonds (Grant no. W.OR16-06). The Dutch SMA register and SMA team are supported by stichting Spieren voor Spieren.

Competing Interest

WLP served as an ad hoc member of the scientific advisory board of Biogen, Avexis and as a member of the Branaplam data monitoring committee (Novartis). BB performed consultancy activities for Scholar Rock and Cytokinetics. WLP and BB report grants from Prinses Beatrix Spierfonds, grants from Stichting Spieren voor Spieren, grants from Vriendenloterij. Other co-authors report no competing interest.

Supplementary files – S1 Simulations DTI and T2 (EPG-T2) explained

DTI simulations

Simulations were performed similar to

1. Froeling M, Nederveen AJAJ, Nicolay K, Strijkers GJGJGJ: DTI of human skeletal muscle: The effects of diffusion encoding parameters, signal-to-noise ratio and T2 on tensor indices and fiber tracts. *NMR Biomed* 2013; 26:1339–1352.
2. Damon BM: Effects of image noise in muscle diffusion tensor (DT)-MRI assessed using numerical simulations. *Magn Reson Med* 2008; 60:934–944.

1. Acquisition parameters:

Same as real data (see Table 1 of manuscript)

2. Tissue parameters

The tissue parameters that were used in the simulations were:

	Muscle compartment	Fat compartment
Proton density	0.9	0.1
T1 relaxation [ms]	1200	300
T2 relaxation [ms]	30	20
Tensor eigen values [10 ⁻³ mm ² /s]	1.88; 1.46; 1.25	0.8; 0.8; 0.8
Derived MD and FA	1.53; 0.21	0.8; 0.0
Tensor eigen vector direction	Along z direction	Random

3. Simulation parameters

- SNR value: 30
- Fat range: 0 to 100% with steps of 5%

4. Simulation

Per compartment (either muscle or fat) the signal was generated as:

$$S_0 = \rho \left(1 - e^{-\frac{TR}{T1}} \right) e$$

$$S_{ib} = S_0 e^{-b \vec{g}_i^T D \vec{g}_i}$$

Here TR is the repetition time, TE the echo time, T1 the longitudinal relaxation time, T2 the transverse relaxation time, and ρ the proton density. The diffusion-weighted signal intensity S_{ib} is related to the non-weighted signal intensity S_0 via the diffusion tensor \mathbf{D} , the b-value b and the gradient directions $\vec{\mathbf{E}}_i$ (Eq. 2). The diffusion tensor \mathbf{D} was decomposed into its eigenvalues λ_i and eigenvectors $\vec{\mathbf{E}}_i$ using

$$\mathbf{D} = \mathbf{E} \cdot \mathbf{\Lambda} \cdot \mathbf{E}^T$$

$$\mathbf{E} = \begin{bmatrix} \vdots & \vdots & \vdots \\ \vec{\mathbf{E}}_1 & \vec{\mathbf{E}}_2 & \vec{\mathbf{E}}_3 \\ \vdots & \vdots & \vdots \end{bmatrix}$$

$$\mathbf{\Lambda} = \begin{bmatrix} \lambda_1 & 0 & 0 \\ 0 & \lambda_2 & 0 \\ 0 & 0 & \lambda_3 \end{bmatrix}$$

The combined signal from water and fat was defined as

$$S_{ib,total} = (1 - f) * S_{ib,muscle} + f * S_{ib,fat}$$

With the fat fraction f ranging from 0 to 1.

In total 10000 signal were generated for each fat fraction after which Rician noise was added. Data was fitted identical to the acquired MRI data as described in the manuscript.

EPG T2 simulations

The EPG signals were simulated according to

1. Marty B, Baudin PY, Reyngoudt H, et al.: Simultaneous muscle water T2 and fat fraction mapping using transverse relaxometry with stimulated echo compensation. NMR Biomed 2016; 29:431-443.

1. Acquisition parameters:

Same as real data (see Table 1 of manuscript)

2. Tissue parameters

The tissue parameters that were used in the simulations were:

	Muscle compartment	Fat compartment water	Fat compartment fat
Relative size	-	10%	90%
T1 relaxation [ms]	1200	1000	500
T2 relaxation [ms]	30	20	175

3. Simulation parameters

- SNR value: 50
- B1 value: 100%
- Fat range: 0 to 100% with steps of 5%

4. Simulation

The measured signal S with size N_{echo} can be approximated using a bi-component EPG model where the signal can be defined as

$$\mathbf{S} = w \mathbf{S}_{water} + f \mathbf{S}_{fat} = [\mathbf{S}_{water} \quad \mathbf{S}_{fat}] \begin{bmatrix} W \\ f \end{bmatrix}$$

With W and f the water and fat signal amplitudes which in the simulation were defined as $W = 1 - f$. The signal at each echo of the water and fat component are S_{water} and S_{fat} , respectively, and are defined as

$$\mathbf{S}_{water} = \sum_{m=1}^M EPG(T_{1,water}, T_{2,water}, B_1, \Delta TE, N_{echo}, \alpha_{ex}^m, \alpha_{ref}^m)$$

$$\mathbf{S}_{fat} = \sum_{m=1}^M (1 - g) EPG(T_{1,fat}, T_{2,fat}, B_1^i, \Delta TE, N_{echo}, \alpha_{ex}^m, \alpha_{ref}^m) + g EPG(T_{1,waterfat}, T_{2,waterfat}, B_1^i, \Delta TE, N_{echo}, \alpha_{ex}^m, \alpha_{ref}^m)$$

With α_{ex} and α_{ref} the flip angle profiles along the slice direction of the excitation and refocusing pulses, respectively, and m the number of samples along the slice profile and g is the water fraction in fat which was 10%.

In total 10000 signal were generated for each fat fraction after which Rician noise was added. Data was fitted identical to the real data as described in the manuscript.

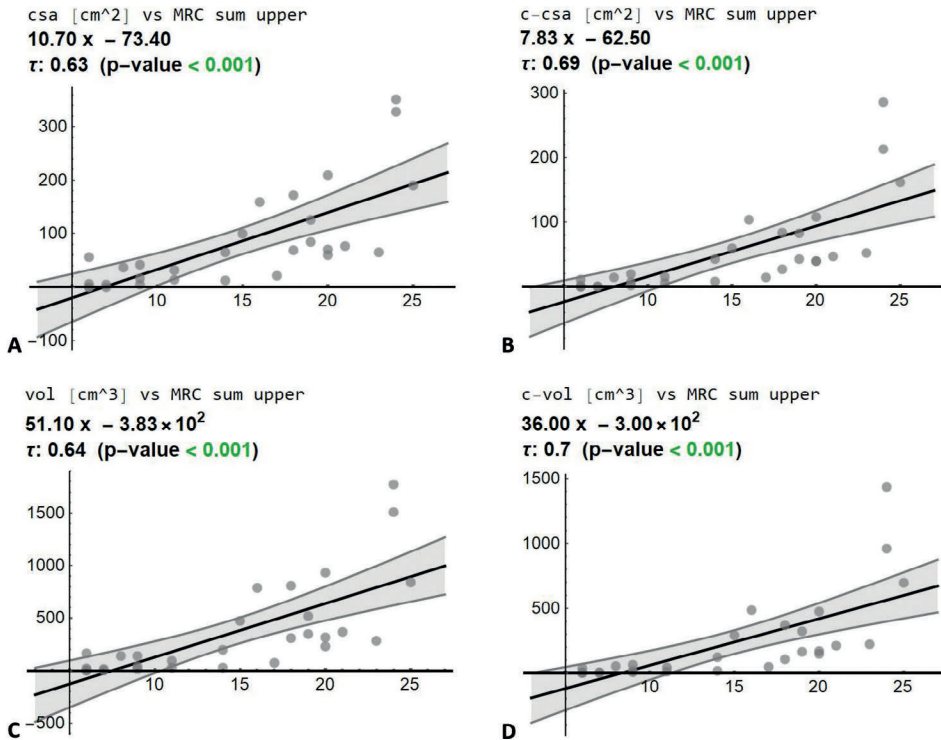
S2 – Cross-sectional area (CSA) and volumes of thigh muscle of SMA patients

Patients	CSA [cm ²]	Contractile-CSA (ccsa) [cm ²]	Volume (vol) [cm ³]	Contractile volume (cvol) [cm ³]
P1	0	0	0	0
P2	350,89	285,57	1774,46	1433,57
P3	77,13	46,62	370,49	209,02
P4	0	0	0	0
P5	55,89	11,63	165,77	36,962
P6	158,72	103,87	788,83	484,03
P7	99,68	59,38	470,44	290,388
P8	0	0	0	0
P9	41,58	19,49	136,22	62,87
P10	4,75	1,99	11,28	5,13
P11	31,43	15,14	93,74	41,89
P12	126,09	83,09	519,51	322,69
P13	11,79	7,99	28,63	18,43
P14	3,98	1,21	16,94	4,02
P15	327,40	213,02	1512,70	957,38
P16	171,65	83,95	810,16	367,15
P17	20,88	14,51	70,91	45,80
P18	69,86	40,12	318,52	170,54
P19	190,28	161,48	839,85	693,63
P20	6,39	1,88	20,03	5,98
P21	13,19	6,05	28,60	12,98
P22	59,69	39,38	233,78	145,88
P23	84,02	43,23	349,23	164,47
P24	65,14	52,54	281,55	220,01
P25	208,82	108,02	932,28	474,73
P26	15,64	6,66	41,05	17,37
P27	65,75	43,00	195,99	121,06
P28	36,65	14,80	137,20	53,83
P29	69,59	27,54	311,01	104,62

Correlation plots of (A) cross-sectional area (CSA); (B) contractile CSA (ccsa); (C) volume and (D) contractile volume (cvol) versus MRC sum score of upper legs.

2

The correlation formula, Kendall's tau correlation coefficient and the p-value (significance level set at <0.05) are shown per correlation plot.



REFERENCES

1. Lefebvre S, Bürglen L, Reboullet S, et al. Identification and characterization of a spinal muscular atrophy-determining gene. *Cell*. 1995;80:155–165. doi:10.1016/0092-8674(95)90460-3.
2. Wadman RI, Stam M, Gijzen M, et al. Association of motor milestones, SMN2 copy and outcome in spinal muscular atrophy types 0-4. *J Neurol Neurosurg Psychiatry*. 2017;88:364–367. doi:10.1136/jnnp-2016-314292.
3. Mercuri E, Darras BT, Chiriboga CA, et al. Nusinersen versus sham control in later-onset spinal muscular atrophy. *N Engl J Med*. 2018;378:625–635. doi:10.1056/NEJMoa1710504.
4. Groen EJN, Talbot K, Gillingwater TH. Advances in therapy for spinal muscular atrophy: Promises and challenges. *Nat Rev Neurol*. 2018;14:214–224. doi:10.1038/nrneuro.2018.4.
5. Shababi M, Lorson CL, Rudnik-Schöneborn SS. Spinal muscular atrophy: A motor neuron disorder or a multi-organ disease? *J Anat*. 2014;224:15–28. doi:10.1111/joa.12083.
6. Wijngaarde CA, Blank AC, Stam M, Wadman RI, Van Den Berg LH, Van Der Pol WL. Cardiac pathology in spinal muscular atrophy: a systematic review. *Orphanet J Rare Dis*. 2017;12(1) doi:10.1186/s13023-017-0613-5.
7. Mercuri E, Finkel R, Montes J, et al. Patterns of disease progression in type 2 and 3 SMA: Implications for clinical trials. *Neuromuscul Disord*. 2016;26(2):126–131. doi:10.1016/j.nmd.2015.10.006.
8. Swoboda KJ, Prior TW, Scott CB, et al. Natural history of denervation in SMA: Relation to age, SMN2 copy number, and function. *Ann Neurol*. 2005;57(5):704–712. doi:10.1002/ana.20473.
9. Strijkers GJ, Araujo ECA, Azzabou N, et al. Exploration of new contrasts, targets, and MR imaging and spectroscopy techniques for neuromuscular disease—A workshop report of working group 3 of the biomedicine and molecular biosciences COST action BM1304 MYO-MRI. *J Neuromuscul Dis*. 2019;6(1):1–30. doi:10.3233/JND-180333.
10. Leroy-Willig A, Willig TN, Henry-Feugeas MC, et al. Body composition determined with MR in patients with Duchenne muscular dystrophy, spinal muscular atrophy, and normal subjects. *Magn Reson Imaging*. 1997;15(7):737–744. doi:10.1016/S0730-725X(97)00046-5.
11. Chan WP, Liu GC. MR imaging of primary skeletal muscle diseases in children. *Am J Roentgenol*. 2002;179(4):989–997. doi:10.2214/ajr.179.4.1790989.
12. Ueno T, Yoshioka H, Iwasaki N, Tanaka R, Saida Y. MR findings of spinal muscular atrophy Type II: sibling cases. *Magn Reson Med Sci MRMS an Off J Japan Soc Magn Reson Med*. 2003;2(4):195–198. doi:10.2463/mrms.2.195.
13. Mercuri E, Pichiecchio A, Allsop J, Messina S, Pane M, Muntoni F. Muscle MRI in inherited neuromuscular disorders: Past, present, and future. *J Magn Reson Imaging*. 2007;25(2):433–440. doi:10.1002/jmri.20804.
14. Oh J, Kim SM, Shim DS, Sunwoo IN. Neurogenic muscle hypertrophy in Type III spinal muscular atrophy. *J Neurol Sci*. Elsevier B.V.; 2011;308(1–2):147–148. doi:10.1016/j.jns.2011.06.023.
15. Brogna C, Cristiano L, Verdolotti T, et al. MRI patterns of muscle involvement in type 2 and 3 spinal muscular atrophy patients. *J Neurol*. 2019;doi:10.1007/s00415-019-09646-w.
16. Sproule DM, Punyanitya M, Shen W, et al. Muscle volume estimation by magnetic resonance imaging in spinal muscular atrophy. *J Child Neurol*. 2011;26(3):309–317. doi:10.1177/0883073810380457.
17. Durmus H, Yilmaz R, Gulsen-Parman Y, et al. Muscle magnetic resonance imaging in spinal muscular atrophy type 3: Selective and progressive involvement. *Muscle and Nerve*. 2017;55(5):651–656. doi:10.1002/mus.25385.

18. Sproule DM, Montgomery MJ, Punyanitya M, et al. Thigh muscle volume measured by magnetic resonance imaging is stable over a 6-month interval in spinal muscular atrophy. *J Child Neurol*. 2011;26(10):1252–1259. doi:10.1177/0883073811405053.
19. Kollmer J, Hilgenfeld T, Ziegler A, et al. Quantitative MR neurography biomarkers in 5q-linked spinal muscular atrophy. *Neurology*. 2019;10.1212/WNL.0000000000007945. doi:10.1212/WNL.0000000000007945.
20. Quijano-Roy S, Avila-Smirnow D, Carlier RY, et al. Whole body muscle MRI protocol: Pattern recognition in early onset NM disorders. *Neuromuscul Disord*. 2012;22doi:10.1016/j.nmd.2012.08.003.
21. Willis TA, Hollingsworth KG, Coombs A, et al. Quantitative Muscle MRI as an Assessment Tool for Monitoring Disease Progression in LGMD2f: A Multicentre Longitudinal Study. *PLoS One*. 2013;8(8) doi:10.1371/journal.pone.0070993.
22. Hooijmans MT, Damon BM, Froeling M, et al. Evaluation of skeletal muscle DTI in patients with duchenne muscular dystrophy. *NMR Biomed*. 2015;28:1589–1597. doi:10.1002/nbm.3427.
23. Bonati U, Holiga Š, Hellbach N, et al. Longitudinal characterization of biomarkers for spinal muscular atrophy. *Ann Clin Transl Neurol*. 2017;4(5):292–304. doi:10.1002/acn3.406.
24. Chabanon A, Seferian AM, Daron A, et al. Prospective and longitudinal natural history study of patients with Type 2 and 3 spinal muscular atrophy: Baseline data NatHis-SMA study. *PLoS One*. 2018;13(7):1–28. doi:10.1371/journal.pone.0201004.
25. Williams SE, Heemskerk AM, Welch EB, Li K, Damon BM, Park JH. Quantitative effects of inclusion of fat on muscle diffusion tensor MRI measurements. *J Magn Reson Imaging*. 2013;38(5):1292–1297. doi:10.1002/jmri.24045.
26. Schlaeger, S, Weidlich, D, Klupp, E et al. Decreased water T2 in fatty infiltrated skeletal muscles of patients with neuromuscular diseases. *NMR Biomed*. 2019;32:e4111. doi:10.1002/nbm.4111.
27. Medical Research Council. Aids to the Examination of the Peripheral Nervous System (Memorandum No. 45). London Her Majesty's Station Off. 1981;
28. Oudeman J, Nederveen AJ, Strijkers GJ, Maas M, Luijten PR, Froeling M. Techniques and applications of skeletal muscle diffusion tensor imaging: A review. *J Magn. Reson. Imaging*. 2016. doi:10.1002/jmri.25016.
29. Froeling M. QMRTools: a Mathematica toolbox for quantitative MRI analysis. *J Open Source Softw*. 2019;doi:10.21105/joss.01204.
30. Reeder SB, Pineda AR, Wen Z, et al. Iterative decomposition of water and fat with echo asymmetry and least-squares estimation (IDEAL): Application with fast spin-echo imaging. *Magn Reson Med*. 2005;54:636–644. doi:10.1002/mrm.20624.
31. Marty B, Baudin P-Y, Reyngoudt H, et al. Simultaneous muscle water T2 and fat fraction mapping using transverse relaxometry with stimulated echo compensation. *NMR Biomed*. 2016;29:431–443. doi:10.1002/nbm.3459.
32. Tax CMW, Otte WM, Viergever MA, Dijkhuizen RM, Leemans A. REKINDLE: Robust Extraction of Kurtosis INDices with Linear Estimation. *Magn Reson Med*. 2015;73:794–808. doi:10.1002/mrm.25165.
33. De Luca A, Bertoldo A, Froeling M. Effects of perfusion on DTI and DKI estimates in the skeletal muscle. *Magn Reson Med*. 2017;78:233–246. doi:10.1002/mrm.26373.
34. Veraart J, Novikov DS, Christiaens D, Ades-aron B, Sijbers J, Fieremans E. Denoising of diffusion MRI using random matrix theory. *Neuroimage*. 2016;142:394–406. doi:10.1016/j.neuroimage.2016.08.016.

35. Schlaffke L, Rehmann R, Rohm M, et al. Multicenter evaluation of stability and reproducibility of quantitative MRI measures in healthy calf muscles. *NMR Biomed.* 2019;1-14. doi:10.1002/nbm.4119.
36. Thomas LW. THE CHEMICAL COMPOSITION OF ADIPOSE TISSUE OF MAN AND MICE. *Q J Exp Physiol Cogn Med Sci.* 1962;doi:10.1113/expphysiol.1962.sp001589.
37. Querleux B, Cornillon C, Jolivet O, Bittoun J. Anatomy and physiology of subcutaneous adipose tissue by in vivo magnetic resonance imaging and spectroscopy: Relationships with sex and presence of cellulite. *Ski Res Technol.* 2002;doi:10.1034/j.1600-0846.2002.00331.x.
38. Keene, K.R., Beenakker J.W.M., Hooijmans M.T., Naarding K.J., Niks E.H., Otto L.A.M., van der Pol W.L., Tannemaat M.R., Kan H.E. FM. T2 mapping in healthy and diseased muscle using optimized extended phase graph algorithms in four clinical cohorts. 2019;conference.
39. Froeling M., Hughes E., Schlaffke L., Kan H.E. HKG. The relation between fat calibration in multi-echo spin-echo water T2 mapping and STEAM fat T2 relaxation measurements. 27th Annu Meet ISMRM. Montreal, Canada.; 2019. p. 1273.
40. Yushkevich PA, Piven J, Hazlett HC, et al. User-guided 3D active contour segmentation of anatomical structures: Significantly improved efficiency and reliability. *Neuroimage.* 2006;31:1116-1128. doi:10.1016/j.neuroimage.2006.01.015.
41. Klein S, Staring M, Murphy K, Viergever MA, Pluim JPW. Elastix: A toolbox for intensity-based medical image registration. *IEEE Trans Med Imaging.* 2010;29:196-205. doi:10.1109/TMI.2009.2035616.
42. Inoue M, Ishiyama A, Komaki H, et al. Type-specific selectivity pattern of skeletal muscle images in spinal muscular atrophy. *Neuromuscul Disord.* 2015;25:S194. doi:10.1016/j.nmd.2015.06.042.
43. Groen EJN, Perenthaler E, Courtney NL, et al. Temporal and tissue-specific variability of SMN protein levels in mouse models of spinal muscular atrophy. *Hum Mol Genet.* 2018;27:2851-2862. doi:10.1093/hmg/ddy195.
44. Lamminen AE. Magnetic resonance imaging of primary skeletal muscle diseases: Patterns of distribution and severity of involvement. *Br J Radiol.* 1990;6:483-486. doi:10.1038/ncb0604-483.
45. Carlier PG. Global T2 versus water T2 in NMR imaging of fatty infiltrated muscles: Different methodology, different information and different implications. *Neuromuscul Disord.* 2014;24:390-392. doi:10.1016/j.nmd.2014.02.009.
46. Azzabou N, De Sousa PL, Caldas E, Carlier PG. Validation of a generic approach to muscle water T2 determination at 3T in fat-infiltrated skeletal muscle. *J Magn Reson Imaging.* 2015;41:645-653. doi:10.1002/jmri.24613.
47. Schlaeger S, Weidlich D, Klupp E, et al. Decreased water T2 in fatty infiltrated skeletal muscles of patients with neuromuscular diseases. *NMR Biomed.* John Wiley and Sons Ltd; 2019;32(8) doi:10.1002/nbm.4111.
48. Ponrartana S, Ramos-Platt L, Wren TAL, et al. Effectiveness of diffusion tensor imaging in assessing disease severity in Duchenne muscular dystrophy: preliminary study. *Pediatr Radiol.* 2015;45(4):582-589. doi:10.1007/s00247-014-3187-6.
49. Arrigoni F, De Luca A, Velardo D, et al. Multiparametric quantitative MRI assessment of thigh muscles in limb-girdle muscular dystrophy 2A and 2B. *Muscle and Nerve.* 2018;58:550-558. doi:10.1002/mus.26189.
50. Dubowitz V, Sewry C. *Muscle Biopsy.* 3rd ed. Saunders Elsevier; 2007.



CHAPTER III

Quantification of disease progression in spinal muscular atrophy with muscle MRI — a pilot study

Louise A.M. Otto¹, Martijn Froeling², Ruben P.A. van Eijk^{1,3}, Fay-Lynn Asselman¹
Renske I. Wadman¹, Inge Cuppen⁴, Jeroen Hendrikse², W-Ludo van der Pol¹

¹Department of Neurology, UMC Utrecht Brain Center, University Medical Center
Utrecht, Utrecht University, the Netherlands

²Department of Radiology, University Medical Center Utrecht, Utrecht University, the
Netherlands

³Biostatistics & Research Support, Julius Center for Health Sciences and Primary Care,
University Medical Center Utrecht, Utrecht University, Utrecht, The Netherlands

⁴Department of Neurology and Child Neurology, UMC Utrecht Brain Center,
University Medical Center Utrecht, Utrecht University, the Netherlands

ABSTRACT

Objectives

Quantitative MRI of muscles is a promising tool to measure disease progression or to assess therapeutic effects in neuromuscular diseases. Longitudinal imaging studies are needed to show sensitivity of qMRI in detecting disease progression in spinal muscular atrophy. In this pilot study we therefore studied one-year changes in quantitative MR parameters in relation to clinical scores.

Methods

We repeated quantitative 3T MR analysis of thigh muscles and clinical testing one year after baseline in 10 treatment-naïve patients with spinal muscular atrophy, 5 with type 2 (21.6 ± 7.0 years) and 5 with type 3 (33.4 ± 11.9 years). MR protocol consisted of DIXON, T2 mapping and diffusion tensor imaging. Temporal relation of parameters was examined with a mixed model.

Results

We detected a significant increase in fat fraction (baseline: 38.2% SE 0.6, follow-up: 39.5% SE 0.6; +1.3%, $p=0.001$) in all muscles. Muscles with moderate to high fat infiltration at baseline show a larger increase over time (+1.6%, $p<0.001$). We did not find any changes in DTI parameters except for low fat infiltrated muscles (m. adductor longus and m. biceps femoris (short head)). T2 of muscles went from 28.2 ms to 28.0 ms ($p=0.07$). Muscle strength and motor function scores were not significantly different between follow-up and baseline.

Conclusion

Longitudinal imaging data show slow disease progression in skeletal muscle of the thigh of (young)-adult patients with spinal muscular atrophy despite stable strength and motor function scores. Quantitative muscle imaging demonstrates potential as a biomarker for disease activity and monitoring of therapy response.

Key words Muscular Atrophy, Spinal; Magnetic Resonance Imaging; Muscle, Skeletal

ABBREVIATIONS

DTI diffusion tensor imaging; FA fractional anisotropy; HFMSE Hammersmith Functional Motor Scale, Expanded; MD mean diffusivity; SMA Spinal Muscular Atrophy; SNR Signal to Noise Ratio; qMRI quantitative MRI

INTRODUCTION

Hereditary proximal spinal muscular atrophy (SMA) is the leading genetic cause of death in infancy and severe impairment in childhood and later life. It is caused by the loss of function of the survival motor neuron (*SMN*) 1 gene and characterized by abnormalities and dysfunction of motor neurons, neuromuscular junction and muscle tissue.(1–5)

The first genetic therapies for SMA were introduced in the past five years with prospects for additional therapies in the near future. Clinical trials have shown that genetic therapies improved infantile survival and motor function in both babies and young children.(6,7) Assessment of treatment efficacy in older children and adults is complicated by the relatively slow progression of the decline of muscle strength and motor function in patients with SMA.(8–12) Sensitive biomarkers to detect decline caused by disease progression and early response to treatment is necessary to evaluate treatment effects at a relatively early stage of treatment to minimize risk and burden to patients and to optimize cost-efficiency.

Quantitative magnetic resonance imaging (qMRI) of muscles is a promising tool to measure disease progression or to assess therapeutic effects in neuromuscular diseases, including SMA.(13–22) We recently reported several unique qMRI characteristics in a cross-sectional study on patients with SMA types 2 and 3. First, quantification of fat infiltration in patients with SMA differentiates between vulnerable and resilient thigh muscles. Second, the bias of fat infiltration resulted in a slight decreased T2. Finally, diffusion tensor imaging (DTI) showed decreased mean diffusivity (MD) in combination with increased fractional anisotropy (FA), which may reflect muscle atrophy.(23) Longitudinal imaging studies are needed to show sensitivity in detecting disease progression. Especially with experimental methods such as quantitative MRI there is a need for reference data, preferably of treatment-naïve patients. As treatment is becoming available for patients, there is subsequent fewer opportunity to obtain data on natural history of disease progression. We repeated qMRI analysis of thigh muscles in treatment-naïve patients with spinal muscular atrophy one year after baseline. We here report on the novel methodology required for analysis of longitudinal imaging data and present the course of qMRI and clinical measures over time. Our data show that qMRI can serve as a biomarker for disease progression.

METHODS

Study population

We invited 31 patients who participated in our prospective baseline study for a follow-up MRI after one year. Exclusion criteria were: any type of invasive ventilation, a postural change of >15% in Forced Vital Capacity (FVC) between sitting and supine position, orthopnea, pronounced swallowing problems, pregnancy, non-MR compatible material in the body or any contra-indication for 3T MR. Additional exclusion criteria for participation were: severe fatty infiltration of muscle tissue after visual evaluation at baseline, the use of any of the available SMA therapies or participation in a clinical trial (fig 1). Ten patients were eligible (3 males and 7 females). Five patients had SMA type 2 (mean age 21.6 ± 7.0 years) and 5 SMA type 3 (mean age 33.4 ± 11.9 years, see table 1). The study was approved by the local ethics committee (no. 17-226/NL61066.041.17) and was conducted in accordance to the declaration of Helsinki.

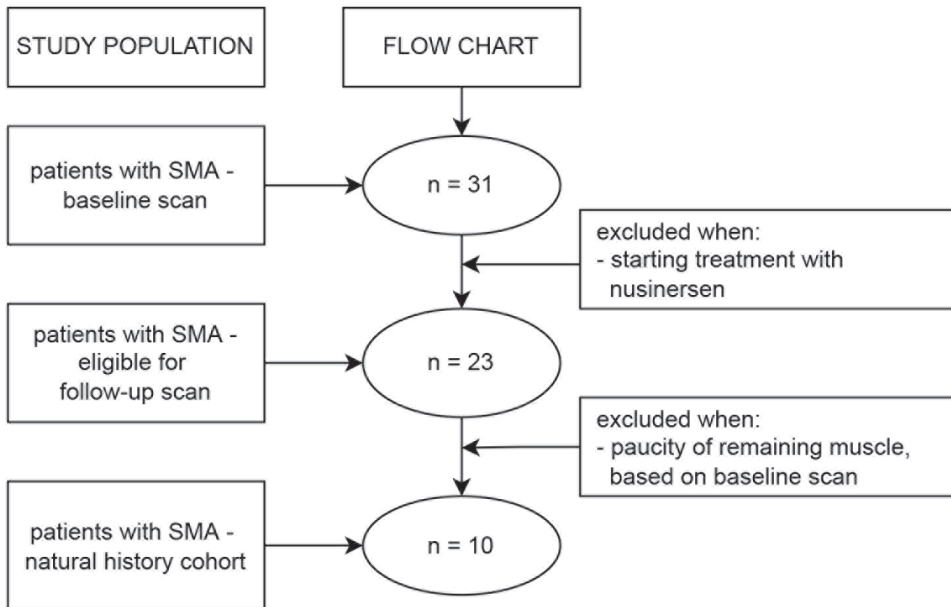


FIGURE 1 Flowchart of study inclusion and follow-up procedure

Table 1 Clinical characteristics

Clinical characteristics	SMA type 2	SMA type 3
N	5	5
Age in years; mean [range]	21.6 [15.7-34.9]	33.4 [18.8-52.8]
Sex (M:F)	0:5	3:2
SMN2 copy number		
3	4	0
4	1	4
5	0	1
Disease duration in months; mean (SD)	250 (82)	234 (120)
Ambulatory status n (%)	0 (0)	5 (100)

Legend Table 1: F= female; M = male; N = number; SD = standard deviation; SMN2 = survival motor neuron 2 gene. Clinical characteristics are reported for patients with SMA type 2 and with type 3.

Clinical evaluation

We assessed motor function with the expanded Hammersmith Functional Motor Scale Expanded (HFMSSE) (range 0-66; a lower score indicates poorer motor ability and function). (24,25) Muscle strength was documented with the Medical Research Council (MRC) scoring system (Medical Research Council, 1976). Additionally, we performed hand-held dynamometry (HHD) of the adductors, quadriceps and hamstring muscles at both sides with a hand-held device (MicroFET2; Hoggan Health Industries Inc., USA). All clinical measurements were performed at baseline and follow-up by the same trained evaluator (LAMO, two years of experience). The clinical evaluation followed directly after MR examination.

MR acquisition

All MR examinations were performed on the same 3 Tesla MR scanner (Philips Ingenia, Philips Medical Systems, the Netherlands) and according to the same protocol as performed at baseline with supine position and feet first, using a 12-channel posterior and 16 channel anterior body coil. Field of view was set according to the position of the image stack of the first scan, which was positioned approximately 175 mm below the femoral head.

The MR protocol comprised of a 4-point DIXON sequence (TR/TE/ 210/2.6/3.36/4.12/4.88 ms; flip angle 10°; voxel size 6x1.5x1.5 mm³; no gap; 25 slices); T2 mapping (17 echoes TR/TE/ΔTE 4598/17/7.6 ms; flip angle 90/180°; voxel size 6x3x3 mm³; slice gap 6mm; 13

slices, no fat suppression) and DTI SE-EPI (TR/TE 5000/57 ms; b-values: 0 (1), 1 (6), 10 (3), 25 (3), 100 (3), 200 (6), 400 (8) and 600 (12) s/mm²; voxel size 6x3x3 mm³; no gap; 25 slices, SPAIR and SPIR fat suppression (fig 2). Total scan time was ~10 minutes. The MR protocol has been validated in a previous multicenter study for reproducibility and high temporal stability.(26) See table 2 for the acquisition parameters.

Table 2 Acquisition parameters of MR protocol. Specifications per sequence at a field strength of 3T

Sequence	4-point DIXON	T2 mapping	DWI
Sequence	Multi acquisition gradient echo	multi echo spin echo	spin echo-EPI
Repetition time (ms)	210	4598	5000
Echo time (ms)	2.6/3.36/4.12/4.88	17x 7.6	57
Flip angle (degrees)	10	90/180	90/180
Acquisition Matrix	320x320		160x92
FOV	480x480		480x276
Resolution (mm ²)	1.5x1.5	3x3	3x3
Slices	25	13	25
Slice thickness (mm)	6	6	6
Slice gap (mm)	0	6	0
b-values (nr of images) (mm/s ²)		0	0 (1), 1 (6), 10 (3), 25 (3), 100 (3), 200 (6), 400 (8), 600 (12)
Fat suppression			Gradient inversion + SPAIR (main fat signal) + SPIR (olefinic fat signal)
SENSE / Partial Fourier	2 / 1	2 / 1	1.9 / 0.75
Acquisition time (min:s)	1:20	3:05	3:30

MR processing

We processed MR data using the custom toolbox QMRITools for **Mathematica** (mfroeling.github.io/QMRITools). All data were checked visually for data quality and motion artifacts (MF and LAMO, 12 years and 2 years experience, respectively). The processing steps have been described previously.(23,26) In short, DIXON data was reconstructed using an IDEAL method with the estimation of B₀ and T₂^{*}, T₂-mapping was processed with extended phase graph (EPG) fitting(27), and DTI with a fitting method (iWLLS with

REKINDLE outlier detection), denoised with principal component analysis (PCA) method and corrected for eddy current distortion and subject motion, Signal to Noise Ratio (SNR) of the DTI data was obtained using the PCA denoising algorithm (fig 2).(28)

Manual segmentation of all datasets was done by one researcher (LAMO, two years of experience). All muscles were segmented for all slices of the imaging stack. However not all muscles could be segmented when they were not clearly present anymore.

3

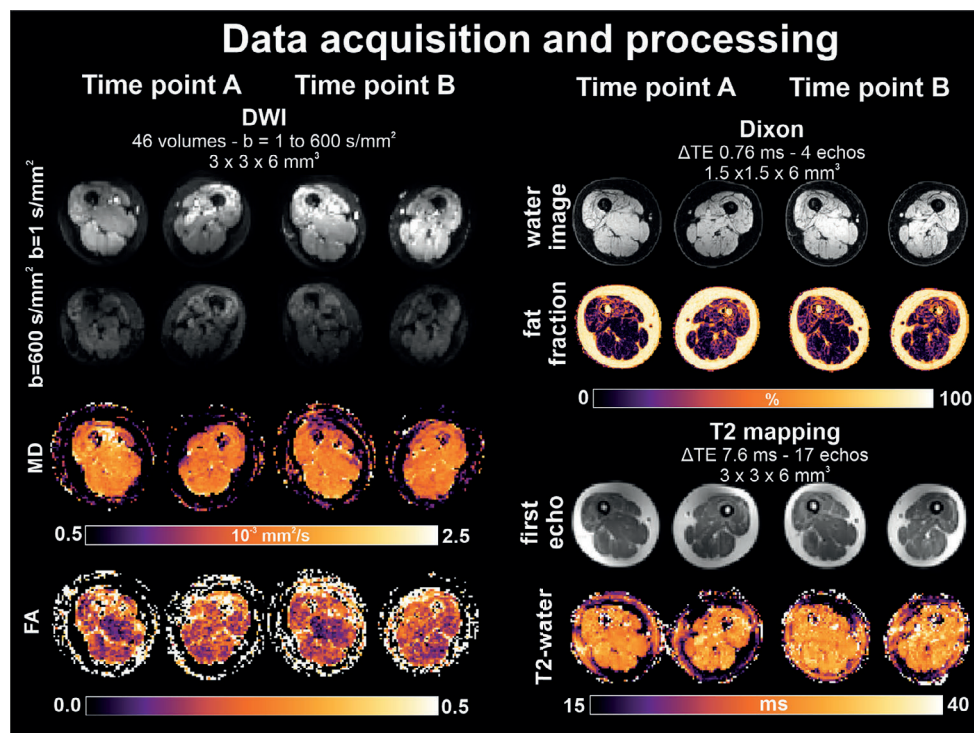


FIGURE 2 Data acquisition and processing of qMRI parameters Legend: diffusion weighted imaging; FA= fractional anisotropy; mm= millimeter; ms = millisecond; MD = mean diffusivity; TE = echo time; s= second. One subject is highlighted to visually present the dataset at time-point A and time-point B (alongside); for each of the parameters the raw data is projected above the processed data. The specifications of the 3 sequences are given

Comparison of imaging stacks

We aligned imaging stacks from baseline (scan A) and follow-up scans (scan B) using multiple converting steps to ensure a match of the muscle segmentations at both time-points. Although care was taken to position and plan scan A and B similarly, they are not identical (fig 3). To select the corresponding anatomy between scans, non-corresponding regions of the muscle segmentations were removed. This was done by registration of the DIXON water image of scan A to scan B using a combined rigid, affine and b-spline registration. With the known transformation of scan A to scan B the manual segmentation was transformed from the image space of scan A to the image space of scan B. Next the union of both the transformed segmentations of scan A and the native segmentation of scan B was taken (fig 3 B). This step ensured the match of voxels, as the shape and position of the leg may vary between scans (fig 3 C). Also, the inverse of the transformation was applied to the segmentations of scan B to move those to the image space of scan A and the union of the native segmentations of scan A and transformed segmentations of scan B was taken. This consecutively led to a match between the two segmentations in the image space of scan A and scan B, to directly compare segmented muscles at the two time-points at exactly the same level and location. Since all data was analyzed in the native space of that dataset, not all muscles contained sufficient voxels for analysis after registration. Therefore, the number of segmented muscles N reported could vary per analysis.

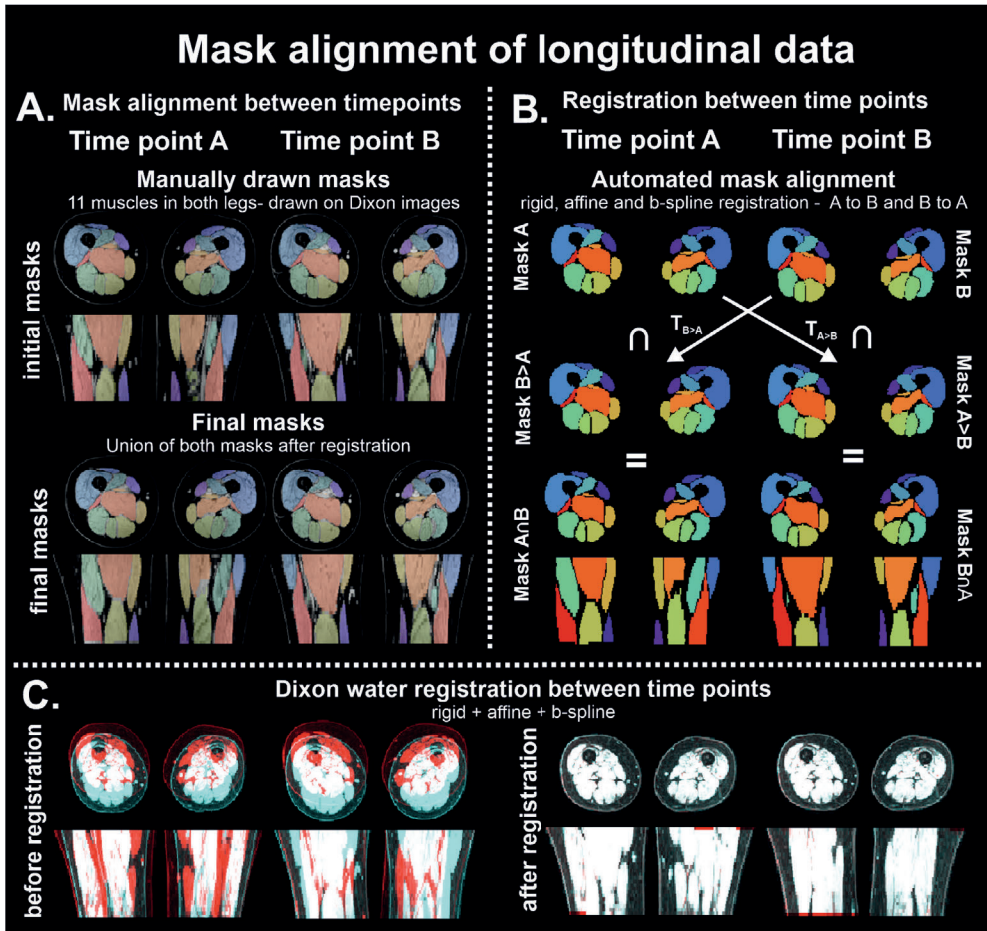


FIGURE 3 Illustration of pipeline and steps of mask alignment of longitudinal data. The methodology of alignment of imaging stacks is illustrated by the steps involving conversion of masks; initial and final masks in panel A and automated steps in mask alignment in panel B. In panel C, the images of time-point A and time-point B are rendered red and blue, to illustrate the incongruency between datasets before (left) and after (right) rigid, affine and b-spline registration. The non-corresponding regions can be identified as they maintain their respective color.

Statistical analysis

Clinical scores and the fat fraction of muscle groups were compared between baseline and follow-up using a paired t-test. In case of missing data, pairwise deletion followed. The change over time in qMRI outcomes was examined using a linear mixed effects model with two random intercepts for *subjects* and *muscle groups* according to an unstructured covariance matrix. Follow-up time as factor and baseline score were incorporated as

fixed effects, with the addition of SNR for DTI parameters. We used the Wald statistic to determine whether a significant change over time occurred. A similar model was created for myometry of the three muscle groups. Threshold of significance was set a $p < 0.05$. Statistical analysis was performed using SPSS version 25 for Windows (SPSS Inc. Chicago). The data that support the findings of this study are available from the corresponding author upon reasonable request.

RESULTS

We included 10 treatment-naïve patients, i.e. none started with nusinersen or other SMA specific treatments during follow-up. Patient characteristics are presented in Table 1. Mean follow-up duration was 13.1 months, of which time between scans was at minimum 368 days and at maximum of 442 days. The full MR protocol could be executed at baseline and follow-up in all 10 selected patients, resulting in a complete dataset of 20 MR scans in total. All but one patient completed the repeated clinical measurements. Muscle ache after the study visit was the only reported adverse event in one patient and resolved spontaneously.

MR processing

After visual inspection of the data no datasets were excluded because of data quality or motion artifacts. SNR of the DTI data did not differ significantly between datasets (mean SNR 17.3 ± 6.8 at first scans, 17.7 ± 8.2 at second scans, mean difference -0.0 ± 4.7 , $p = 0.25$).

Quantitative MR markers over time

Results from the linear mixed model of each of the qMRI parameters at time-point A and B are given in table 3, visually presented for type 2 and type 3 (fig 4) and are plotted against fat fraction (fig 5).

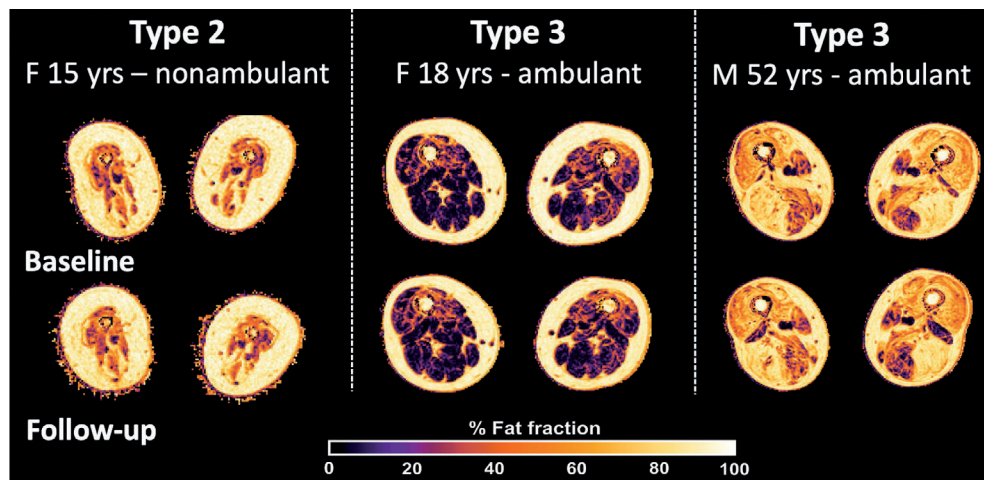


FIGURE 4 Visual overview of fat infiltration at baseline and at follow-up for type 2 and type 3. The color bar at the bottom indicates the gradient of fat fraction, ranging from lesser fat fraction in dark tones fading to lighter colors indicating higher fat fraction.

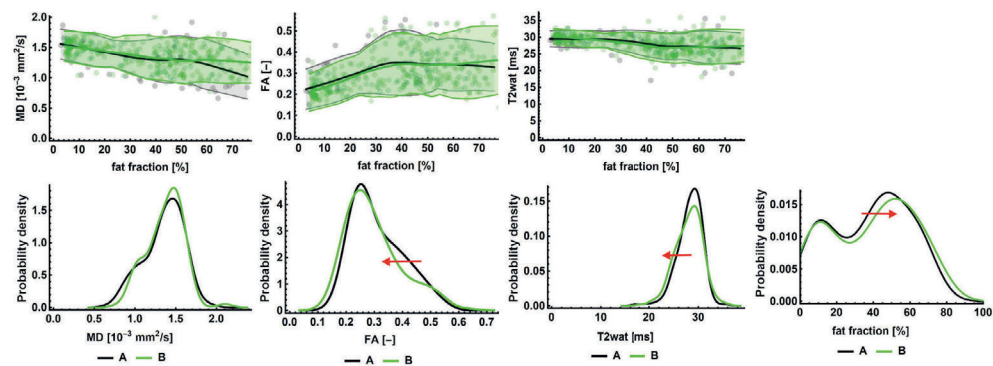


FIGURE 5 Histogram and plots of qMRI parameters at both time-points. In the upper row, MD, FA and T₂ are plotted against fat fraction, with each of the individual datapoints as dots, reduced to an average line using local regression with 95%-CI (shaded area). The bottom row represents the histograms of each of the qMRI parameters, the red arrow indicates significant changes and its direction. Timepoint A is indicated in grey, and time-point B in green.

Mean fat fraction was 38.2% (SE 0.6) at baseline, and measured 39.5% (SE 0.6) at follow-up. Combined analysis showed an increase in fat fraction of all muscles over time (slope +1.3 %/time; 95%-CI 0.51 – 2.05) but only hamstrings showed a significant increase in fat fraction when analyzing muscle groups individually (from 37.1% to 38.7% (p=0.04); adductors increased from 33.1 to 34.1% (+1.0%, p=0.47) and quadriceps muscles from 44.0 to 44.5% (+0.5%, p=0.40).

The histogram (fig 5) of fat fraction showed bimodal distribution reflecting muscles with relatively high and low fat infiltration. The m. adductor longus and the short head of m. biceps femoris are consistently less fat infiltrated than other muscles, with a fat fraction of $\leq 30\%$ (see Table 4). When we excluded these two muscles from the mixed model analysis, the slope of fat fraction over time increased to $+1.6\%$ (95%-CI 0.8 – 2.4, $p<0.001$). Change of fat fraction of the adductor longus and biceps femoris over time was -0.5% (95% CI -2.5 – 1.5, $p=0.63$).

Removal of other muscles from the generalized linear model did not change the outcome. Subsequently, results from other qMRI parameters were analyzed with and without the incorporation of these two muscles.

Albeit the histograms from time-point A and B mostly overlapped, there were significant changes in T2 and fractional anisotropy (FA) over time (fig 5). T2 decreased from 28.2 ms (SE 0.2) to 28.0 ms (SE 0.2, $p=0.07$), and further decreased after the exclusion of the m. adductor longus and m. biceps femoris (short head) (difference -0.4 ms, $p=0.02$). FA decreased from 0.32 (SE 0.01) to 0.31 (SE 0.01, $p<0.01$) when all muscles are analyzed simultaneously. However, when analyzed individually only FA of the adductor longus and biceps femoris (short head) showed a significant decrease of 0.03 ($p<0.01$). MD was not significantly different between time-points, with or without the exclusion of the two aforementioned muscles. The outcome of these analyses did not change after correction for SNR which is expected since there was no significant difference in SNR between timepoints.

Table 4 Fat fraction, CSA and c-CSA of muscles at time point A and B

Muscle	Fat fraction (%)	CSA (cm ²)	c-CSA (cm ²)	n - A	Fat fraction (%)	CSA (cm ²)	c-CSA (cm ²)	n - B
	- A <i>Mean, SD</i>	- A <i>total</i>	- A <i>total</i>		- B <i>Mean, SD</i>	- B <i>total</i>	- B <i>total</i>	
Adductor longus	24.49 ± 14.39	75.87	53.33	17	24.87 ± 14.88	69.84	47.38	17
Adductor magnus	40.20 ± 19.34	203.15	145.42	17	42.97 ± 28.92	189.43	132.98	17
Biceps femoris (long)	39.05 ± 19.34	113.99	78.94	18	40.23 ± 20.77	111.53	76.27	18
Biceps femoris (short)	30.73 ± 25.47	78.01	59.29	16	28.19 ± 25.64	78.71	59.71	15
Gracilis	32.33 ± 20.05	63.72	44.20	19	33.89 ± 22.59	55.62	38.44	18
Rectus femoris	38.01 ± 20.37	58.84	40.32	17	37.65 ± 19.87	58.03	39.84	17
Sartorius	41.46 ± 18.77	45.61	27.68	16	41.92 ± 18.61	44.87	26.73	16
Semimembranosus	41.09 ± 19.17	118.58	76.87	20	42.69 ± 20.98	110.72	71.01	20
Semitendinosus	38.22 ± 17.42	79.72	49.22	20	41.25 ± 20.44	77.54	47.32	20
Vastus intermedius	37.51 ± 24.84	71.75	56.41	6	35.16 ± 23.74	65.72	51.97	6
Vastus lateralis	47.94 ± 23.09	225.27	127.24	16	49.31 ± 24.32	212.81	119.41	16
Vastus medialis	47.82 ± 21.42	109.58	66.93	20	49.20 ± 22.31	107.48	63.29	20
TOTAL \ - all muscles	38.38 ± 21.34	1244.07	825.86	202	39.42 ± 22.60	1182.29	774.34	200

Legend table 4: c-CSA = contractile cross-sectional area, cm= centimeter, CSA = cross-sectional area, n = number of measurements per time-point A/B, SD = standard deviation. Mean values are descriptive, cross-sectional means.

Table 3 Quantitative MRI parameters over time

qMRI parameter	N muscle	Time-point A Mean (SE)	Time-point B Mean (SE)	Difference (SE)	95%-CI	p-value
ALL MUSCLES						
Fat fraction (%)	402	38.22 (0.64)	39.50 (0.64)	1.28 (0.39)	0.51 – 2.05	0.001
CSA (cm ²)	401	6.21 (0.12)	5.95 (0.12)	-0.25	-0.61 – 0.10	0.15
c-CSA (cm ²)	401	4.12 (0.06)	3.90 (0.06)	-0.23	-0.41 – -0.05	0.016
T ₂ (ms)	386	28.21 (0.16)	27.97 (0.16)	-0.24 (0.14)	-0.51 – 0.02	0.074
MD (10-3 mm ² /s)	360	1.35 (0.01)	1.37 (0.01)	0.02 (0.01)	-0.01 – 0.04	0.121
FA	360	0.32 (0.01)	0.31 (0.01)	-0.01 (0.00)	-0.02 – 0.00	0.007
Analysis of muscles, without m. adductor longus and m. biceps femoris (short head)						
Fat fraction (%)	337	40.37 (0.73)	41.96 (0.73)	1.59 (0.42)	0.76 – 2.4	<0.001
CSA (cm ²)	336	6.49 (0.13)	6.20 (0.13)	-0.28 (0.18)	-0.67 – 0.10	0.143
c-CSA (cm ²)	336	4.24 (0.07)	4.00 (0.07)	-0.25 (0.09)	-0.44 – -0.05	0.017
T ₂ (ms)	325	28.02 (0.17)	27.66 (0.17)	-0.36 (0.15)	-0.65 – 0.06	0.018
MD (10-3 mm ² /s)	302	1.34 (0.01)	1.36 (0.02)	0.02 (0.01)	-0.01 – 0.05	0.114
FA	302	0.31 (0.01)	0.31 (0.01)	-0.01 (0.00)	-0.02 – 0.00	0.106
Analysis of muscles, m. adductor longus and m. biceps femoris (short head) only						
Fat fraction (%)	65	27.03 (0.86)	26.54 (0.89)	0.49 (1.02)	-2.55 – 1.56	0.631
CSA (cm ²)	65	4.76 (0.12)	4.65 (0.12)	-0.11 (0.12)	-0.36 – 0.14	0.355
c-CSA (cm ²)	65	3.49 (0.10)	3.36 (0.10)	-0.13 (0.08)	-0.29 – 0.03	0.110
T ₂ (ms)	61	29.23 (0.30)	29.61 (0.30)	0.38 (0.30)	-0.22 – 0.99	0.211
MD (10-3 mm ² /s)	58	1.43 (0.02)	1.44 (0.02)	-0.00 (0.02)	-0.04 – 0.05	0.856
FA	58	0.33 (0.01)	0.29 (0.01)	-0.03 (0.01)	-0.06 – -0.01	0.003

Legend table 3. qMRI= quantitative MRI; c-CSA; contractile cross-sectional area; CI = confidence interval; CSA: cross-sectional area;FA = fractional anisotropy; N= number; MD = mean diffusivity; ms =millisecond ; mm= millimeter; s= second.

Results from the linear mixed model after correction for baseline. All data are represented by mean with standard errors, unless otherwise stated. The number of muscles that could be segmented is reported per qMRI parameter in the second column.

Clinical assessments at baseline and follow-up

Clinical assessments are summarized in table 5. Hamstrings generated the highest mean muscle force, followed by the adductors and lastly the quadriceps, as measured by HHD.

HFMSE, MRC scores and HHD were not significantly different between baseline and follow-up.

Table 5 Clinical measurements at baseline and follow-up

Clinical measurements	Baseline	Follow-up	Statistics
HFMSE score			
mean (SD) [score range 0-66]	27.9 (27.7)	25.1 (27.6) *	p= 0.364
MRC sum score			
mean (SD) [score range 44-210]	142.7 (41.6)	141.6 (41.8) *	p= 0.257
MRC sum score thigh			
mean (SD) [score range 6-30]	16.3 (5.7)	16.5 (5.7)	p= 0.169
HHD of muscle group (N)			
mean [95%-CI]			
<i>Adductors</i>	39.4 [8.0-70.9]	45.6 [14.2-77.1]	p= 0.221
<i>Hamstrings</i>	47.1 [5.0-89.1]	59.1 [17.1-101.1]	p= 0.058
<i>Quadriceps</i>	16.0 [-7.9-39.8]	20.2 [-3.6-44.1]	p= 0.226

Legend Table 5,* n=9; CI = confidence interval; HHD = hand-held dynamometry; HFMSE = Hammersmith Functional Motor Scale Expanded; MRC = Medical Research Council; N = Newton; SD = standard deviation

Clinical characteristics are reported for patients with SMA type 2 and with type 3. Clinical measurements are reported as means with standard deviation, or the 95%-CI in case we used a mixed model. P-values of paired t-testing and of the mixed model of clinical measurements are reported.

DISCUSSION

We here show that qMRI parameters obtained from thigh muscles of patients with SMA type 2 and 3 change significantly in the course of one year whereas strength and motor function remain unchanged. Previous studies consistently showed that clinical assessments lack sensitivity to detect changes in follow-up periods shorter than 2-5 years.(8,11,12,29-31)

This study, therefore, demonstrates that qMRI can detect subclinical disease progression and therefore is a promising biomarker.

Comparison of longitudinal imaging datasets is challenging and may impede clinical application. When comparing structures between imaging stacks or analyzing whole muscle volume two components are of importance; accuracy of segmentation and the match of anatomical locations. Slice-by-slice manual segmentation has yet demonstrated good-to-excellent reliability.(32) For the latter, we describe in this study a method to overcome the misalignment that is inherent to comparing scans from two time-points. We chose to segment and analyze all muscles separately and only use those regions that were

present and consistently segmented in consecutive scans. In this way, only muscle tissue that was present in both examinations on the same location was used for analysis. With this approach whole muscle can be compared individually, whilst retaining its multitude of information and without subsampling or deformation of the parameter maps. Our methodology thus allowed to include all 25 slices of the imaging stack, spanning 15 cm, which benefitted accuracy and statistical power. In comparison, a previous longitudinal study in SMA that employed the DIXON sequence and compared 3 slices of the imaging stack failed to detect significant changes (+2.3% after one year).(13)

The pace of fatty degeneration in SMA is slow and comparable to other neuromuscular diseases that are generally characterized by a yearly progression rate of <5%. (15,21,33,34) Other longitudinal studies in muscular dystrophies show that only few functional tests were able to detect changes in that timespan whilst fat infiltration progressed on MRI.(15,21,35–37) SMA is furthermore characterized by a higher overall fat infiltration, although there are few longitudinal studies in treatment-naïve adult patients with other neuromuscular diseases for comparison.(15,20,21,33) The increase in fat fraction seems to occur at the cost of contractile muscle tissue, as illustrated by the significant decrease in contractile-CSA over the course of one year. In line with previous clinical observations(8,9,38), qMRI data show clear differences between muscles. The pattern of relatively vulnerable and spared muscles that is characteristic of SMA is reflected by the bimodal distribution of fat fraction. Two separate peaks indicate the difference between low and high levels of fatty infiltration. This difference is clearly muscle specific but probably not static. Data from a cross-sectional study in SMA indicate that the adductor longus and biceps femoris muscles eventually show fatty replacement exceeding 30% of muscle volume up to end-stage full fatty replacement.(23) The lack of a clear spectrum may suggest that fatty infiltration is not a continuous process but can rather quickly convert at some tipping point towards high fatty content. This hypothesis is also supported by the finding that fat infiltration occurs at a slow yearly speed in muscles with less than 30% of fat infiltration as compared to a rapid yearly increase in muscles with fat infiltration > 30%.

Also, we noticed a very small (-0.2 ms) but significant decrease in T2 over time. We think the decrease is related to the bias of a simultaneous increase of fat fraction as increasing fat replacement results in lowering of T2, as we observed in our previous study.(23,27) Although T2 mapping is often used as a meaningful outcome measure in other neuromuscular diseases, its application as a biomarker for SMA, therefore, seems irrelevant, although its value in monitoring treatment effect remains to be determined.

The DTI measures MD and FA did not show significant changes over time in moderate to severely affected muscles. We observed a small significant change in FA only in low fat-infiltrated muscles, i.e. the adductor longus and biceps femoris (short head) that persisted after correction for SNR.(39) The decrease in FA in does probably not represent increased permeability of cell membranes because MD values did not change accordingly. Possible alternative explanations for the observed FA decrease in low fat-infiltrated muscles are increased strain while other muscles deteriorate, resulting in swelling. FA decrease may also reflect a distinct moment in (early) muscle pathology. Whether DTI changes are preceding fat infiltration remains inconclusive and has to be demonstrated by additional measurements in an early phase of muscle pathology in young children. Because of the small standard deviation of MD and FA (0.1 and 0.2 respectively) on both time-points, we hypothesize that DTI can still be sensitive measure for evaluating treatment effects despite not qualifying as a biomarker for disease progression in untreated patients. In the cross-sectional cohort, which was a inhomogeneous group that included patients from 7 to 73 years, the overall change of FA was 0.2 over the span of 60 years.(23) Now, we observe that FA, similar to MD, is not sensitive as measure for change within one year. Nonetheless, previous work has also shown that FA in affected muscle is different from healthy muscle, and that what is considered healthy muscle in SMA has comparable FA values as muscle of controls.(23) This broad range of FA and the possibility for normalization of FA values holds potential when monitoring treatment response.

All clinical measurements were done by one evaluator. Previous studies have shown that the intra-rater reliability of these measurements in SMA are 0.959 for HFMSE(40) and >0.91 for HHD.(41) Additionally, research in DMD showed that MRC reliability within a study improved when consecutive evaluations are done by the same evaluator.(42) Clinical measures appear insensitive to minor changes, as reflected by the stable MRC score, or can show day-to-day variation, as illustrated by the HHD results. We thus propose MRI as a more objective method for monitoring patients. Good correlation of DIXON-FF and moderate correlation of DTI parameters with clinical measures has been established in a cross-sectional study in SMA.(23) The small sample size is a clear limitation to this study. However, SMA is rare and the fact patients are often severely impaired complicates MRI studies. Muscle MRI of lower extremities in SMA therefore seems limited to young and adolescent patients with type 2 and young to adult patients with type 3. qMRI of the upper extremities could represent a future alternative, after the solution of some logistic and technical issues including positioning of the patient (especially those with contractures) and the fact that arms cannot be imaged simultaneously, resulting in prolonged scanning

time. This study on natural history of disease progression excluded patients that started treatment; they are still undergoing follow-up measurements. There are subsequent fewer opportunities to gather reference data from treatment-naïve patients since treatment is becoming widely available for patients.

To conclude, longitudinal imaging data show slow disease progression in skeletal muscles of the thigh of (young)-adult patients with SMA despite stable strength and motor function scores. As multiple disease-modifying therapies have become available since the start of this study, this dataset, on treatment-naïve patients, provides insight in the natural history of SMA. This pilot study demonstrates the potential of quantitative MRI as a biomarker for disease activity and monitoring of therapy response.

Acknowledgements

We thank all SMA patients and their families for their participation. We thank Christa van Ekris for her assistance at patients visits.

Funding

This work was supported by the Prinses Beatrix Spierfonds (Grant no. W.OR16-06). The Dutch SMA register is supported by stichting Spieren voor Spieren.

Competing Interest

WLP is a member of the scientific advisory board of SMA Europa and served as an ad hoc member of the scientific advisory boards of Biogen and Avexis and as a member of a data monitoring committee for Novartis. WLP receives grants from Prinses Beatrix Spierfonds and stichting Spieren voor Spieren. Other co-authors report no competing interest.

REFERENCES

1. Lefebvre S, Bürglen L, Reboullet S, et al. Identification and characterization of a spinal muscular atrophy-determining gene. *Cell*. 1995;80(1):155–165. doi:10.1016/0092-8674(95)90460-3.
2. Munsat TL, Davies KE. International SMA Consortium Meeting (26–28 June 1992, Bonn, Germany). *Neuromuscul Disord*. 1992. p. 423–428doi:10.1016/S0960-8966(06)80015-5.
3. Wadman RI, Stam M, Gijzen M, et al. Association of motor milestones, SMN2 copy and outcome in spinal muscular atrophy types 0–4. *J Neurol Neurosurg Psychiatry*. 2017;88:364–367. doi:10.1136/jnnp-2016-314292.
4. Swoboda KJ, Prior TW, Scott CB, et al. Natural history of denervation in SMA: Relation to age, SMN2 copy number, and function. *Ann Neurol*. 2005;57:704–712. doi:10.1002/ana.20473.
5. Martínez-Hernández R, Soler-Botija C, Also E, et al. The developmental pattern of myotubes in spinal muscular atrophy indicates prenatal delay of muscle maturation. *J Neuropathol Exp Neurol*. 2009;68(5):474–481. doi:10.1097/NEN.0b013e3181a10ea1.
6. Groen EJN, Talbot K, Gillingwater TH. Advances in therapy for spinal muscular atrophy: Promises and challenges. *Nat Rev Neurol*. 2018;14:214–224. doi:10.1038/nrneuro.2018.4.
7. Schorling DC, Pechmann A, Kirschner J. Advances in Treatment of Spinal Muscular Atrophy - New Phenotypes, New Challenges, New Implications for Care. *J. Neuromuscul. Dis*. 2020.doi:10.3233/JND-190424.
8. Piepers S, Van Den Berg LH, Brugman F, et al. A natural history study of late onset spinal muscular atrophy types 3b and 4. *J Neurol*. 2008;255(9):1400–1404. doi:10.1007/s00415-008-0929-0.
9. Deymeer F, Serdaroglu P, Parman Y, Poda M. Natural history of SMA IIIb: Muscle strength decreases in a predictable sequence and magnitude. *Neurology*. 2008;71(9):644–649. doi:10.1212/01.wnl.0000324623.89105.c4.
10. Souchon F, Simard LR, Lebrun S, Rochette C, Lambert J, Vanasse M. Clinical and genetic study of chronic (types II and III) childhood onset spinal muscular atrophy. *Neuromuscul Disord*. 1996;6(6):419–424. doi:10.1016/S0960-8966(96)00379-3.
11. Kaufmann P, McDermott MP, Darras BT, et al. Prospective cohort study of spinal muscular atrophy types 2 and 3. *Neurology*. 2012;79(18):1889–1897. doi:10.1212/WNL.0b013e318271f7e4.
12. Wijngaarde CA, Stam M, Otto LAM, et al. Muscle strength and motor function in adolescents and adults with spinal muscular atrophy. *Neurology*. 2020;95(14):e1988–e1998. doi:10.1212/WNL.0000000000010540.
13. Bonati U, Holiga Š, Hellbach N, et al. Longitudinal characterization of biomarkers for spinal muscular atrophy. *Ann Clin Transl Neurol*. 2017;4(5):292–304. doi:10.1002/acn3.406.
14. Carlier PG, Marty B, Scheidegger O, et al. Skeletal Muscle Quantitative Nuclear Magnetic Resonance Imaging and Spectroscopy as an Outcome Measure for Clinical Trials. *J Neuromuscul Dis*. 2016;3:1–28. doi:10.3233/JND-160145.
15. Fischmann A, Hafner P, Fasler S, et al. Quantitative MRI can detect subclinical disease progression in muscular dystrophy. *J Neurol*. 2012;259(8):1648–1654. doi:10.1007/s00415-011-6393-2.
16. Arrigoni F, De Luca A, Velardo D, et al. Multiparametric quantitative MRI assessment of thigh muscles in limb-girdle muscular dystrophy 2A and 2B. *Muscle and Nerve*. 2018;58:550–558. doi:10.1002/mus.26189.
17. Fischer D, Bonati U, Wattjes MP. Recent developments in muscle imaging of neuromuscular disorders. *Curr Opin Neurol*. 2016;doi:10.1097/WCO.0000000000000364.

18. Arpan I, Willcocks RJ, Forbes SC, et al. Examination of effects of corticosteroids on skeletal muscles of boys with DMD using MRI and MRS. *Neurology*. 2014;83(11):974–980. doi:10.1212/WNL.0000000000000775.
19. Forbes SC, Willcocks RJ, Rooney WD, Walter GA, Vandenborne K. MRI quantifies neuromuscular disease progression. *Lancet Neurol*. 2016. doi:10.1016/S1474-4422(15)00320-8.
20. Willcocks RJ, Rooney WD, Triplett WT, et al. Multicenter prospective longitudinal study of magnetic resonance biomarkers in a large duchenne muscular dystrophy cohort. *Ann Neurol*. 2016;79(4):535–547. doi:10.1002/ana.24599.
21. Willis TA, Hollingsworth KG, Coombs A, et al. Quantitative Muscle MRI as an Assessment Tool for Monitoring Disease Progression in LGMD2l: A Multicentre Longitudinal Study. *PLoS One*. 2013;8(8) doi:10.1371/journal.pone.0070993.
22. Hollingsworth KG, Garrod P, Eagle M, Bushby K, Straub V. Magnetic resonance imaging in duchenne muscular dystrophy: Longitudinal assessment of natural history over 18 months. *Muscle and Nerve*. 2013;48(4):586–588. doi:10.1002/mus.23879.
23. Otto LAM, van der Pol W-L, Schlaffke L, et al. Quantitative MRI of skeletal muscle in a cross-sectional cohort of Spinal Muscular Atrophy patients with types 2-3. *NMR Biomed*. 2020; doi:10.1002/nbm.4357.
24. O'Hagen JM, Glanzman AM, McDermott MP, et al. An expanded version of the Hammersmith Functional Motor Scale for SMA II and III patients. *Neuromuscul Disord*. 2007;17(9–10):693–697. doi:10.1016/j.nmd.2007.05.009.
25. Mercuri E, Messina S, Battini R, et al. Reliability of the Hammersmith functional motor scale for spinal muscular atrophy in a multicentric study. *Neuromuscul Disord*. 2006;16(2):93–98. doi:10.1016/j.nmd.2005.11.010.
26. Schlaffke L, Rehmann R, Rohm M, et al. Multicenter evaluation of stability and reproducibility of quantitative MRI measures in healthy calf muscles. *NMR Biomed*. 2019;1–14. doi:10.1002/nbm.4119.
27. Keene KR, Beenakker JM, Hooijmans MT, et al. T2 relaxation time mapping in healthy and diseased skeletal muscle using extended phase graph algorithms. *Magn Reson Med*. 2020; doi:10.1002/mrm.28290.
28. Veraart J, Novikov DS, Christiaens D, Ades-aron B, Sijbers J, Fieremans E. Denoising of diffusion MRI using random matrix theory. *Neuroimage*. 2016;142:394–406. doi:10.1016/j.neuroimage.2016.08.016.
29. Mercuri E, Finkel R, Montes J, et al. Patterns of disease progression in type 2 and 3 SMA: Implications for clinical trials. *Neuromuscul Disord*. 2016;26(2):126–131. doi:10.1016/j.nmd.2015.10.006.
30. Sivo S, Mazzone E, Antonaci L, et al. Upper limb module in non-ambulant patients with spinal muscular atrophy: 12 month changes. *Neuromuscul Disord*. 2015;25(3):212–215. doi:10.1016/j.nmd.2014.11.008.
31. Kaufmann P, McDermott MP, Darras BT, et al. Observational study of spinal muscular atrophy type 2 and 3: Functional outcomes over 1 year. *Arch Neurol*. 2011;68(6):779–786. doi:10.1001/archneurol.2010.373.
32. Pons C, Borotikar B, Garetier M, et al. Quantifying skeletal muscle volume and shape in humans using MRI: A systematic review of validity and reliability. *PLoS One*. 2018; doi:10.1371/journal.pone.0207847.

33. Morrow JM, Sinclair CDJ, Fischmann A, et al. MRI biomarker assessment of neuromuscular disease progression: A prospective observational cohort study. *Lancet Neurol.* 2016;15(1):65–77. doi:10.1016/S1474-4422(15)00242-2.
34. Figueroa-Bonaparte S, Llauger J, Segovia S, et al. Quantitative muscle MRI to follow up late onset Pompe patients: A prospective study. *Sci Rep.* 2018;8(1)doi:10.1038/s41598-018-29170-7.
35. Andersen G, Dahlqvist JR, Vissing CR, Heje K, Thomsen C, Vissing J. MRI as outcome measure in facioscapulohumeral muscular dystrophy: 1-year follow-up of 45 patients. *J Neurol.* 2017;doi:10.1007/s00415-016-8361-3.
36. Janssen BH, Voet NBM, Nabuurs CI, et al. Distinct disease phases in muscles of facioscapulohumeral dystrophy patients identified by MR detected fat infiltration. *PLoS One.* 2014;doi:10.1371/journal.pone.0085416.
37. Dahlqvist JR, Fornander F, de Stricker Borch J, Oestergaard ST, Poulsen NS, Vissing J. Disease progression and outcome measures in spinobulbar muscular atrophy. *Ann Neurol.* 2018;doi:10.1002/ana.25345.
38. Wadman RI, Wijngaarde CA, Stam M, et al. Muscle strength and motor function throughout life in a cross-sectional cohort of 180 patients with spinal muscular atrophy types 1c–4. *Eur J Neurol.* 2018;25(3):512–518. doi:10.1111/ene.13534.
39. Froeling M, Nederveen AJ, Nicolay K, Strijkers GJ. DTI of human skeletal muscle: The effects of diffusion encoding parameters, signal-to-noise ratio and T2 on tensor indices and fiber tracts. *NMR Biomed.* 2013;26(11):1339–1352. doi:10.1002/nbm.2959.
40. Glanzman AM, Mazzone ES, Young SD, et al. Evaluator Training and Reliability for SMA Global Nusinersen Trials. *J Neuromuscul Dis.* 2018;doi:10.3233/JND-180301.
41. Merlini L, Mazzone ES, Solari A, Morandi L. Reliability of hand-held dynamometry in spinal muscular atrophy. *Muscle and Nerve.* 2002;26(July):64–70. doi:10.1002/mus.10166.
42. Florence JM, Pandya S, King WM, et al. Intrarater reliability of manual muscle test (Medical Research Council scale) grades in Duchenne's muscular dystrophy. *Phys Ther.* 1992;doi:10.1093/ptj/72.2.115.



CHAPTER IV

Monitoring nusinersen treatment effects in children with spinal muscular atrophy with quantitative muscle MRI

Louise A.M. Otto¹, M. Froeling², Ruben P.A. van Eijk^{1,3}, Renske I. Wadman¹, Inge Cuppen⁴,
Danny R. van der Woude⁵, Bart Bartels⁵, Fay-Lynn Asselman¹, J. Hendrikse²,
W.L. van der Pol¹

1 Department of Neurology, UMC Utrecht Brain Center, University Medical Center Utrecht,
Utrecht University, Utrecht, The Netherlands

2 Department of Radiology, University Medical Center Utrecht, Utrecht University, Utrecht,
The Netherlands

3 Biostatistics & Research Support, Julius Center for Health Sciences and Primary Care,
University Medical Center Utrecht, Utrecht University, Utrecht, The Netherlands

4 Department of Neurology and Child Neurology, UMC Utrecht Brain Center, University
Medical Center Utrecht, Utrecht University, Utrecht, The Netherlands

5 Department of Child Development and Exercise Center, University Medical Center Utrecht,
Utrecht University, the Netherlands

Submitted

ABSTRACT

Introduction Spinal muscular atrophy (SMA) is caused by deficiency of survival motor neuron (SMN) protein. Intrathecal nusinersen treatment increases SMN protein in motor neurons and has been shown to improve motor function in children with SMA. We used quantitative MRI to gain insight in microstructure and fat content of muscle during treatment and to explore its use as biomarker for treatment effect.

Methods We used a quantitative MRI protocol before start of treatment and following the 4th and 6th injection of nusinersen in 8 children with SMA type 2 and 3 during the first year of treatment. The MR protocol allowed DIXON, T2 mapping and diffusion tensor imaging acquisitions. We also assessed muscle strength and motor function scores.

Results Fat fraction of all thigh muscles except for the m. adductor longus increased in all patients during treatment (+3.2%, $p=0.02$). DTI parameters changed in hamstrings towards values observed in healthy muscle with similar trends in other muscle groups. T2 showed no significant changes over time (-0.7 ms, $p=0.3$).

Conclusion Thigh muscles of children with SMA treated with nusinersen showed ongoing fatty infiltration and normalization of thigh muscle microstructure during the first year of nusinersen treatment. Quantitative muscle MRI shows potential as biomarker for the effects of SMA treatment strategies.

Keywords spinal muscular atrophy, nusinersen, quantitative MRI, muscle MRI, diffusion tensor imaging

Abbreviations AD, axial diffusivity; DMD, Duchenne Muscular Dystrophy; DTI, diffusion tensor imaging; FA, fractional anisotropy; FOV, field of view; HFMSE, Hammersmith Functional Motor Scale, Expanded; HHD, hand-held dynamometry; MD, mean diffusivity; MRC, Medical Research Council; PCA, principal component analysis; qMRI, quantitative MRI; RD, radial diffusivity; SMA, spinal muscular atrophy; SMN, survival motor neuron; SNR, signal to noise ratio; SE-EPI, spin-echo echo planar imaging; SPAIR, spectral attenuated inversion recovery; SPIR, spectral presaturation with inversion recovery.

INTRODUCTION

Proximal hereditary spinal muscular atrophy (SMA) is caused by loss of function of the survival motor neuron (*SMN1*) gene and the resulting deficiency of cellular SMN protein. SMA is characterized by severe and progressive muscle weakness and is the most important genetic cause of infantile death or severe impairment later in life.(1) SMN protein is ubiquitously expressed and has several important cellular functions.(2) The highly homologous *SMN2* gene ensures the production of residual amounts of full-length protein, but this is insufficient to avoid degeneration of the motor unit.(3) Alpha motor neurons are most sensitive to SMN deficiency, but SMN deficiency probably also affects the structural integrity and function of other tissues, such as muscle.(4,5)

The antisense oligonucleotide (ASO) nusinersen modulates *SMN2* mRNA splicing and is the first approved drug for SMA. It is used to treat an increasing number of patients worldwide. After intrathecal administration, it upregulates SMN production in the spinal cord and brain.(6,7) Randomized trials have shown that nusinersen treatment improves survival in infants and motor function in approximately half of young children with SMA.(8,9) Real life data in older patients also show treatment effects in subgroups.(10,11) The clinical motor function scales that have been used in natural history studies to assess disease progression lack sensitivity to detect relevant changes in the shorter run.(12,13) New, sensitive biomarkers that can differentiate responders from non-responders would therefore help to improve cost-effectiveness and reduce the patient burden that is associated with unsuccessful treatment.

Magnetic resonance imaging (MRI) has been used as an *in vivo* outcome measure in trials to measure treatment effect in patients with neuromuscular disorders such as Duchenne Muscular Dystrophy (DMD).(14–16) We recently showed that quantitative MRI (qMRI) of thigh muscles can detect subclinical disease progression in the course of one year in treatment-naïve adult patients with SMA.(13) This MR protocol assesses the ratio of healthy muscle versus fat fraction (DIXON); microstructural changes in remaining muscle tissue using diffusion tensor imaging (DTI) and possible inflammatory changes (T2 mapping). In the current study, we used this MR protocol in a cohort of 8 young children with SMA type 2 and type 3 (age range 7-13 years) prior to and in the course of the first year of treatment (at 4th and 6th injection) to investigate if qMRI has potential as a biomarker to detect treatment effects. The data presented here show that qMRI detects early changes during treatment and is therefore a promising tool for treatment evaluation.

METHODS

Study population

We consecutively enrolled 8 children with genetically confirmed SMA before they started treatment with nusinersen. Four children had SMA type 2 (i.e. onset between 6-18 months and able to sit independently at any moment in life) and 4 had SMA type 3 (i.e. onset after 18 months and able to walk independently at any moment in life).⁽¹⁷⁾ Mean age was 9.0 years (range 7.6 - 13.8 years). Clinical characteristics are presented in table 1. The inclusion criterium was an age older than 6 years at the start of nusinersen treatment. From this age children can express voluntary participation to scanning procedures without sedation. Exclusion criteria were any type of invasive ventilation, orthopnea, pronounced swallowing disorders, discontinuation of nusinersen treatment during the study, or any other contra-indication for 3 Tesla MR.

The study was approved by the local ethics committee (no. 17-226/NL61066.041.17) and conducted in accordance with codes of conduct for research in children and the Helsinki declaration (latest amendment Fortaleza, October 2013). In children under 12 years, parents gave oral and written consent. We monitored children for signs of resistance against any of the procedures. Children of 12 years and older and their parents both gave oral and written consent.

Table 1 Patient characteristics at baseline

	Patients (n=8)
Mean age in years [range]	9.0 [7.7-13.8]
Sex (M:F)	5:3
SMA type (Type 2 : Type 3)	4:4
<i>SMN2</i> copy number *	
3	5
4	3
Mean disease duration in months [range]	93 [69-148]
Ambulatory status (ambulant : non-ambulant)	3:5

Legend table 1: F= female; M= male. *SMN2 copy number was determined with MLPA analysis (SALSA MLPA kit P060 version B2; www.mlpa.com)

Clinical evaluation

Two trained physiotherapists (DvdW, BB) assessed motor function with the Hammersmith Functional Motor Scale Expanded (HFMSE) before the 1st and after the 4th (i.e. 2 months after start of treatment) and 5th injection (i.e. 6 months after start of treatment). In addition to routine clinical evaluation with HFMSE, we assessed muscle strength either prior to the injection or directly following the MR examination. The same evaluator (LAMO) performed all strength measurements using the Medical Research Council (MRC) scale and hand-held dynamometry (MicroFET2; Hoggan Health Industries Inc., USA) of the quadriceps, hamstrings and adductors of both sides according standard procedures.(18) We report muscle strength as a composite MRC score of all 42 muscle groups (flexors and extensors of the neck, upper arms, wrists, fingers, hips, knees, feet and deltoids, pectoralis, supraspinatus, infraspinatus, finger abductors, hip abductor and – adductor and hallucis longus muscle) and as MRC sum score of the upper leg muscles (quadriceps, hamstrings and adductors).

MR acquisition

Baseline scans were performed prior to the first injection with nusinersen. The second and third scan were scheduled at the 4th injection (i.e. 2 months after start of treatment) and at the 6th injection (10 months after start of treatment). We used the same 3T MR scanner (Philips Ingenia, Philips Medical Systems, the Netherlands) for all but one patient. We had to reschedule this patient to another scanner from the same vendor because it was out-of-service due to maintenance. Patients were scanned in supine position, feet-first with a 12-channel posterior coil and 16-channel anterior body coil. The image stack was centered mid-femoral, the distance from the top of the FOV to the upper limit of the femoral head was noted for each patient to ensure same positioning for follow-up scans. We designed the protocol to be short (total scan time ~10 minutes) in order to be tolerated by young children. The MR protocol consisted of the following three sequences; 4-point DIXON (TR/TE/ 210/2.6/3.36/4.12/4.88 ms; flip angle 10°; voxel size 6x1.5x1.5 mm³; no gap; 25 slices); T2 mapping (17 echoes TR/TE/ΔTE 4598/17/7.6 ms; flip angle 90/180°; voxel size 6x3x3 mm³; slice gap 6mm; 13 slices, no fat suppression) and DTI SE-EPI (TR/TE 5000/57 ms; b-values: 0 (1), 1 (6), 10 (3), 25 (3), 100 (3), 200 (6), 400 (8) and 600 (12) s/mm²; voxel size 6x3x3 mm³; no gap; 25 slices, SPAIR and SPIR fat suppression. The MR protocol has been validated in a multicenter study on healthy controls and has been used in previous imaging studies in SMA.(13,19,20)

MR processing

We obtained the following quantitative parameters; fat fraction (%) from DIXON; T₂ relaxation times (ms); mean diffusivity (MD) and the directional parameters fractional anisotropy (FA), radial diffusivity (RD) and axial diffusivity (AD) from DTI. We used a custom toolbox for processing of MR data (QMRITools for Mathematica -mfroeling.github.io/QMRITools). Two of the authors (MF and LAMO, 13 years and 3 years of experience, respectively) checked data for motion artifacts and quality. We reconstructed DIXON data with an IDEAL method with estimation of B₀ and T₂^{*}, T₂-mapping data with extended graph (EPG) fitting(21) and DTI data with iWLLS method with REKINDLE outlier detection. We used principle component analysis (PCA) for denoising and for obtaining the signal to noise ratio (SNR) of DTI data and corrected for subject motion and eddy current distortion.(22) For a detailed description of the processing steps we refer to previous work.(19,20)

Comparison of imaging stack

The field of view (FOV) comprised 12 individual muscles per leg; m. adductor magnus, m. adductor longus, m. rectus femoris, the three vasti muscles, m. semimembranosus, m. semitendinosus, m. biceps femoris (long and short head) and the m. sartorius and m. gracilis. One of the authors (LAMO) performed manual segmentation of these muscles for each leg with ITK-SNAP(23) (version 3.6) and at each time-point. As positioning of patients may slightly vary between scans, we used multiple converting steps for alignment to ensure evaluation of the same muscle location at each time-point.(13) In short, we used the registration of the DIXON water image of each of the scans for combined rigid, affine and b-spline registration to the other two time-points (in the assumption that each participant had a total of three scans). The manual segmentation, or mask, at each time-point was transformed accordingly. We took the union of the transformed segmentation and the native segmentation for each time-point. We then repeated this step, where each time-point served as reference and starting point for the converting steps. Finally, only a match between the three segmentations in the image space of those three scans was taken for analysis which assures that we evaluated exactly the same muscle location at all timepoints.

Statistical analysis

We compared clinical scores and qMRI outcomes with linear mixed effects models. We plotted all outcomes as function of the continuous variable time (in years) and estimated the average time trend for qMRI data by incorporating a random intercept and slope for

time per subject, as well as a random intercept for muscle. Also, we clustered the muscles in a muscle group (hamstrings, adductors, quadriceps).

The fixed part of the model contained the baseline score and an effect for time. We used the Wald statistic to determine significance (threshold set at $p < 0.05$).

We will refer to patients who were still able to walk as 'walkers' and patients who had lost or never acquired the ability to walk as 'sitters' (i.e. both type 2 and non-ambulant type 3). Due to the limited sample size, we use only descriptive statistics for the findings in clinical subgroups. We used SPSS for statistical analysis (version 25 for Windows, SPSS Inc. Chicago) and ggplot2 function in RStudio (version 1.3.959, RStudio PBS) for the figures. All source codes and data are available upon request.

RESULTS

Study population

We had to exclude one participant after the 4th injection since he/she wanted to participate in a clinical trial (see flowchart in Fig 1). All other 7 participants continued nusinersen treatment.

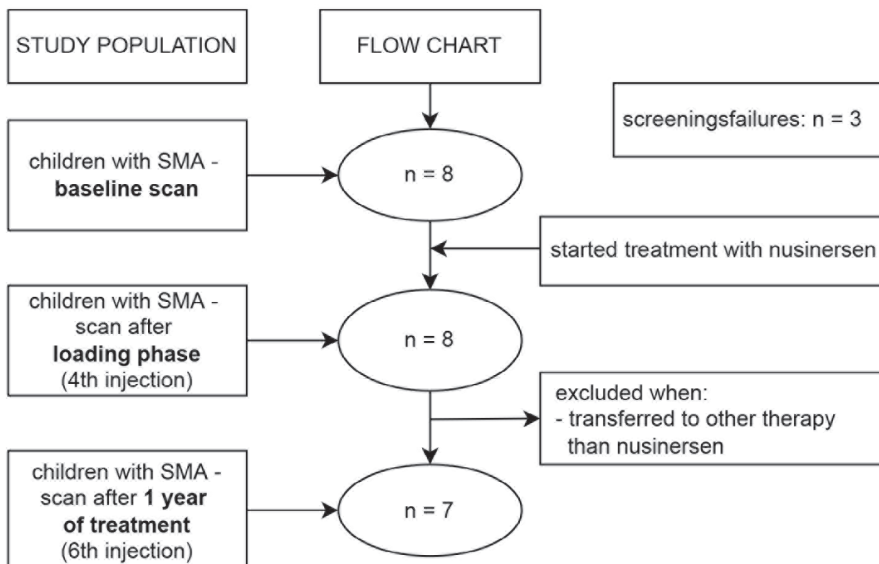


FIGURE 1 Flowchart of study procedure

Clinical evaluation

Clinical scores are presented in table 2. HFMSE scores were higher at 5th injection compared to baseline in four out seven children. The mean change of the HFMSE score after 6 months of treatment was +1.6 points (95%CI -0.20 to 3.50, $p=0.084$). Two out of seven children showed an increase in HFMSE score measured at 6th or 7th injection of ≥ 3 points. (24)

We could not obtain full MRC scores of 2 patients at two visits because of fatigue. We therefore only obtained MRC scores of muscle groups of the thigh. At the group level, the MRC sum score increase was +5.4 points during the first year of treatment (95%CI 0.70 to 10.10, $p=0.028$). At individual level, the range of MRC sum change was 0 to 11 points (i.e. 1 subject remained stable). The change in MRC sum scores of thigh muscles after one year was not significantly different from baseline (+0.3, 95%CI -0.70 to 1.30, $p=0.50$) but we did detect variability between subjects; MRC sum score changes of the thigh varied from a decrease of 1 point (2 subjects), stable (1 subject), to an increase of 1 (3 subjects) or 2 points (1 subject).

Quantitative muscle strength (as measured by HHD) of adductors and hamstrings increased significantly in the course of one year (+6.8 N 95%CI 3.3 to 10.3, baseline 21.8, $p<.001$ and +8.9 N 95%CI 4.5 to 13.3, baseline 22.1, $p<.001$, respectively). HHD of quadriceps was 4.3N at baseline and showed no significant change (+1.0 N 95% CI -2.4 to 4.3, $p=0.56$).

Table 2 Clinical parameters over time

Clinical measurements	n	Baseline (SE)	Slope / year [95%-CI]	p-value
HFMSE	23	31.8 (0.7)	+1.6 [-0.2 - 3.5]	0.084
MRC sum score	20 †	130.8 (1.4)	+5.4 [0.7 - 10.1]	0.028*
MRC sum score upper leg	23	18.5 (0.4)	+0.3 [-0.7 - 1.3]	0.504
HHD (N)				
<i>Adductors</i>	40	21.8 (0.9)	+6.8 [3.3 - 10.3]	<0.001*
<i>Hamstrings</i>	46	22.2 (1.9)	+8.9 [4.5 - 13.3]	<0.001*
<i>Quadriceps</i>	40	4.3 (1.6)	+1.0 [-2.4 - 4.3]	0.557

Legend table 2: * = $p<0.05$; † = missing data; CI = confidence interval; HHD = hand-held dynamometry; HFMSE = Hammersmith Functional Motor Scale Expanded, score range 0-66; MRC = Medical Research Council, sum score range 44-210, sum score upper leg range 6-30; N = Newton; n = number of observations included in analysis; s = second; SE = standard error

MR acquisition and processing

We obtained baseline scans the day before (7 patients) or one month before (1 patient) the first administration of nusinersen. We performed the second scan one day prior to the 4th injection (1 patient); on the day of the 4th injection (4 patients) or in the period following the 4th injection (2 patients; 2 weeks since and 5 months, respectively) and the third scan on the day of the 6th injection in 3 patients, after 1 month (2 patients) or 2 months (2 patients) following the 6th injection. We excluded one patient after the 4th injection because of his/her wish to participate in a clinical trial with another drug.

None of the datasets had to be excluded for motion artifacts or data quality, resulting in a total of 25 datasets. 90% of muscles could be segmented, whilst extensive fatty degeneration precluded segmentation in the remainder (Table 2).

Muscle fat fraction changes in the course of one year (DIXON)

Figure 2 depicts the cross-sectional image of fat infiltration of thigh muscles of each participant at baseline. Table 3 summarizes quantitative MR data over time. The average fat fraction of participants was 44.2% (95% CI 43.5 to 44.9 at baseline). Quantification of fat infiltration showed an increase of 3.2% in fat fraction during treatment (95% CI 0.9 to 5.5, $p=0.015$). Figure 3 (panel A) shows the slope of fat fraction of individual patients over time, and their relation with motor function scores (panel B).

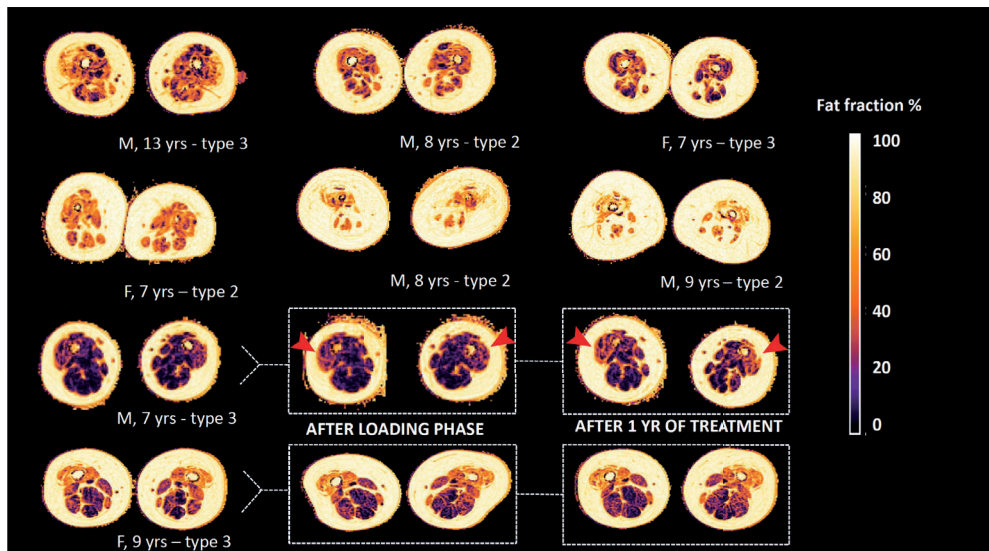


FIGURE 2 Status of fat infiltration at baseline of participants. Legend: M = male, F = female, yr(s) = year(s) Overview of the status of fat infiltration of all participants, as measured by the DIXON sequence;

in the bottom two rows we highlight the three consecutive scans of two subjects. Note the visible change of color in the anterior compartment of one male subject, as indicated by the red arrows, that indicates progression of fat infiltration

Fat infiltration exceeded 40% in all muscles at baseline, except for the m. semimembranosus and the m. adductor longus. Notably, the m. adductor longus had the lowest fat fraction, which decreased in the course of one year (21.5% to 19.4%). The highest increase in fat fraction was in the m. rectus femoris (+10%) and lowest in the m. sartorius (+1.5%) after one year. At the level of muscle groups, the quadriceps (consisting of the m. rectus femoris and vasti) showed the greatest fat increase; +5.8% (95% CI 2.7 to 8.9, baseline 44.5, $p=0.003$). The fat fraction of the adductor muscle group (m. adductor magnus and longus) increased by 1.5% (95% CI 0.3 to 2.7, $p=0.014$), and that of hamstrings (m. semimembranosus, m. semitendinosus and m. biceps femoris) by +3.3% (95% CI 1.1 to 5.5, $p=0.65$). Figure 4 presents the fat fraction changes over time of the muscle groups and highlights one muscle per muscle group, i.e. m. adductor longus, m. rectus femoris and m. semimembranosus. We did not find a significant decrease in contractile volume over time (Table 3). At baseline and after the 6th injection, fat fraction negatively correlated with contractile volume of thigh muscle ($R=-0.25$, $p=0.001$ and $R=-0.32$, $p<0.001$, respectively). However, the change in fat fraction did not correlate with a change in contractile volume ($R=-0.15$, $p=0.086$).

Table 3 Quantitative parameters over time

qMRI parameter	N	Baseline (SE)	Slope / year [95%-CI]	p-value
Fat fraction (%)	499	44.2 (0.3)	+3.2 [0.9 – 5.5]	0.015*
<i>Adductors</i>		43.7 (1.3)	+1.5 [0.3 – 2.7]	0.014*
<i>Hamstrings</i>		44.0 (0.2)	+3.3 [1.3 – 5.4]	0.652
<i>Quadriceps</i>		44.5 (0.5)	+ 5.8 [2.7 – 8.9]	0.003*
Volume (cm³)	502	12.3 (0.2)	+1.2 [-0.4 – 2.9]	0.133
<i>Adductors</i>		12.6 (0.1)	+0.7 [-0.7 – 2.2]	0.263
<i>Hamstrings</i>		12.4 (0.2)	+1.2 [-1.1 – 3.6]	0.293
<i>Quadriceps</i>		11.9 (0.4)	+1.5 [-1.0 – 4.0]	0.194
Contractile volume (cm³)	502	6.8 (0.2)	+0.5 [-0.6 – 1.6]	0.343
<i>Adductors</i>		7.0 (0.2)	+0.4 [-0.8 – 1.6]	0.498
<i>Hamstrings</i>		6.9 (0.2)	+0.7 [-1.2 – 2.6]	0.399
<i>Quadriceps</i>		6.7 (0.1)	+0.0 [-0.9 – 0.9]	0.927
T2 (ms)	497	26.76 (0.24)	-0.72 [-2.51 – 1.06]	0.293
<i>Adductors</i>		27.00 (0.59)	-1.28 [-4.06 – 1.51]	0.299
<i>Hamstrings</i>		29.93 (0.40)	-0.19 [-1.48 – 1.11]	0.745
<i>Quadriceps</i>		26.61 (0.22)	-0.84 [-2.17 – 0.49]	0.176

MD ($10^{-3} \text{ mm}^2/\text{s}$)	493	1.58 (0.02)	-0.05 [-0.12 – 0.02]	0.130
<i>Adductors</i>		1.65 (0.05)	-0.03 [-0.20 – 0.15]	0.714
<i>Hamstrings</i>		1.59 (0.04)	-0.09 [-0.16 – -0.03]	0.007*
<i>Quadriceps</i>		1.57 (0.07)	-0.03 [-0.13 – 0.07]	0.597
FA	493	0.36 (0.01)	-0.02 [-0.04 – 0.01]	0.110
<i>Adductors</i>		0.35 (0.01)	-0.03 [-0.07 – 0.01]	0.133
<i>Hamstrings</i>		0.35 (0.01)	-0.02 [-0.04 – 0.00]	0.084
<i>Quadriceps</i>		0.36 (0.01)	-0.01 [-0.05 – 0.02]	0.410
AD ($10^{-3} \text{ mm}^2/\text{s}$)	493	2.19 (0.04)	-0.11 [-0.22 – 0.01]	0.061
<i>Adductors</i>		2.30 (0.06)	-0.10 [-0.39 – 0.19]	0.431
<i>Hamstrings</i>		2.16 (0.07)	-0.19 [-0.29 – -0.09]	<0.001*
<i>Quadriceps</i>		2.19 (0.08)	-0.06 [-0.19 – 0.08]	0.405
RD ($10^{-3} \text{ mm}^2/\text{s}$)	492	1.04 (0.02)	-0.03 [-0.10 – 0.04]	0.386
<i>Adductors</i>		1.06 (0.03)	+0.04 [-0.09 – 0.17]	0.468
<i>Hamstrings</i>		1.06 (0.04)	-0.06 [-0.14 – 0.01]	0.089
<i>Quadriceps</i>		1.01 (0.03)	-0.02 [-0.11 – 0.06]	0.487

Legend table 3: * = $p < 0.05$; AD = axial diffusivity; CI = confidence interval; FA = fractional anisotropy; mm = millimeter; MD = mean diffusivity; ms = millisecond; n = number of observations included in analysis; RD = radial diffusivity; s = second; SE = standard error.

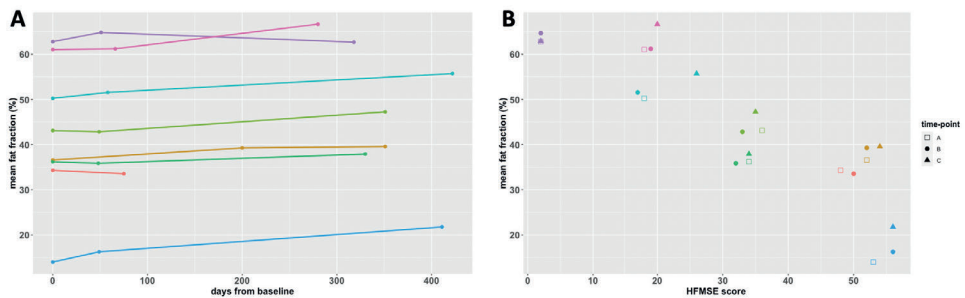


FIGURE 3 Fat fraction over time and relation with motor function score. Legend: HFMSE = Hammersmith Functional Motor Scale, Expanded

Panel A presents the trajectory of fat fraction of subjects over time, the timing of each scan is presented as bullet. In panel B the timing of scans is presented as A (baseline); B (after loading phase) and C (one year on treatment) and fat fraction at each time-point is presented in relation to the score on the HFMSE scale. Subjects go by the same color in the panels.

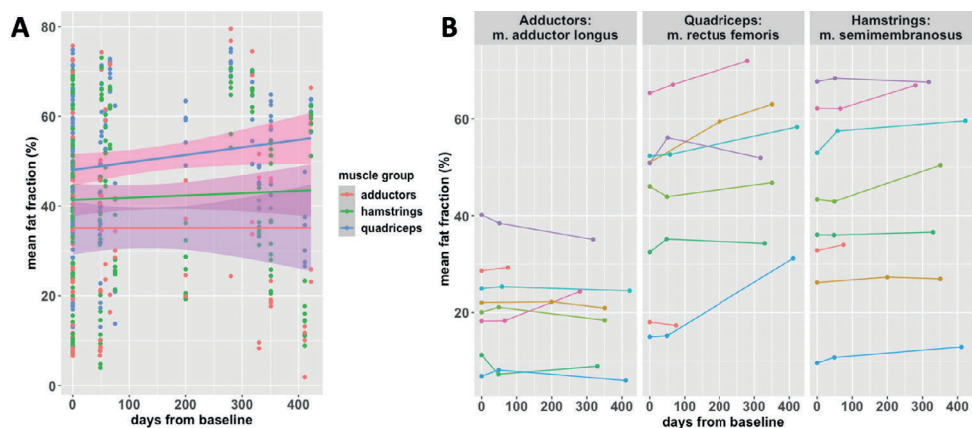


FIGURE 4 Trajectory of fat fraction for muscles over time. Panel A represent the trajectory of fat fraction for the three muscle groups; adductors, hamstrings and quadriceps. Note the steeper increase of quadriceps in fat fraction over time. In panel B one muscle per muscle group is highlighted, and the trajectory of each subject is given. The color coding of subjects corresponds with figure 3. The adductor longus seems to decrease in fat fraction over time; the rectus femoris shows a steep increase in subjects, one subject (blue line) that started with low fat infiltration demonstrates a great increase from baseline. In the m. semimembranosus, fat fraction increase is more modest and gradual over time

Fat fraction in relation to clinical characteristics

Three patients were walkers and 5 were sitters (1 subject with type 3 and 4 with type 2). Figure 5 shows the histogram and slope of fat infiltration for both groups. Walkers had a lower average fat fraction of thigh muscles at baseline than sitters (baseline 28.2% versus 50.7%; +2.6% versus +3.0% over time, respectively). In parallel, we observed a decrease (between 1.3 to 5.8%) in fat fraction in walkers in the m. adductor longus, the m. adductor magnus, m. semimembranosus and m. semitendinosus. Walkers had a higher HFMSE score at baseline.

QMRI results of three children with motor function improvement showed the most pronounced change in fat fraction. The fat fraction distribution of this group was bimodal with low and high fat infiltration peaks (Fig 5-C). This pattern of two peaks persisted and evenly shifted towards higher fat infiltration in the course of one year. In contrast, the fat distribution of thigh muscles of the other children did not show a bimodal distribution, but a broad slope from moderate to high (50 to 70%) fat fraction. At baseline, the fat fraction of children with the most pronounced motor function improvement was lower compared to

children with modest or no motor function change (33.6% vs 50.8%). However, increase in fat fraction in the course of one year was greater (+5.4% vs. +2.4%) (Fig 5-D).

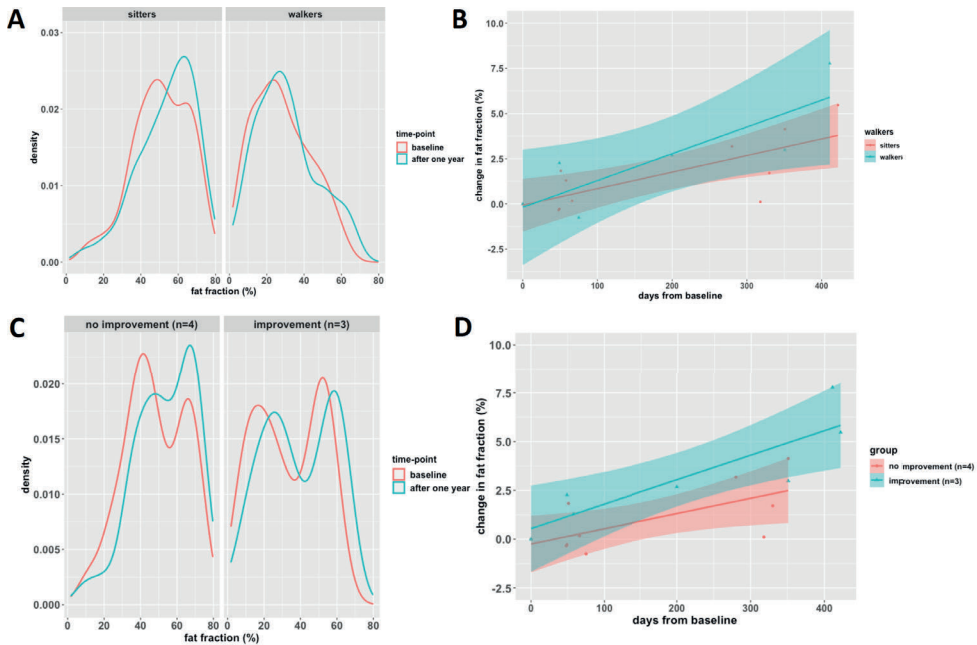


FIGURE 5 Plots of fat fraction over time for walkers vs. sitters and motor function improvement group. The top row (A-B) presents the fat fraction when subjects are classified upon ambulatory status at baseline as 'sitters' or 'walkers'. Note the lower average fat fraction in walkers (panel A). Furthermore, the confidence interval of change in fat fraction of the groups mostly overlaps. The bottom row (C-D) presents the fat fraction when subjects are further subclassified based on their motor function score change. Note the bimodal fat distribution in responders panel a, and the seemingly steeper slope of change in fat fraction of responders

Quantitative MR parameter: T2

T2 imaging had a slope of -0.7 ms (95% CI -0.2 to 0.1 , baseline 26.7 ms) in the course of one year. The changes compared to baseline were not significant ($p=0.29$) either on the group level or for individual muscle groups.

Quantitative MR parameters: MD, FA, AD and RD

We observed a non-significant negative slope for all DTI parameters MD, FA, AD and RD when we performed combined analysis of all leg muscles (table 2). The negative slopes

of MD and AD seem mainly driven by a significant decrease seen in the hamstrings (slope MD: $-0.1 \text{ mm}^2/\text{s}/\text{year}$, $p < 0.01$ and slope AD: $-0.19 \text{ mm}^2/\text{s}/\text{year}$, $p < 0.001$, respectively), while values did not change significantly in quadriceps and adductors. FA showed the strongest negative decrease for the hamstrings ($-0.02/\text{year}$, $p = 0.084$), but similar to RD not for all muscle groups.

DISCUSSION

In this study we describe quantitative MR parameter changes in thigh muscles of 8 children with SMA aged 7 to 13 years during one-year treatment with nusinersen. Segmentation of individual muscles allowed comparison of longitudinal MR data for the monitoring of treatment effects. The DIXON and DTI suggest simultaneous and divergent processes. We observed continued fatty degeneration of muscle groups that were already affected at the start of treatment. In parallel, DTI results showed improvements in the microstructure of muscle tissue. Together, these alterations differ from the changes observed in treatment-naïve adult patients in whom the natural disease progression is characterized by progressive fatty degeneration at the loss of contractile muscle tissue.⁽¹³⁾ Our data show that although progression of fatty infiltration of thigh muscles is also present in young children with SMA who are treated, contractile volume of thigh muscles remains stable.

Fatty replacement increased despite treatment, in line with previous observations⁽²⁵⁾, although the rates at which this happened differed between muscle groups, possibly reflecting differences in vulnerability of muscle groups. The quadriceps, which is a relatively weak muscle group in SMA,^(20,26–28) showed the highest one-year increase in fat, followed by the hamstrings, whilst the anatomy and function of the adductors was relatively preserved. The m. adductor longus was the only muscle in which average fat content decreased during treatment in all children. This is consistent with observations in three treated adults by Savini et al.⁽²⁵⁾ The gains in HFMSE scores that we observed in a subgroup of children indicate that treatment success is not explained by a reverse of fatty degeneration. We observed specific patterns of fat distribution that may have biomarker value. A bimodal distribution of the level of fatty infiltration was common in children with motor function gains. We previously observed a similar pattern in some adults.⁽¹³⁾ This pattern most likely indicates the presence of muscles that may still respond to treatment (i.e. low levels of fat; $< 30\%$). Disease progression may eventually change this bimodal distribution in a single broad peak reflecting end-stage fat infiltration (i.e. fat levels $> 50\%$). Therefore, the value of bimodal fatty distribution as qMRI biomarker deserves further study.

Diffusion tensor imaging provides the directional properties of water diffusion. The relation between each of the directional parameters can be used to probe tissue microarchitecture. (29) For example, the finding of lowered average diffusion in a increased anisotropic medium was an indication of shrinkage of the cellular compartment, i.e. muscle atrophy,(30) as we established in a previous study on thigh muscles in patients with SMA.(20)

The mean diffusivity (MD) at baseline was higher than measured in adult patients with SMA(20), probably due to lower levels of fat infiltration in children,(31,32) but still lower compared to values known of healthy muscles (i.e. 1.4 and 1.5)(19,33). Fractional anisotropy (FA) at baseline was high compared to findings in healthy muscles. After start of nusinersen treatment, we observed significant changes towards normal DTI values in hamstrings with similar trends in other muscle groups. A decrease in FA is explained by an axial diffusivity (AD) decrease, while radial diffusivity (RD) remains constant. This means that during treatment diffusion restriction in axial directions increases, implicating that atrophy is gradually reversed.(34) A FA decrease in response to treatment has recently also been observed in lower leg muscle in a case-study in two patients.(35) The trend of normalization of MD, RD and AD values could reflect a decrease of membrane permeability, or an increase of intracellular actin and myosine.(36) We hypothesize that these changes indicate normalization of muscle microstructure. Taken together, our data suggest that treatment effects are first seen in the restoration of structurally abnormal but viable muscle tissue, rather than in a decrease of fatty infiltration of muscle tissue.

The sample size is a limitation of this study. However, the analysis of individually segmented muscles increased statistical power. Despite extensive fatty replacement, we were able to include muscles with up to 80% fat fraction in our final analysis. Since we did not include a matched group of control subjects, patients served as their own reference. Theoretically, the observed changes in DTI parameters could reflect natural history rather than treatment effects. This is unlikely, since the increase of fat replacement is similar to observations in adults and natural history of children from the age of 6 years on is characterized by slowly progressive decline in muscle strength.(12) We therefore think it is highly unlikely that pathophysiological processes captured by qMRI differ between children and adults. Larger sample sizes and a reference cohort will be almost impossible to obtain now that treatment has become part of standard care.

To conclude, quantitative MR parameters of the DIXON and DTI sequence provided insight into parallel ongoing fatty infiltration with microstructural normalization of thigh muscles

in young patients during their first year of nusinersen treatment. Quantitative MRI could serve as a biomarker for treatment effects at the tissue level and possibly even to identify responders.

Acknowledgements

We thank all children who participated in this study and their families. We thank Christa van Ekris, Astrid Verhoef, Kim Holtmaat, Lisa de Koning, dr. Marloes Stam and all students who facilitated this study. This work was supported by Prinses Beatrix Spierfonds (grant number W.OR 16-06) and Stichting Spieren voor Spieren.

Competing Interests

WLP has served as an ad hoc member of the scientific advisory boards of Biogen and Avexis and as a member of a data monitoring committee for Novartis. WLP receives grants from Prinses Beatrix Spierfonds and stichting Spieren voor Spieren. The other authors report no conflicts of interest.

REFERENCES

1. Lefebvre S, Bürglen L, Reboullet S, et al. Identification and characterization of a spinal muscular atrophy-determining gene. *Cell*. 1995;80(1):155–165. doi:10.1016/0092-8674(95)90460-3.
2. Groen EJM, Talbot K, Gillingwater TH. Advances in therapy for spinal muscular atrophy: Promises and challenges. *Nat Rev Neurol*. 2018;14:214–224. doi:10.1038/nrneuro.2018.4.
3. Simic G. Pathogenesis of proximal autosomal recessive spinal muscular atrophy. *Acta Neuropathol*. 2008. p. 223–234doi:10.1007/s00401-008-0411-1.
4. Hamilton G, Gillingwater TH. Spinal muscular atrophy: Going beyond the motor neuron. *Trends Mol Med*. 2013;19:40–50. doi:10.1016/j.molmed.2012.11.002.
5. Jing Yeo CJ, Darras BT. Overturning the Paradigm of Spinal Muscular Atrophy as just a Motor Neuron Disease. *Pediatr Neurol*. 2020;doi:10.1016/j.pediatrneurol.2020.01.003.
6. Finkel RS, Chiriboga CA, Vajsar J, et al. Treatment of infantile-onset spinal muscular atrophy with nusinersen: a phase 2, open-label, dose-escalation study. *Lancet* (London, England). Elsevier; 2016;388(10063):3017–3026. doi:10.1016/S0140-6736(16)31408-8. Accessed February 3, 2017.
7. Finkel R, Chiriboga C, Vajsar J, et al. Interim results of a phase 2 clinical study of nusinersen (ISIS-SMNRX) in patients with infantile-onset spinal muscular atrophy. *Ann Neurol*. 2016;doi:10.1002/pon.4272.
8. Finkel RS, Mercuri E, Darras BT, et al. Nusinersen versus sham control in infantile-onset spinal muscular atrophy. *N Engl J Med*. 2017;377:1723–1732. doi:10.1056/NEJMoa1702752.
9. Mercuri E, Darras BT, Chiriboga CA, et al. Nusinersen versus sham control in later-onset spinal muscular atrophy. *N Engl J Med*. 2018;378:625–635. doi:10.1056/NEJMoa1710504.
10. Hagenacker T, Wurster CD, Günther R, et al. Nusinersen in adults with 5q spinal muscular atrophy: a non-interventional, multicentre, observational cohort study. *Lancet Neurol*. 2020;doi:10.1016/S1474-4422(20)30037-5.
11. Maggi L, Bello L, Bonanno S, et al. Nusinersen safety and effects on motor function in adult spinal muscular atrophy type 2 and 3. *J Neurol Neurosurg Psychiatry*. 2020;doi:10.1136/jnnp-2020-323822.
12. Wijngaarde CA, Stam M, Otto LAM, et al. Muscle strength and motor function in adolescents and adults with spinal muscular atrophy. *Neurology*. 2020;95(14):e1988–e1998. doi:10.1212/WNL.0000000000010540.
13. Otto LAM, Froeling M, van Eijk RPA, et al. Quantification of disease progression in spinal muscular atrophy with muscle MRI—a pilot study. *NMR Biomed*. 2021;doi:10.1002/nbm.4473.
14. Arpan I, Willcocks RJ, Forbes SC, et al. Examination of effects of corticosteroids on skeletal muscles of boys with DMD using MRI and MRS. *Neurology*. 2014;83(11):974–980. doi:10.1212/WNL.0000000000000775.
15. Bonati U, Hafner P, Schädelin S, et al. Quantitative muscle MRI: A powerful surrogate outcome measure in Duchenne muscular dystrophy. *Neuromuscul Disord*. 2015;25(9):679–685. doi:10.1016/j.nmd.2015.05.006.
16. Hooijmans M, Wokke B, Goemans N, et al. Longitudinal quantitative muscle magnetic resonance imaging (qMRI) in five boys with Duchenne muscular dystrophy (DMD), on and off treatment with drisapersen. *Neuromuscul Disord*. 2015;doi:10.1016/j.nmd.2015.06.053.
17. Wadman RI, Stam M, Gijzen M, et al. Association of motor milestones, SMN2 copy and outcome in spinal muscular atrophy types 0-4. *J Neurol Neurosurg Psychiatry*. 2017. p. 364–367doi:10.1136/jnnp-2016-314292.

18. Beenakker EAC, Van der Hoeven JH, Fock JM, Maurits NM. Reference values of maximum isometric muscle force obtained in 270 children aged 4-16 years by hand-held dynamometry. *Neuromuscul Disord.* 2001;doi:10.1016/S0960-8966(01)00193-6.
19. Schlaffke L, Rehmann R, Rohm M, et al. Multicenter evaluation of stability and reproducibility of quantitative MRI measures in healthy calf muscles. *NMR Biomed.* 2019;1-14. doi:10.1002/nbm.4119.
20. Otto LAM, van der Pol W-L, Schlaffke L, et al. Quantitative MRI of skeletal muscle in a cross-sectional cohort of Spinal Muscular Atrophy patients with types 2-3. *NMR Biomed.* 2020;doi:10.1002/nbm.4357.
21. Keene KR, Beenakker JM, Hooijmans MT, et al. T2 relaxation time mapping in healthy and diseased skeletal muscle using extended phase graph algorithms. *Magn Reson Med.* 2020;doi:10.1002/mrm.28290.
22. Veraart J, Novikov DS, Christiaens D, Ades-aron B, Sijbers J, Fieremans E. Denoising of diffusion MRI using random matrix theory. *Neuroimage.* 2016;142:394-406. doi:10.1016/j.neuroimage.2016.08.016.
23. Yushkevich PA, Piven J, Hazlett HC, et al. User-guided 3D active contour segmentation of anatomical structures: Significantly improved efficiency and reliability. *Neuroimage.* 2006;31(3):1116-1128. doi:10.1016/j.neuroimage.2006.01.015.
24. Mercuri E, Darras BT, Chiriboga CA, et al. Nusinersen versus sham control in later-onset spinal muscular atrophy. *N Engl J Med.* 2018;378(7):625-635. doi:10.1056/NEJMoa1710504.
25. Savini G, Asteggiano C, Paoletti M, et al. Pilot Study on Quantitative Cervical Cord and Muscular MRI in Spinal Muscular Atrophy: Promising Biomarkers of Disease Evolution and Treatment? *Front Neurol.* 2021;12doi:10.3389/fneur.2021.613834.
26. Piepers S, Van Den Berg LH, Brugman F, et al. A natural history study of late onset spinal muscular atrophy types 3b and 4. *J Neurol.* 2008;255(9):1400-1404. doi:10.1007/s00415-008-0929-0.
27. Wadman RI, Wijngaarde CA, Stam M, et al. Muscle strength and motor function throughout life in a cross-sectional cohort of 180 patients with spinal muscular atrophy types 1c-4. *Eur J Neurol.* 2018;25(3):512-518. doi:10.1111/ene.13534.
28. Brogna C, Cristiano L, Verdolotti T, et al. MRI patterns of muscle involvement in type 2 and 3 spinal muscular atrophy patients. *J Neurol.* 2019;doi:10.1007/s00415-019-09646-w.
29. Budzik JF, Balbi V, Verclytte S, Pansini V, Le Thuc V, Cotten A. Diffusion tensor imaging in musculoskeletal disorders. *Radiographics.* 2014;34(3)doi:10.1148/rg.343125062.
30. Oudeman J, Nederveen AJ, Strijkers GJ, Maas M, Luijten PR, Froeling M. Techniques and applications of skeletal muscle diffusion tensor imaging: A review. *J Magn. Reson. Imaging.* 2016. doi:10.1002/jmri.25016.
31. Williams SE, Heemskerk AM, Welch EB, Li K, Damon BM, Park JH. Quantitative effects of inclusion of fat on muscle diffusion tensor MRI measurements. *J Magn Reson Imaging.* 2013;38(5):1292-1297. doi:10.1002/jmri.24045.
32. Hooijmans MT, Damon BM, Froeling M, et al. Evaluation of skeletal muscle DTI in patients with duchenne muscular dystrophy. *NMR Biomed.* 2015;28:1589-1597. doi:10.1002/nbm.3427.
33. Monte JR, Hooijmans MT, Froeling M, et al. The repeatability of bilateral diffusion tensor imaging (DTI) in the upper leg muscles of healthy adults. *Eur Radiol.* 2020;doi:10.1007/s00330-019-06403-5.

34. Heemskerk AM, Strijkers GJ, Drost MR, Van Bochove GS, Nicolay K. Skeletal muscle degeneration and regeneration after femoral artery ligation in mice: Monitoring with diffusion MR imaging. *Radiology*. 2007;doi:10.1148/radiol.2432060491.
35. Barp A, Carraro E, Albamonte E, et al. Muscle MRI in two SMA patients on nusinersen treatment: A two years follow-up. *J Neurol Sci*. 2020;doi:10.1016/j.jns.2020.117067.
36. Anneriet M, Heemskerk, Bruce M. Damon. Diffusion Tensor MRI Assessment of Skeletal Muscle Architecture. *Curr Med Imaging Rev*. 2007;doi:10.2174/157340507781386988.



CHAPTER V

Quantitative MR neurography of the sciatic nerve in patients with spinal muscular atrophy: a longitudinal study during nusinersen treatment

Louise A.M. Otto¹, M. Froeling², Ruben P.A. van Eijk^{1,3}, Fay-Lynn Asselman¹,
Inge Cuppen⁴, J. Hendrikse², W.L. van der Pol¹

1 Department of Neurology, UMC Utrecht Brain Center, University Medical Center Utrecht, Utrecht University, Utrecht, The Netherlands

2 Department of Radiology, University Medical Center Utrecht, Utrecht University, Utrecht, The Netherlands

3 Biostatistics & Research Support, Julius Center for Health Sciences and Primary Care, University Medical Center Utrecht, Utrecht University, Utrecht, The Netherlands

4 Department of Neurology and Child Neurology, UMC Utrecht Brain Center, University Medical Center Utrecht, Utrecht University, Utrecht, The Netherlands

Submitted

ABSTRACT

Introduction New treatment strategies for spinal muscular atrophy (SMA) have been shown to improve motor function in a subgroup of children and adults, but a proportion does not respond to treatment. Sensitive outcomes measures that are able to monitor treatment effects at an early stage, such as potentially quantitative MRI, could help to understand the heterogeneity in treatment response.

Methods We applied a MR neurography protocol, consisting of DIXON, T2 mapping, DTI and proton density, in a cross-sectional cohort of 16 treatment-naïve children and adults with SMA, and explored associations between MRN parameters and clinical characteristics: HFMSE and measures of muscle strength. We subsequently applied the protocol longitudinally in 7 young children receiving nusinersen treatment before starting treatment, and after the 4th and 6th injection of nusinersen.

Results The cross-sectional area (CSA) of the sciatic nerve increased with age in SMA patients ($R=0.76$, $p<0.001$) and showed a moderate correlation with HHD results ($R=0.38$, $p=0.045$). AD correlated with HFMSE score and MRC sum score of hamstrings/adductors ($R=0.48$, $p=0.012$ and $R=0.42$, $p=0.023$). None of the qMRN parameters changed over the course of one year of treatment, despite increase in clinical scores.

Conclusion Quantitative MR neurography of the sciatic nerve was feasible in adults and children with SMA and showed correlation with clinical characteristics. The added value of qMRN markers in the evaluation of treatment in SMA remains to be demonstrated in future studies of larger sample size.

Keywords spinal muscular atrophy, nusinersen, magnetic resonance neurography, diffusion tensor imaging

Abbreviations AD, axial diffusivity; ALS, amyotrophic lateral sclerosis; CMAP, compound muscle action potential; CMT1, Charcot-Marie-Tooth disease type 1; CSA, cross-sectional area; DTI, diffusion tensor imaging; EPG, extended graph; FA, fractional anisotropy; HHD, hand-held dynamometry; HFMSE, Hammersmith Functional Motor Scale, Expanded; MD, mean diffusivity; MLPA, multiplex ligation-dependent probe amplification; MRC, Medical Research Council; MRN, magnetic resonance neurography; N, Newton; PCA, principal component analysis; PD, proton density; RD, radial diffusivity; SD, standard deviation; SE-EPI, spin-echo echo planar imaging; SMA, spinal muscular atrophy; SMN, survival motor neuron; SNR, signal to noise ratio; SPAIR, spectral attenuated inversion recovery; SPIR, spectral presaturation with inversion recovery; TSE ,turbo spin-echo; qMRI, quantitative MRI; qMRN, quantitative MRN

INTRODUCTION

Hereditary proximal spinal muscular atrophy (SMA) is the most common genetic cause of infant death and significant disability later in life. It is caused by the deletion or loss of function of the *SMN1* gene resulting in cellular SMN protein deficiency. A point mutation in exon 7 of the second, highly homologous *SMN 2* skews splicing of pre-mRNA towards an mRNA that lacks exon 7, next to a smaller fraction of full length mRNA that ensures residual full-length SMN protein production. *SMN2* copy number variation inversely correlates with disease severity and explains a large part of the variability seen in SMA.(1,2)

Spinal cord alpha-motor neurons are the most susceptible cell type for SMN deficiency, despite the fact that SMN protein is ubiquitously expressed and involved in multiple generic cellular functions.(3) Alpha-motor neuron loss, axonal degeneration and neuromuscular junction dysfunction are important characteristics of motor unit pathology in SMA and explain the often severe and progressive muscle atrophy and weakness.(4) New treatment strategies that target *SMN2* are the antisense oligonucleotide nusinersen and the small molecule Risdiplam, and have been shown to improve motor function in a subgroup of children and adults with SMA.(5,6)

A significant proportion of patients does not respond to treatment in terms of muscle strength or motor function improvement.(7,8) Sensitive outcomes measures that are able to monitor treatment effects at an early stage could help to understand the heterogeneity in treatment response. Quantitative magnetic resonance imaging (qMRI) is a technique that can be applied to study tissue properties *in vivo* before or during treatment, as has been demonstrated by imaging studies of the cervical spinal cord and skeletal muscle. (9–12)

Quantitative MRI has also been applied to analyze peripheral nerves and provides insight in the microstructural properties of nerve. Thus far, pilot studies showed that quantitative MR neurography (qMRN) can detect peripheral nerve atrophy in SMA. A number of modalities, i.e. magnetization transfer ratio, apparent T2-relaxation time and proton spin density, have been proposed as novel imaging biomarkers that require additional validation studies. (13,14) Diffusion tensor imaging (DTI) is a tool to study microstructure of tissue and has been applied in peripheral neuropathies(15–17) including CMT1 and in amyotrophic lateral sclerosis (ALS),(18,19) where it appeared sensitive to detect disease progression and increased axonal degeneration within a time period of 6 months.(19)

To explore quantitative MR neurography as potential monitoring biomarker for treatment effects in SMA, we conducted an exploratory study on the sciatic nerve in two cohorts of SMA patients, i.e. one with and one without nusinersen treatment. First, we established our MRN protocol, consisting of DIXON, T2 mapping, DTI and proton density, in a cross-sectional cohort of 16 treatment-naïve children and adults. We explored associations between MRN parameters and clinical characteristics. Our secondary aim was to evaluate the feasibility of the MR protocol longitudinally in 8 young children receiving nusinersen treatment, before start of treatment and after the 4th and 6th injection of nusinersen.

METHODS

Patients

We enrolled 16 patients with SMA and genetically confirmed *SMN1* loss of function. Six had SMA type 2 (onset between 6-18 months and highest acquired motor milestone 'independent sitting') and 10 with SMA type 3 (onset after 18 months and highest acquired motor milestone 'independent walking'). Mean age was 17.0 years (age range 7.6-54.7 years). From this cohort (further referred to as cohort 1- the cross-sectional cohort), we followed up on 7 pediatric patients that would frequent the hospital for treatment with nusinersen (cohort 2 – longitudinal cohort). These 7 patients were longitudinally followed at the 4th and 6th intrathecal injection with nusinersen (see flowchart in figure 1). This group consisted of 4 children with SMA type 2 and 3 with SMA type 3 (mean age 8.3, range 7.6-9.4 years). Patients were included from an age older than 6 years, and for longitudinal analysis, when 3 measurements points were available; see complete individual data in figure 4. Exclusion criteria were orthopnea, pronounced swallowing disorders that would put at risk for asphyxia during scanning, any type of invasive ventilation, non-MR compatible material in the body or other contra-indication for 3T MR. Patients' characteristics of the two cohorts are summarized in table 1.(20)

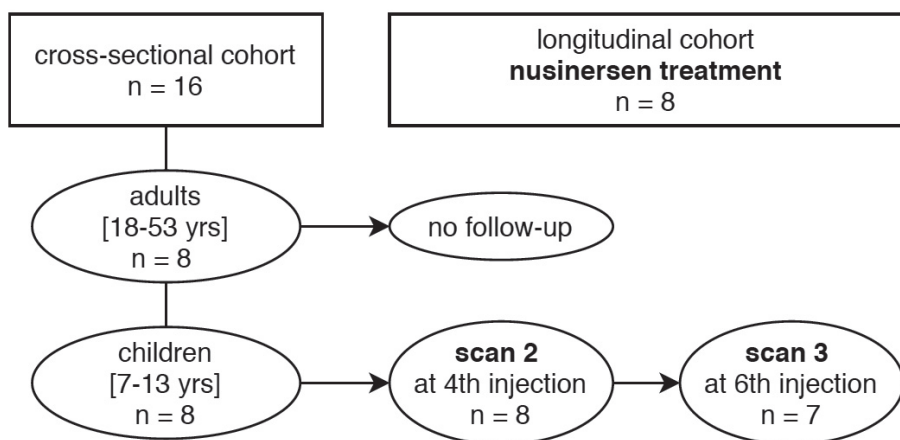


FIGURE 1 flowchart study procedure

Table 1 Patient characteristics

Parameter	SMA population n = 16 <i>cross-sectional cohort</i>	SMA – children n = 7 <i>longitudinal cohort</i>
Age [yrs] (range)	22.8 ± 17.3 (7.7 – 54.8)	8.3 ± 0.7 (7.7 – 9.4)
Sex [m:f]	9:7	4:3
SMA subtype (type 2 : type 3)	6:10	4:3
Disease duration [months]	208 ± 174	85 ± 9.0
SMN2 copy number		
[n patients]		
3 copies	7	5
4 copies	8	2
5 copies	1	0
HFMSE score *(range 0-66)	34 ± 22	32 ± 16
MRC sum score (range 2-10)	6.8 ± 1.8	7.2 ± 1.5
<i>Adductors/hamstrings</i>		
HHD [N] (range)	92.8 ± 90.5 (0.0 – 303.1)	40.8 ± 21.5 (0.0 – 66.3)

Legend: * = one observation missing; HFMSE = Hammersmith Functional Motor Scale, Expanded, f= female, m = male, MRC = Medical Research Council, n = number, N = Newton, yrs = years. SMN2 copy number was determined with MLPA.

Clinical assessment

All patients underwent clinical testing, either at least 2 hours prior to scanning to not affect the MR examination, or following scanning. The clinical assessment consisted of evaluation of motor function with the Hammersmith Functional Motor Scale Expanded (HFMSSE) and of muscle strength of the lower legs with the Medical Research Council (MRC) Scale and hand-held myometry (MicroFet2; Hoggan Health Industries Inc. USA). The HFMSSE was administered in adult patients by a trained evaluator (LO), pediatric patients were evaluated by two trained physiotherapist; before the 1st injection and after the 4th (i.e. 2 months) and 5th injection (i.e. approximately 6 months). Additionally, LO assessed muscle strength at each scanning visit for all patients, for treated children this consisted of testing at the 1st, 4th and 6th injection (i.e. after 10-12 months) - either prior to the injection or after the MR examination on the same day. Muscle strength is reported as sum score of the hamstrings and adductors of both legs, as the muscles of these groups (m. semitendinosus, m. semimembranosus, m. biceps femoris and m. adductor magnus) are innervated by the sciatic nerve.

MR acquisition

MR datasets of left and right sciatic nerve at the thigh level were acquired on a 3T MR Scanner (Ingenia, Philips, Best, the Netherlands). Patients were scanned feet-first in supine position with a 12-channel receiving coil and 16-channel anterior body coil. The protocol had a duration of 9:45 minutes and consisted of the following sequences:

- i. Proton density (PD) weighted turbo spin-echo (TSE) for anatomical reference (TR/TE 2041/15 ms; field of view 403 x 352 mm²; matrix size 672 x 585; acquisition voxel size 0.6x0.6x4mm³; reconstruction voxel size 0.3x0.3x4mm³; slice gap 1mm; 17 slices, SPAIR fat suppression, SENSE with Partial Fourier reconstruction);
- ii. Four-point DIXON to determine the fat content of the nerve (TR/TE/210/2.6/3.36/4.12/4.88 ms; flip angle 10°; voxel size 6x1.5x1.5 mm³; no gap; 25 slices);
- iii. T2 mapping (17 echoes TR/TE/ΔTE 4598/17/7.6 ms; flip angle 90/180°; voxel size 6x3x3 mm³; slice gap 6mm; 13 slices, no fat suppression);
- iv. SE-EPI sequence to acquire DTI parameters (TR/TE 5000/57 ms; b-values: 0 (1), 1 (6), 10 (3), 25 (3), 100 (3), 200 (6), 400 (8) and 600 (12) s/mm²; voxel size 6x3x3 mm³; 25 slices without gap; SPAIR and SPIR fat suppression).

MR processing

We processed data using a custom pipeline (QMRI Tools for Mathematica – m.froeling.github.io/QMRITools). We checked data for data quality and motion artifacts. The processing steps have been described in previous work.(21) In short, DIXON was reconstructed with an IDEAL method with estimation of B_0 and T_2^* , T_2 mapping with an extend graph (EPG) fitting and DTI with iWLLS fitting with REKINDLE outlier detection and principle component analysis (PCA) for denoising and obtaining the signal to noise (SNR) ratio, and data was corrected for eddy current distortion and subject motion.

We segmented the sciatic nerve on the PD-sequence that provided anatomical reference for bilateral segmentation with the use of ITK-snap(22) (version 3.6)(see figure 2). Then, segmentations were transformed using rigid, affine and b-spline registration to the image space of the quantitative sequences DTI, T_2 mapping and DIXON. Transformation was checked visually by two authors (MF, LO) for the whole the image stack to rule out misalignment.

5

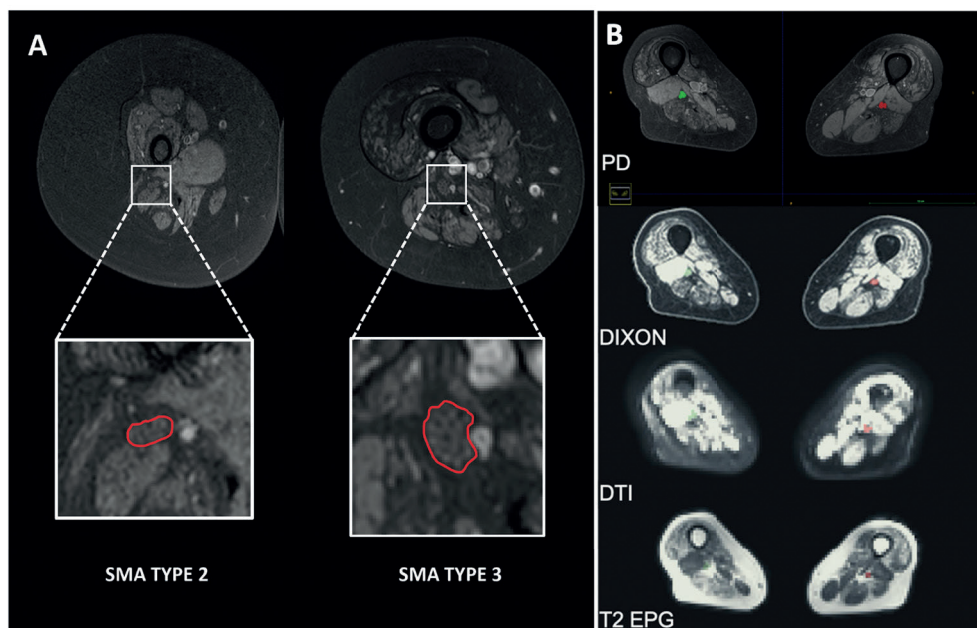


FIGURE 2 Nerve segmentation and mask overlay on other sequences. Panel A shows the sciatic nerve in the right leg in two subjects with SMA, type 3 and type 2. The insert gives the enlarged picture of the nerve with the outer edges circled in red. Panel B depicts the mask of the nerve in the PD sequence, and consecutively transformed to the other image spaces DIXON, DTI and T_2 -EPG

Statistical analysis

Differences in clinical scores between type 2 and type 3 was examined with a student's t-test. We explored the relation of qMR metrics with clinical scores in the cross-sectional cohort with linear regression and Pearson's correlation formula. Then, we determined the rate of change in qMRN parameters during the first year of treatment with a linear mixed model that incorporated time since baseline as fixed effect, and a random intercept for patients using an unstructured covariance matrix. P-values were determined using the likelihood ratio test.

RESULTS

Clinical characteristics

We obtained HFMSE scores from all but one patient. SMA patients exhibited a broad range on the HFMSE score (see table 1). There was no significant linear relation between age and HFMSE score ($R=-0.05$, $p=0.8$). The sum MRC score of adductors and hamstrings was not significantly different for type 2 (mean 5.7, range 2-8 points) versus type 3 patients (mean 7.3, range 6-8 points, $p=0.08$). HHD results were significantly lower in type 2 compared to type 3 patients (mean 31 ± 27 N, range 14-66 N versus 125 ± 96 N, 19-303 N, respectively, $p<0.001$). There was no significant correlation between HHD results and age ($R=0.20$, $p=0.3$).

Children from cohort 2 scored between 2 and 53 points on the HFMSE scale at the start of the treatment and demonstrated a yearly increase of +2.5 points (SE 0.6, $p<0.001$). Muscle strength of hamstrings and adductors remained stable after the 6th injection on the MRC scale (baseline 7.2, $p=0.41$), HHD results of hamstrings/adductors showed an improvement (+19 N, SE 4.1, baseline 41 N, $p<0.001$).

MR acquisition and processing

All but one patient was scanned on the same MR scanner. All data was checked visually. In total, we included 16 datasets for cross-sectional analysis and 21 datasets for longitudinal analysis of treatment. Segmentation of both nerves was successful in 23 of the 27 cases, we obtained unilateral measurements in 4 cases because of motion distortion. There was no misalignment upon visual inspection.

MR metrics of the cross-sectional cohort

Table 2 shows the mean value of each of the quantitative MRN parameters. The cross-sectional area (CSA) of the sciatic nerve increased with age in SMA patients ($R=0.76$, $p<0.001$). Figure 3 shows that this strong correlation is comparable for type 2 and type 3 ($R=0.71$, $p=0.02$ and $R=0.76$, $p<0.001$), although type 2 exhibited a lower cross-sectional area of the nerve at younger age and the subsequent increase was less. Furthermore, CSA showed a moderate but significant positive correlation with HHD results ($R=0.38$, $p=0.045$), but not with HFMSE and MRC sum score of adductors and hamstrings. Table 3 presents the correlation values of MR metrics and clinical data.

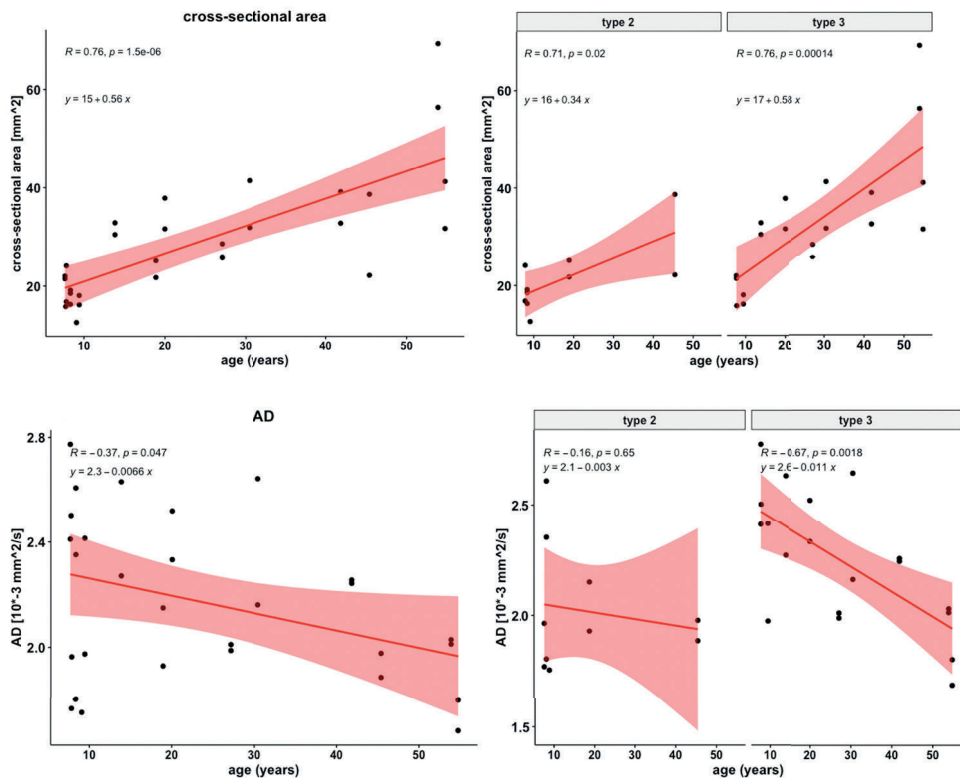


FIGURE 3 MR parameters CSA and AD across age in SMA. Regression plot with R and line function for the cross-sectional population (left column) and subdivided into SMA type 2 and type 3 (right column). The top row represents the plots for the cross-sectional area, and the bottom row for axial diffusivity (AD)

There was no significant correlation of fat fraction and age or clinical scores. T2 mapping of nerve was not related with age ($R=-0.01$, $p=0.98$), and not significantly correlated with HF MSE score and MRC sum score of hamstrings/adductors ($R=-0.37$, $p=0.058$ and $R=-0.35$, $p=0.061$, respectively). Of the DTI parameters, AD was the sole parameter that showed a significant decrease with age ($R=-0.37$, $p=0.047$). Furthermore, AD correlated with HF MSE score and MRC sum score of hamstrings/adductors ($R=0.48$, $p=0.012$ and $R=0.42$, $p=0.023$). The other parameters FA, MD and RD demonstrated decrease with age, although this was not statistically significant. MD showed a positive significant correlation with MRC sum score of hamstrings/adductors ($R=0.38$, $p=0.040$). FA and RD were not significantly associated with clinical scores.

Table 2 – Means of quantitative MRN parameters

Parameter – Mean ± SD	Cross-sectional Cohort n = 16	Nusinersen cohort – baseline n = 7	Nusinersen cohort – at 4 th injection* n = 7	Nusinersen cohort – at 6 th injection** n = 7
Follow-up duration [days] (range)	N/A	0 (0)	75 ± 55 (48 – 200)	351 ± 48 (280 – 422)
CSA [mm²]	29.0 ± 12.7	18.3 ± 3.3	18.3 ± 3.5	18.7 ± 2.2
T2 [ms]	26.5 ± 3.0	25.6 ± 2.0	25.6 ± 2.2	26.3 ± 2.0
Fat fraction [%]	47.7 ± 9.3	50.6 ± 7.9	48.9 ± 13.4	48.1 ± 6.9
DTI – FA	0.49 ± 0.1	0.49 ± 0.1	0.51 ± 0.1	0.50 ± 0.1
DTI – MD [x10⁻³mm²/s]	1.37 ± 0.2	1.41 ± 0.3	1.42 ± 0.2	1.35 ± 0.2
DTI – AD [x10⁻³mm²/s]	2.17 ± 0.3	2.21 ± 0.4	2.27 ± 0.3	2.15 ± 0.4
DTI – RD [x10⁻³mm²/s]	0.98 ± 0.2	1.00 ± 0.3	1.00 ± 0.2	0.95 ± 0.2

Legend: * follow-up duration 74 ± 49 days (range 48 – 200 days); ** follow-up duration 351 ± 48 days (range 280 – 422 days); AD= axial diffusivity, CSA = cross-sectional area, FA = fractional anisotropy, MD= mean diffusivity, mm= millimeter, ms= millisecond, N/A = not applicable, n= number of patients in cohort, RD = radial diffusivity, s= second, SD = standard deviation.

Table 3 – Correlation matrix of MRI metric and clinical characteristics

	Age [yrs]	HFMSE	MRC sum adductors/ hamstrings	HHD sum adductors/ hamstrings
CSA [mm²]	0.76* (<0.001)	0.14 (0.49)	0.03 (0.87)	0.38* (0.045)
T2 [ms]	-0.01 (0.97)	-0.37 (0.058)	-0.35 (0.061)	-0.10(0.61)
Fat fraction [%]	0.14 (0.47)	-0.35 (0.070)	-0.13 (0.49)	-0.27 (0.16)
DTI – FA	-0.21 (0.29)	0.06 (0.77)	-0.04 (0.83)	0.02 (0.91)
DTI – MD	-0.25 (0.19)	0.37 (0.060)	0.38* (0.040)	0.18 (0.35)
[x10⁻³mm²/s]				
DTI – AD	-0.37* (0.047)	0.48* (0.012)	0.42* (0.023)	0.25 (0.20)
[x10⁻³mm²/s]				
DTI – RD	-0.12 (0.53)	0.23 (0.26)	0.29 (0.13)	0.10 (0.59)
[x10⁻³mm²/s]				

Legend: * = threshold for significance is set at $p < 0.050$, AD= axial diffusivity, CSA = cross-sectional area, FA = fractional anisotropy, HFMSE = Hammersmith Functional Motor Scale, Expanded, HHD = hand-held dynamometry, MD= mean diffusivity, mm= millimeter, ms= millisecond, MRC = Medical Research Council, RD = radial diffusivity, s= second, yrs= years

MR metrics of patients on treatment

The slope of each MR metric in treated patients is presented in table 4. Patients receiving treatment showed no significant increase in cross-sectional area (+0.7 mm², $p=0.39$). T2 values remained stable over the course of one year (change of +0.85 ms, $p=0.23$) and fat fraction demonstrated a non-significant decrease (-2.0%, $p=0.40$). None of the DTI parameters showed significant changes over one year. All DTI parameters tended to decrease over the course of one year of treatment. The change of CSA and AD in subjects during treatment is illustrated in figure 4.

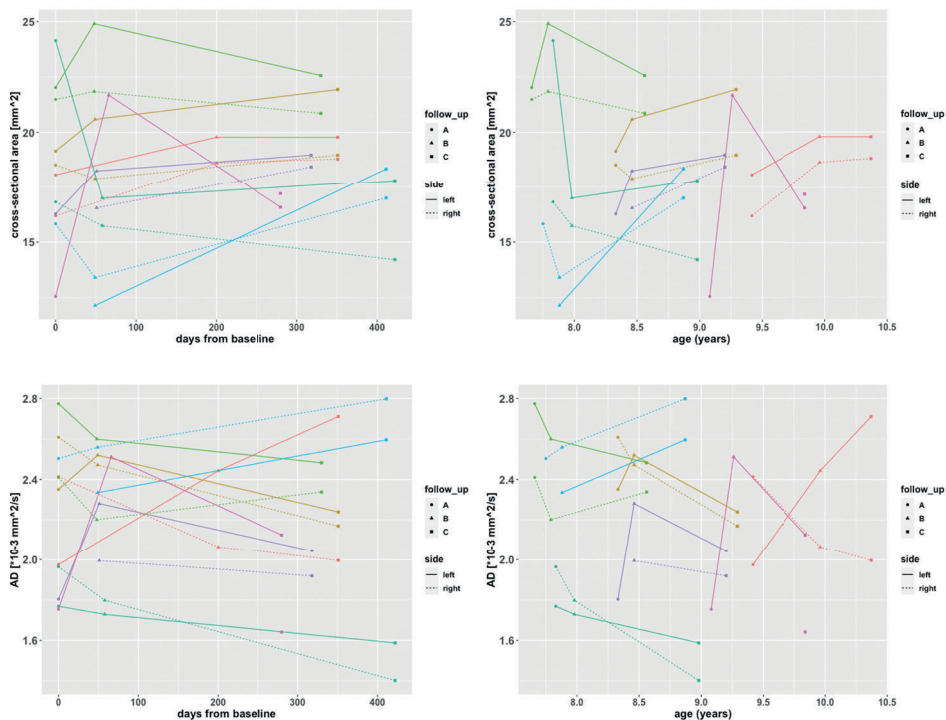


FIGURE 4 Longitudinal change of CSA and AD of treated patients. Trajectory of cross-sectional area (CSA -top row) and axial diffusivity (AD - bottom row) over the course of time since baseline (left column) and of increasing age (right column). Measurements of the left side are represented by the dotted line, and of the right side as continuous line, each subject has its distinct color. The follow-up period is indicated by the round (time-point A), the triangular (B) and the rectangular (C) shape

DISCUSSION

In this study we explored multiple quantitative MR parameters of the sciatic nerve in a cohort of treatment-naïve patients with SMA with a wide age range (7-53 years) and a second cohort of children who were treated with nusinersen. The association of cross-sectional area and of AD with clinical characteristics in treatment naïve patients suggested that qMRN might have biomarker value for monitoring disease progression or treatment effects. However, MR parameters of nerve did not exhibit a linear pattern during treatment in children. We noticed improvements in clinical scores that were not accompanied by significant changes in quantitative MRN markers nor for the nerve cross-sectional area.

In healthy subjects the sciatic nerve is a big structure that is well identifiable on DIXON and shows bright with DTI on the lower b-values, contrasting with its surroundings. In

patients we observed nerve atrophy and an altered anatomy that impeded identifying the sciatic nerve on these sequences. We thus selected the high-resolution PD sequence as reference data for segmentation. The transformation of the mask to fit each sequence allowed us to obtain the quantitative measures of the nerve. The transformation to another image space introduces a small deviation in the mask, that could be missed upon visual inspection. However, the match of our MR data with reference values from other research on sciatic nerve emphasizes the correct positioning of the mask.(18,19,23,24)

Nerve atrophy has been established as a feature of motor neuron disease, including ALS and SMA.(13,25) Kollmer et al. demonstrated with quantitative MR neurography that nerve cross-sectional area (CSA) was significantly reduced in the upper and lower leg of SMA patients compared to age and gender-matched controls.(13,14) As these studies measured at different segments of the sciatic nerve and nerve thickness varies per segment, direct comparison of cross-sectional area results was not possible. More so, there is little data on nerve thickness in children.(26,27) Based on our data we cannot fortify whether we have demonstrated nerve atrophy in SMA due to the lack of healthy controls. Nonetheless, the positive correlation between CSA and age in SMA implies that, in spite of assumed nerve atrophy, the sciatic nerve maintained the ability to grow over time, as seen in healthy subjects.(28) CSA did not correlate with measures of motor function or muscle strength scored with the MRC scale, in line with previous research.(14) but was positively associated with muscle strength on a continuous scale measured with HHD. Children who received treatment exhibited an increase in CSA (+0.8 mm²/year). This is in line with the determined increase of 0.6 mm² per year based on cross-sectional data and could be either partly explained by physiological aging, as we established a positive correlation of nerve area and age in SMA, or by potential treatment effects on nerve structure. The similarity of the trajectories of the nerves of each subject (figure 4) suggests that either of the hypotheses occur simultaneously and symmetrically. Nonetheless, the improvement in clinical scores was not reflected in a significant increase in CSA. CSA is considered a semi-quantitative measure and can be user biased. Its potential as a biomarker therefore remains undetermined.

None of the DTI parameters changed significantly in children during treatment. This could be due to the misrepresentation of DTI properties of younger subjects, as we demonstrated that this did not follow a linear pattern with increasing age. There are few reference studies for nerve DTI parameters in young, growing children. Although no longitudinal studies are available, MR neurography in young adolescents showed indeed a greater dependence on demographic determinants (such as weight and height) compared to adults, which

is probably due to body development.(27) Other studies on nerve DTI in peripheral nerve disease or injury have mostly described FA as parameter sensitive to change. FA of nerve gradually decreases with physiological aging, and a decrease indicates axonal degeneration in disease conditions.(29–31) Furthermore, FA together with RD marked the regenerative phase following nerve injury in rodents and correlated with axonal and myelin regeneration on histology.(32) FA thus theoretically seemed a potential candidate to study axonal degeneration attributed to motor neuron loss in SMA and to evaluate treatment directed at motor neurons. Other research on nerve DTI also described the potential of AD, as it was able to discriminate between ALS and MMN(16), or able to detect changes in nerve roots of the spinal cord in SMA versus healthy controls.(11)

In our study, FA demonstrated no significant changes during treatment. In contrast to FA, AD showed moderate correlation with most clinical parameters. However, the improvements seen in clinical parameters such as HFMSE and HHD during treatment were not paralleled by significant changes in AD. We believe this could be due to a lack of Power.

The limited sample size and the absence of reference data of young children only allows careful conclusions on the trends we witnessed during treatment. The primary recommendation for future studies is extending the sample size in order to validate these preliminary findings, both with patients and with young controls of which the current literature is lacking. Furthermore, we suggest data acquisition at higher resolution to obtain data of greater accuracy, which will probably result in a prolonged scan time.

In the interpretation of DTI results, we identified a potential bias from noise, although the surrounding tissue was suppressed. More so, the CSA of the nerve influences MD and FA results due to partial volume effects of outer voxels surrounding a round structure, like the nerve. In other words, a bigger nerve takes up more volume within a voxel thus eliminating the amount of contaminating signal from the outer corner.(28) In smaller nerves, like in SMA, this imposes challenges for the interpretation of results. Furthermore, electrophysiological assessment could be used to match the MR data, but previous research has already shown that CMAP amplitudes were not related to CSA.(14) Also, CMAP amplitudes do not exhibit a significant decline with age in SMA patients.(33)

Quantitative MR neurography of the sciatic nerve showed association with clinical scores and demonstrated changes of the nerve during treatment. Statements about possible nerve regeneration during treatment are too premature but subtle alterations in cross-sectional area could be an indicator of treatment-related effects. Quantitative MR neurography in SMA has been the interest of recent studies and may have sufficient

sensitivity to determine alterations of the nerve when compared to controls, which has resulted in several promising markers. This study demonstrates the complexity of validating such biomarkers. Possibly, the microstructural changes in the nerve during treatment are too modest to be picked up by qMRN techniques. In contrast, similar quantitative imaging markers (fat fraction, T2 mapping and DTI) demonstrated changes in skeletal muscle during the first year of nusinersen treatment.⁽¹²⁾ Further studies on a larger cohort of treated patients, with nusinersen or other disease modifying therapies, are therefore needed to decide on useful quantitative MRN markers in SMA.

This study served as a pilot experiment to explore the potential of qMRN markers in monitoring treatment effects. Quantitative MR neurography of the sciatic nerve was feasible in adults and children with SMA and showed correlation with clinical characteristics. The added value of qMRN markers in the evaluation of treatment in SMA remains to be demonstrated in future studies of larger sample size.

5

Acknowledgements

We thank all participants from this study and their families. We thank Christa van Ekris for her assistance in this study. This work was supported by Prinses Beatrix Spierfonds (grant number W.OR 16-06) and Stichting Spieren voor Spieren.

Competing Interests

WLP has served as an ad hoc member of the scientific advisory boards of Biogen and Avexis and as a member of a data monitoring committee for Novartis. WLP receives grants from Prinses Beatrix Spierfonds and stichting Spieren voor Spieren. The other authors report no conflicts of interest.

REFERENCES

1. Wadman RI, Jansen MD, Stam M, et al. Intragenic and structural variation in the SMN locus and clinical variability in spinal muscular atrophy. *Brain Commun.* 2020;doi:10.1093/braincomms/fcaa075.
2. Lunn MR, Wang CH. Spinal muscular atrophy. *Lancet.* 2008;371(9630):2120–2133. doi:10.1016/S0140-6736(08)60921-6.
3. Groen EJN, Talbot K, Gillingwater TH. Advances in therapy for spinal muscular atrophy: Promises and challenges. *Nat Rev Neurol.* 2018;14:214–224. doi:10.1038/nrneurol.2018.4.
4. Wadman RI, Vrancken AFJE, Van Den Berg LH, Van Der Pol WL. Dysfunction of the neuromuscular junction in spinal muscular atrophy types 2 and 3. *Neurology.* 2012;doi:10.1212/WNL.0b013e3182749eca.
5. Mercuri E, Finkel RS, Muntoni F, et al. Diagnosis and management of spinal muscular atrophy: Part 1: Recommendations for diagnosis, rehabilitation, orthopedic and nutritional care. *Neuromuscul Disord.* 2018;doi:10.1016/j.nmd.2017.11.005.
6. Mercuri E, Baranello G, Kirschner J, et al. O.41Sunfish part 1: 18-month safety and exploratory outcomes of risdiplam (RG7916) treatment in patients with type 2 or 3 spinal muscular atrophy. *Neuromuscul Disord.* 2019;29doi:10.1016/j.nmd.2019.06.595.
7. Hagenacker T, Wurster CD, Günther R, et al. Nusinersen in adults with 5q spinal muscular atrophy: a non-interventional, multicentre, observational cohort study. *Lancet Neurol.* 2020;doi:10.1016/S1474-4422(20)30037-5.
8. Kariyawasam D, D'silva A, Howells J, et al. Motor unit changes in children with symptomatic spinal muscular atrophy treated with nusinersen. *J Neurol Neurosurg Psychiatry.* 2021;92(1)doi:10.1136/jnnp-2020-324254.
9. Barp A, Carraro E, Albamonte E, et al. Muscle MRI in two SMA patients on nusinersen treatment: A two years follow-up. *J Neurol Sci.* 2020;doi:10.1016/j.jns.2020.117067.
10. Otto LAM, Froeling M, van Eijk RPA, et al. Quantification of disease progression in spinal muscular atrophy with muscle MRI—a pilot study. *NMR Biomed.* 2021;doi:10.1002/nbm.4473.
11. Stam M, Haakma W, Kuster L, et al. Magnetic resonance imaging of the cervical spinal cord in spinal muscular atrophy. *NeuroImage Clin.* 2019;doi:10.1016/j.nicl.2019.102002.
12. Otto LAM, Froeling M, van Eijk RPA, et al. Quantitative muscle MRI in monitoring disease progression and nusinersen treatment effects in spinal muscular atrophy. *Proc Int Soc Magn Reson Med.* 2021.
13. Kollmer J, Hilgenfeld T, Ziegler A, et al. Quantitative MR neurography biomarkers in 5q-linked spinal muscular atrophy. *Neurology.* 2019;10.1212/WNL.0000000000007945. doi:10.1212/WNL.0000000000007945.
14. Kollmer J, Kessler T, Sam G, et al. Magnetization transfer ratio: a quantitative imaging biomarker for 5q spinal muscular atrophy. *Eur J Neurol.* 2020;doi:10.1111/ene.14528.
15. Heckel A, Weiler M, Xia A, et al. Peripheral nerve diffusion tensor imaging: Assessment of axon and myelin sheath integritye0130833. *PLoS One.* 2015;doi:10.1371/journal.pone.0130833.
16. Haakma W, Jongbloed BA, Froeling M, et al. MRI shows thickening and altered diffusion in the median and ulnar nerves in multifocal motor neuropathy. *Eur Radiol.* 2017;doi:10.1007/s00330-016-4575-0.
17. M.H.J. VR, H.S. G, J. H, W.L. VDP. Diffusion tensor imaging of the brachial plexus in inflammatory neuropathies. *J Neuromuscul Dis.* 2019;doi:http://dx.doi.org/10.3233/JND-199002.

18. Kim HS, Yoon YC, Choi BO, Jin W, Cha JG, Kim JH. Diffusion tensor imaging of the sciatic nerve in Charcot–Marie–Tooth disease type I patients: a prospective case–control study. *Eur Radiol*. 2019;doi:10.1007/s00330-018-5958-1.
19. Simon NG, Lagopoulos J, Paling S, et al. Peripheral nerve diffusion tensor imaging as a measure of disease progression in ALS. *J Neurol*. 2017;doi:10.1007/s00415-017-8443-x.
20. Otto LAM, van der Pol W-L, Schlaffke L, et al. Quantitative MRI of skeletal muscle in a cross-sectional cohort of Spinal Muscular Atrophy patients with types 2-3. *NMR Biomed*. 2020;doi:10.1002/nbm.4357.
21. Otto LAM, Froeling M, Van Den Berg LH, Hendrikse J, van der Pol W-L. Muscle MRI in a cross-sectional cohort of patients with Spinal Muscular Atrophy types 2-3. *J Neuromuscul Dis*. 2019;6(suppl2):S54–S55. doi:10.3233/JND-199002.
22. Yushkevich PA, Piven J, Hazlett HC, et al. User-guided 3D active contour segmentation of anatomical structures: Significantly improved efficiency and reliability. *Neuroimage*. 2006;31(3):1116–1128. doi:10.1016/j.neuroimage.2006.01.015.
23. Bernabeu A, Láopez-Celada S, Alfaro A, Mas JJ, Sánchez-González J. Is diffusion tensor imaging useful in the assessment of the sciatic nerve and its pathologies? Our clinical experience. *Br J Radiol*. 2016;doi:10.1259/bjr.20150728.
24. Mathys C, Aissa J, Zu Hörste GM, et al. Peripheral Neuropathy: Assessment of Proximal Nerve Integrity By Diffusion Tensor Imaging. *Muscle Nerve*. 2013;doi:10.1002/mus.23855.
25. Schreiber S, Vielhaber S, Schreiber F, Cartwright MS. Peripheral nerve imaging in amyotrophic lateral sclerosis. *Clin. Neurophysiol*. 2020;doi:10.1016/j.clinph.2020.03.026.
26. Roux A, Tréguier C, Bruneau B, et al. Localized hypertrophic neuropathy of the sciatic nerve in children: MRI findings. *Pediatr Radiol*. 2012;doi:10.1007/s00247-012-2418-y.
27. Hofstadler B, Bäumer P, Schwarz D, et al. MR Neurography: Normative Values in Correlation to Demographic Determinants in Children and Adolescents. *Clin Neuroradiol*. 2020;30(4)doi:10.1007/s00062-019-00834-9.
28. Vos SB, Jones DK, Viergever MA, Leemans A. Partial volume effect as a hidden covariate in DTI analyses. *Neuroimage*. 2011;doi:10.1016/j.neuroimage.2011.01.048.
29. Wako Y, Nakamura J, Eguchi Y, et al. Diffusion tensor imaging and tractography of the sciatic and femoral nerves in healthy volunteers at 3T. *J Orthop Surg Res*. 2017;doi:10.1186/s13018-017-0690-0.
30. Tanitame K, Iwakado Y, Akiyama Y, et al. Effect of age on the fractional anisotropy (FA) value of peripheral nerves and clinical significance of the age-corrected FA value for evaluating polyneuropathies. *Neuroradiology*. 2012;doi:10.1007/s00234-011-0981-9.
31. Werring DJ, Clark CA, Barker GJ, Thompson AJ, Miller DH. Diffusion tensor imaging of lesions and normal-appearing white matter in multiple sclerosis. *Neurology*. 1999;doi:10.1212/wnl.52.8.1626.
32. Morisaki S, Kawai Y, Umeda M, et al. In vivo assessment of peripheral nerve regeneration by diffusion tensor imaging. *J Magn Reson Imaging*. 2011;doi:10.1002/jmri.22442.
33. Wijngaarde CA, Stam M, Otto LAM, et al. Muscle strength and motor function in adolescents and adults with spinal muscular atrophy. *Neurology*. 2020;95(14):e1988–e1998. doi:10.1212/WNL.0000000000010540.



CHAPTER VI

Can quantitative MRI detect pre-symptomatic abnormalities in SMA? A case-report

Louise A.M. Otto¹, Martijn Froeling², H. Stephan Goedee¹, Boudewijn T.H.M. Sleutjes¹,
Jeroen Hendrikse², W. Ludo van der Pol²

¹ Department of Neurology, UMC Utrecht Brain Center, University Medical Center Utrecht,
Utrecht University, Utrecht, The Netherlands

² Department of Radiology, University Medical Center Utrecht, Utrecht University, Utrecht,
The Netherlands

Submitted

ABSTRACT

Pre-symptomatic treatment of hereditary proximal spinal muscular atrophy (SMA) is increasingly advocated as best practice. However, for a small minority of patients with late onset SMA it is unclear whether the possible gains of chronic pre-symptomatic treatment outweighs the increased burden and the risk of long-term side effects. Biomarkers sensitive enough to reveal the time at which individuals turn from asymptomatic to pre-symptomatic could be helpful to determine the best moment to start treatment. In this case report we describe the use of quantitative MRI (qMRI) of the thigh in an apparently asymptomatic patient. Although qMRI parameters were within the normal range, it revealed the presence of fasciculations. The presence of fasciculations could be an early pre-symptomatic sign that deserves further research.

INTRODUCTION

Hereditary spinal muscular atrophy (SMA) is a rare genetic disease that is caused by the homozygous deletion of the *survival motor neuron (SMN) 1* gene.(110) First symptoms of muscle weakness most often present at birth or during the first years of childhood and result in stalled gross motor development. The (in)ability to achieve specific motor milestones, such as sitting and walking independently is used for clinical classification in infantile/childhood-onset SMA type 1 (non-sitters), type 2 (sitters) and type 3 (walkers). (204) Late (adolescent or adult) onset SMA (classified as type 4) is rare and contributes marginally to SMA prevalence.(205) Variation in the copy number of the second human SMN-gene, *SMN2*, explains a large part of the clinical variation in severity, with an inverse relation between copy number and severity.(206) Late onset SMA is therefore associated with a higher *SMN2* copy number, i.e. at least 4 *SMN2* copies.(205)

Genetic treatment strategies are increasingly used to treat SMA. These include the *SMN2* splicing modifiers Nusinersen (an antisense oligonucleotide) and Risdiplam (a small molecule) and the associated adenovirus (AAV)-based *SMN1* gene therapy named Zolgensma. In symptomatic cases, treatment on average improves survival (type 1) and motor function (types 1-3).(143) Presymptomatic treatment probably improves outcome and is therefore considered crucial for achieving optimal cost-effectiveness. However, it is likely that late-onset SMA poses a dilemma to an early start of treatment strategies that need to be repeated (i.e. Nusinersen and Risdiplam). Presymptomatic treatment of patients with 4 *SMN2* copies or more who could become symptomatic 20 years later would obviously increase patient burden and reduce cost-effectiveness.

Biomarkers that reveal presymptomatic onset of SMA could therefore be helpful to determine the optimal moment to start treatment. We previously developed a quantitative magnetic resonance imaging (qMRI) protocol of the thighs that provides multidimensional insight in SMA pathophysiology. The DIXON sequences allow quantification of fatty replacement of muscle tissue, while diffusion tensor imaging (DTI) documents atrophy of viable muscle tissue.(192) We here describe the application of qMRI in an adult pre-symptomatic patient with a homozygous *SMN1* deletion and 4 *SMN2* copies.

Case report

The patient is a 21-year-old man who had been genetically screened for *SMN1* deletion after birth because of a positive family history for SMA on mother's side (infantile-onset type 1 in a cousin and another family member with mild, type 3 form SMA). He had not experienced complaints of muscle weakness. He had normal gross motor development

and exercised without complaints. He reported an episode of spontaneous twitching of the limbs for which further neurological work-up (epilepsy in particular) had not provided an explanation. He was referred for treatment advice shortly after the news about Nusinersen reimbursement in the Netherlands became public. On neurological examination, there were no signs of muscle weakness or areflexia, nor of tongue fasciculations. We observed a mild tremor of the fingers. Genetic testing showed a homozygous deletion of the *SMN1* gene and the presence of 4 *SMN2* copies. Nerve conduction studies of the median and ulnar nerve showed normal compound action potential (CMAP) amplitudes. Evaluation of isokinetic strength and muscular endurance of the quadriceps/hamstrings and the biceps/triceps with a Biodex System 4 pro dynamometer (Biodex Medical Systems, Inc., Shirley, NY, USA) showed to be normal.

Quantitative muscle MRI

He underwent an MR examination of thigh muscles on a 3T MR scanner (Philips Ingenia, Philips Medical Systems, Eindhoven, The Netherlands). The MR protocol was extensively described elsewhere(154). Briefly, the protocol included a fourpoint Dixon sequence (TR/TE/210/2.6/3.36/4.12/4.88 ms; flip angle 10°; voxel size 6 × 1.5 × 1.5 mm³; 25 slices; no gap); T2 mapping (17 echoes TR/TE/ΔTE 4598/17/7.6 ms; flip angle 90/180°; voxel size 6 × 3 × 3 mm³; slice gap 6 mm; 13 slices; no fat suppression) and DTI spin echo echoplanar imaging (TR/TE 5000/57 ms; bvalues 0 (1), 1 (6), 10 (3), 25 (3), 100 (3), 200 (6), 400 (8) and 600 (12) s/mm²; voxel size 6 × 3 × 3 mm³; 25 slices; no gap; spectral attenuated inversion recovery (SPAIR) and spectral presaturation with inversion recovery (SPIR) fat suppression). The total scan time was ~10 minutes.(172) Segmentation of thigh muscles was performed as described previously.(192) In short, the out-phase image of the DIXON sequence was used for manual segmentation with open-source software (ITK-SNAP version 3.6(135)) of 12 individual thigh muscles on the 25 slices of the image stack, accounting for 24 analyzed muscles per subject. From these, we extracted well-established MR parameters including fat fraction, T2 time of muscle tissue and the diffusion metrics fractional anisotropy (FA) and mean diffusivity (MD) (table 1). We checked for motion artifacts and noticed signal voids, indicating fasciculations or contractions caused by activations of the motor unit. For each voxel, fasciculation of contractions were quantified according to the method described by Steidle et al. using the data with a b-value > 150 s/mm².(207) For every slice, clusters of activation were selected that existed of at least 4 connecting voxels. Finally, the total number of clusters and their size were calculated.

We used qMRI data from 4 previously enrolled healthy control subjects (males, mean age 27.8 yrs [24-31.5]) that were scanned on the same scanner as a reference. Their qMRI examination covered the same field of view of the thigh and the total scan time was similar.

Results

Results of qMRI are shown in Table 1. Quantitative MR parameters had a similar range as observed in age and gender matched control subjects. We unexpectedly observed fasciculations during MRI (Figure 1), which resulted in a MR signal attenuation, or 'signal voids', on the diffusion weighted images which is presumably based on intravoxel reordering of tissue water.(207,208) The total count of fasciculations was higher in the SMA subject compared to control subjects.

Table 1 Results MR examination

MR parameter	SMA subject (n=1) mean (SD) [range] N muscles = 24 (left + right)	Control subjects (n=4) (age/gender matched) mean (SD) [range] N muscles = 96
Fat fraction (%)	5.9 (0.9) [3.8-8.2]	6.7 (1.7) [3.6-10.2]
T2 (ms)	28.8 (1.6) [23.4-30.6]	29.3 (0.9) [27.2-31.6]
FA ^a	0.23 (0.03) [0.19-0.30]	0.22 (0.04) [0.15-0.34]
MD ^b (*10 ⁻³ mm ² /s)	1.63 (0.1) [1.38-1.81]	1.53 [0.1] [1.03-1.71]
Fasciculation count	45.5 (69.8) [-]	13.5 (10.9) [-]
Total count	1229	229

^a FA: Fractional anisotropy; ^b MD: mean diffusivity, mm: millimeter, ms: millisecond, s: second, N muscles is defined as the sum of the 12 muscle of the left and right leg

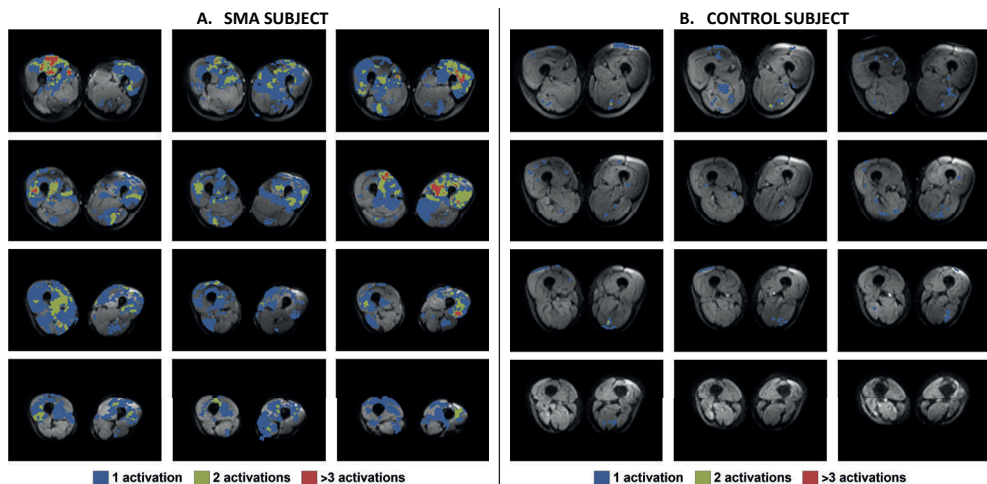


FIGURE 1 Presence of fasciculations in a control subject versus SMA subject. Fasciculation count in the upper leg (proximal to distal) for a control subject (A) versus the SMA subject (B). The number of registered activations is colorcoded and represents the fasciculation count.

Discussion

We used our previously developed qMRI protocol in an individual with a confirmed *SMN1* deletion, a postural tremor and normal muscle strength and motor function. We did not document early signs of SMA pathology on MRI, i.e. fatty infiltration or muscle atrophy, but recorded recurrent fasciculations. This case report indicates that DIXON and DTI sequences may have limited sensitivity to detect pre-symptomatic changes in muscle. Asymptomatic carriership has been described but is rare.(33) Natural history studies of SMA type 3b/4 documented onset from the second decade to 30-40 years of age.(205,209) It is therefore possible that the patient presented here is truly asymptomatic.

qMRI analysis showed frequent fasciculations. Fasciculations can be an early sign of alpha-motor neuron dysfunction that results in spontaneous motor unit firing and subsequent muscle twitching. They are a prominent clinical characteristic of amyotrophic lateral sclerosis (ALS) and other motor neuron disease (MND). Fasciculations in the tongue are a common characteristic in SMA(174). Their presence in other muscles has not been studied in detail in patients with SMA; fasciculations were present in 45% of symptomatic type 4 patients in one study.(209) The presence of fasciculations in pre-symptomatic patients has understandably not been studied at all. Since fasciculations are non-specific for MND and can also occur in healthy subjects, we cannot determine whether their presence is unique for this patient, are characteristic of asymptomatic individuals with homozygous loss of function of *SMN1*, or precede changes in nerve and muscle that may ultimately cause motor function loss. (210,211)

Screening for the presence of fasciculations could be a helpful approach in pre-symptomatic cases in the future. Diffusion weighted imaging can be modeled to study motor unit morphology and function.(212,213) Also, computer-aided ultrasound of muscle, a more versatile technique than qMRI, can be used to detect fasciculations(214,215) which makes them interesting tools for future studies.

Newborn screening for SMA will result in an increasing number of pre- or asymptomatic referrals for treatment. Some authors have argued for early treatment of all cases(143), but this may be at odds with reimbursement policies in some countries. More specifically, the possibility of unnecessary chronic treatment for periods of 10 years or longer may trigger discussions of cost-effectiveness and patient burden. The fact that the presence of 4 copies is associated with a wide range of phenotypes, from 'sitters' (type 2) to adult onset underlines the need for clinical tools that allow an early detection of symptoms, i.e. before weakness sets in.(174) Monitoring of fasciculations could therefore provide an interesting

new approach for pre-symptomatic cases. The patient presented in this case report will therefore be monitored every year with EMG, qMRI, ultrasound and quantitative muscle testing. If applied on a broader scale, this could provide important insights in the sensitivity of such tools for truly pre-symptomatic cases with late onset.

REFERENCES

- Lefebvre S, Bürglen L, Reboullet S, et al. Identification and characterization of a spinal muscular atrophy-determining gene. *Cell*. 1995;80:155–165. doi:10.1016/0092-8674(95)90460-3.
- Zerres K, Davies KE. 59th ENMC International Workshop: Spinal Muscular Atrophies: Recent progress and revised diagnostic criteria 17-19 April 1998, Soestduinen, The Netherlands. *Neuromuscul Disord*. 1999;doi:10.1016/S0960-8966(99)00016-4.
- Piepers S, Van Den Berg LH, Brugman F, et al. A natural history study of late onset spinal muscular atrophy types 3b and 4. *J Neurol*. 2008;doi:10.1007/s00415-008-0929-0.
- Wadman RI, Stam M, Gijzen M, et al. Association of motor milestones, SMN2 copy and outcome in spinal muscular atrophy types 0-4. *J. Neurol. Neurosurg. Psychiatry*. 2017;doi:10.1136/jnnp-2016-314292.
- Schorling DC, Pechmann A, Kirschner J. Advances in Treatment of Spinal Muscular Atrophy - New Phenotypes, New Challenges, New Implications for Care. *J. Neuromuscul. Dis*. 2020;doi:10.3233/JND-190424.
- Otto LAM, Froeling M, Van Den Berg LH, Hendrikse J, van der Pol W-L. Muscle MRI in a cross-sectional cohort of patients with Spinal Muscular Atrophy types 2-3. *J Neuromuscul Dis*. 2019;6(suppl2):S54–S55. doi:10.3233/JND-199002.
- Otto LAM, van der Pol W-L, Schlauffke L, et al. Quantitative MRI of skeletal muscle in a cross-sectional cohort of Spinal Muscular Atrophy patients with types 2-3. *NMR Biomed*. 2020;doi:10.1002/nbm.4357.
- Otto LAM, Froeling M, van Eijk RPA, et al. Quantification of disease progression in spinal muscular atrophy with muscle MRI—a pilot study. *NMR Biomed*. 2021;doi:10.1002/nbm.4473.
- Yushkevich PA, Piven J, Hazlett HC, et al. User-guided 3D active contour segmentation of anatomical structures: Significantly improved efficiency and reliability. *Neuroimage*. 2006;31:1116–1128. doi:10.1016/j.neuroimage.2006.01.015.
- Steidle G, Schick F. Addressing spontaneous signal voids in repetitive single-shot DWI of musculature: Spatial and temporal patterns in the calves of healthy volunteers and consideration of unintended muscle activities as underlying mechanism. *NMR Biomed*. 2015;28(7)doi:10.1002/nbm.3311.
- Schwartz M, Steidle G, Martirosian P, et al. Spontaneous mechanical and electrical activities of human calf musculature at rest assessed by repetitive single-shot diffusion-weighted MRI and simultaneous surface electromyography. *Magn Reson Med*. 2018;79(5)doi:10.1002/mrm.26921.
- Oprea GE, Kröber S, McWhorter ML, et al. Plastin 3 is a protective modifier of autosomal recessive spinal muscular atrophy. *Science* (80-). 2008;doi:10.1126/science.1155085.
- Souza PVS, Pinto WBVR, Ricarte A, et al. Clinical and radiological profile of patients with spinal muscular atrophy type 4. *Eur J Neurol*. 2021;doi:10.1111/ene.14587.
- Wadman RI, Stam M, Gijzen M, et al. Association of motor milestones, SMN2 copy and outcome in spinal muscular atrophy types 0-4. *J. Neurol. Neurosurg. Psychiatry*. 2017. p. 364–367;doi:10.1136/jnnp-2016-314292.
- Sleutjes BTHM, Gligorijević I, Montfoort I, van Doorn PA, Visser GH, Blok JH. Identifying fasciculation potentials in motor neuron disease: A matter of probability. *Muscle and Nerve*. 2016;53(2)doi:10.1002/mus.24712.
- De Carvalho M, Swash M. Cramps, muscle pain, and fasciculations: Not always benign? *Neurology*. 2004;63(4)doi:10.1212/01.WNL.0000134609.56166.15.

Heskamp L, Birkbeck MG, Whittaker RG, Schofield IS, Blamire AM. The muscle twitch profile assessed with motor unit magnetic resonance imaging. *NMR Biomed.* 2021;34(3)doi:10.1002/nbm.4466.

Whittaker RG, Porcari P, Braz L, Williams TL, Schofield IS, Blamire AM. Functional magnetic resonance imaging of human motor unit fasciculation in amyotrophic lateral sclerosis. *Ann Neurol.* 2019;85(3) doi:10.1002/ana.25422.

Gijsbertse K, Bakker M, Sprengers A, et al. Computer-aided detection of fasciculations and other movements in muscle with ultrasound: Development and clinical application. *Clin Neurophysiol.* 2018;129(12)doi:10.1016/j.clinph.2018.09.022.

Duarte ML, Iared W, Oliveira ASB, dos Santos LR, Peccin MS. Ultrasound versus electromyography for the detection of fasciculation in amyotrophic lateral sclerosis: Systematic review and meta-analysis. *Radiol. Bras.* 2020.doi:10.1590/0100-3984.2019.0055.



CHAPTER VII

General discussion

This thesis explored feasibility of quantitative muscle and nerve MRI as a biomarker for SMA. In an initial pilot study that preceded the work described here, we focused on qMRI of the cervical spinal cord.(1) Although this study showed spinal cord atrophy and DTI changes in cervical nerve roots that correspond with the characteristic pattern of muscle weakness in SMA, continuation of spinal cord qMRI was unattractive for a number of reasons. First, the imaging protocol would require further technical optimization to reduce scanning time to be applicable for clinical practice.

Second, it would be interesting to extend spinal cord imaging to the lower thoracic and lumbar segments, for the latter innervates the more affected lower limbs in SMA. However, imaging these segments is even more challenging as they are more prone to susceptibility artifacts due to the presence of air trapped in lung tissue. Similarly, the presence of spinal rods following scoliosis surgery introduces beam scattering artifacts that impedes image acquisition. Around 34% of our cohort has scoliosis material in situ (reference data of 2019) (2), making spinal cord imaging as potential biomarker applicable to a small proportion of the population, both in research as in clinical setting.

Hence, we extended the imaging projects and our search for quantitative biomarker to other tissues affected by SMA pathology, i.e muscle and peripheral nerve.

Spinal muscular atrophy encompasses a wide range in disease severity. We wanted to assess applicability of muscle qMRI across the broad spectrum of SMA (**chapter 2**) and therefore included patients from 7 years up to 73 years with type 2 and type 3 in a cross-sectional study on muscle involvement and properties of muscle. We did not enroll patients at the extremes of the severity spectrum, i.e. with type 1c and type 4, for reasons of severity and rarity, respectively. Nevertheless, the study provided insight in muscle involvement in SMA across the largest part of the disease spectrum. The progressive nature of SMA was reflected by the more severe fatty infiltration of upper leg muscles in older patients. Patients with SMA type 2 had earlier onset of fatty infiltration and therefore a higher fat fraction in all muscle groups than patients with type 3 at a similar age. The scans confirmed relative vulnerability of muscle tissue; the anterior compartment was conspicuously more fat-infiltrated than the other muscle compartments, which is in agreement with prominent quadriceps weakness seen in patients and with previous imaging reports (3–5), while the hamstrings were relatively spared in patients with SMA type 3.(6) The severe fat infiltration we witnessed in some patients with type 3 did not impede them to walk. Since knee flexors have been identified to be involved in the compensatory gait pattern in SMA patients, progression of fatty infiltration in hamstrings may ultimately lead to loss of ambulation.

(7) Progression of muscle replacement by fat is continuous, eventually leading to total fat replacement, which was already observed in patients with type 2 and type 3a under the age of 30 years. However, and as outlined below, the data may suggest that fat replacement, when set in motion, arrives at a tipping point beyond which muscle tissue continues to be replaced even after the start of treatment. This would imply that optimizing treatment primarily depends on an early start.

The SMA literature tends to emphasize differences between type 2 and 3, or non-walkers and walkers. However, we did not observe a clear distinction in DIXON qMRI between SMA types. In fact, there was less of a distinction between patients who learned to stand but not walk (i.e. 'SMA type 2b') and type 3a than between patients with SMA type 3 with early (type 3a) and late (type 3b) disease onset. This is in line with clinical observations among Dutch patients with SMA type 3. In particular children who learn to walk, but lose ambulation before the age of 10 years have a severity profile later in life that is very similar to patients with type 2b(3,8) , while truly late onset (i.e. type 3b-4) carries a much better prognosis.(9) Our data therefore confirm that disease course is reflected by the quality of muscle tissue.(10)

Muscle weakness in SMA is not uniform but shows a pattern of relative sparing. This is not unique to SMA. Other neuromuscular disease also present with a characteristic selectivity pattern, which actually triggered research to establish muscle MRI as a diagnostic tool.(11) In line with previous observations, we observed relative sparing of the m. adductor longus and gracilis, sartorius, semimembranosus and rectus femoris muscles.(4,12–15) Causes of selective vulnerability of muscle are unknown although the following mechanisms may contribute.

First, selective muscle vulnerability may result from motor neuron pathology or the somatotopic location of motor neuron pools in the spinal cord. Proximal and axial muscles, which are known to be most affected in SMA from clinical and from imaging studies, are located in the medial column.(16) Distal muscles are innervated from the lateral column and are relatively longer preserved.(3–5) Why the medial column would be more vulnerable than the lateral column remains to be clarified.(17,18) Moreover, these are findings from mouse studies and remain to be confirmed in humans. Regardless, clinically, muscle weakness eventually progresses into general involvement, irrespective of the medial and lateral column.(3,17)

The theory of segmental vulnerability has been refuted previously. The general idea was that specific segments of the spinal cord were more vulnerable than others, i.e. C5, C7 and L3-4, corresponding with deltoid, triceps brachii and quadriceps muscles.(3,8) In a more in-depth analysis, we could not corroborate a segmental distribution of muscle weakness based on cross-sectional data of 180 patients.(3)

Differences in innervation density could provide an alternative explanation. Differences in motor unit size of muscles could determine their vulnerability. Reinnervation that follows motor neuron degradation in SMA causes the remaining motor units to enlarge, but is insufficient to compensate for motor unit loss.(19) Muscles with fewer motor units could therefore be more vulnerable and thereby weaker.(20) This would imply that muscles that generally contain larger motor units could be prone to faster deterioration, when subsequent motor unit loss result in more noticeable effects. To the best of my knowledge, there is no atlas of motor unit sizes in the human body. However, it seems plausible that the function of anti-gravity muscles such as triceps brachii and quadriceps would require fewer innervating axons than muscles that need more finetuning, such as muscles for hand function and eye movements. It is interesting that newly developed techniques, such as CMAP scan, may be useful to gain insight in how treatment alters motor unit numbers and sizes.(21) CMAP scan provides information on motor unit composition as 'steps' in the curve that constitute the CMAP obtained during increasing stimulus intensity.(19) The CMAP scan is currently only used for the median nerve and thenar muscles. Broader application of the CMAP scan could contribute to our general understanding of motor unit function in SMA to validate this hypothesis for selective vulnerability but will be technically challenging.

Importantly, muscle itself is affected by SMN deficiency. SMN levels in muscle of SMA patients were reduced compared to controls.(22–24) Mouse studies demonstrate SMN requirements of muscle in the developmental stage that decrease over time. SMA mice present with very low levels of SMN in muscle, already in the presumably pre-symptomatic period.(25) Regardless of the low SMN requirements in muscle compared to motor neurons, SMN depletion has its effects on many levels.

In patients, dysregulated muscle growth and structural alterations were observed.(26–29) In a mouse model, selective depletion of SMN in muscle led to muscle fiber defects, neuromuscular junction abnormalities and poor motor function.(30) Furthermore, Kim et al. showed in mouse models for SMA that selective depletion of SMN in muscle triggers NMJ alterations retrogradely.(30) This strongly implies that SMN depletion in muscle further contributes to the disease, and is not only affected 'upstream' by denervation following

motor neuron stress or death. The restoration of SMN after onset of muscle pathology indeed reversed the disease in mice, which is promising for systemic and muscle-targeted therapies.(30) The mechanisms by which SMN depletion could lead to selective vulnerability remain to be established. SMN protein plays a role in actin regulation and mitochondrial function. We can hypothesize that this causes heterogeneity in vulnerability, based on differences in muscle fiber type distribution or metabolic requirements in muscles. Although there are more questions than answers regarding the role of SMN in muscle function, it seems safe to assume that muscle pathology can only truly be attenuated if SMN repletion strategies reach the muscle too, or other strategies rescue downstream effects of SMN deficiency.

Given the extent of pathological findings in each of the constituents of the motor unit, i.e. the motor neuron, the nerve, the neuromuscular junction and the muscle, it seems more plausible that selective muscle weakness due to SMN deficiency is multifactorial. We have only just begun to understand the vulnerability of motor neurons in SMA, but the paradigm of SMA as pure motor neuron disease has shifted to a systemic and developmental disease. Comparing the effects of targeted therapy, aimed at motor neurons only, versus systemic treatment is crucial to optimize treatment protocols in the future. MRI is one of such modalities that allows examination of tissue, such as muscle and nerve and assessment of their (relative) involvement in SMA pathology. Studying tissue involvement under two conditions, i.e. with and without disease modifying treatment, will give us insight into disease progression at the tissue level, which precedes improvements or deterioration of clinical deficits. Quantitative MR parameters can teach us more about tissue involvement and based on the results of our work we hypothesize that qMRI could serve as a biomarker for disease progression or treatment effect.

Quantification of fat infiltration of muscle

We used the DIXON technique to quantify fat infiltration. This is the best known and most widely used and described qMRI parameter. Manual segmentation allows quantification of the fat content of each muscle individually and has been a big step forward in understanding disease course in other neuromuscular disorders, including Duchenne muscular dystrophy (DMD). In comparison with standard T1-weighted imaging, the DIXON technique allows a better estimation of fat fraction in muscle by differentiating more precisely between water and fat signal.(31,32) It is based on the chemical shift difference of water and fat, and the 4-point DIXON provides 4 images for post-processing which is slightly more accurate than the common 3-point sequence.(33)

Previous smaller imaging studies on muscle involvement in SMA, and quantitative MRI work on DMD suggested that DIXON could be useful to monitor disease progression in SMA. In **chapter 2**, we show that muscles of our included SMA patients had an almost 5-times increased fat content compared to controls (48% fat fraction versus 8%). Fat infiltration was progressive even in one year. This finding is quite striking if one considers that natural clinical history studies suggest that deterioration of muscle *function* can only be detected in much longer intervals, i.e 2-5 years.(34,35) In adults (**chapter 3**), fat fraction increased with 1.3% in one year. As expected, this increase in fat content was not mirrored by a deterioration of motor function on clinical scales. We therefore conclude that the DIXON method detects subclinical disease progression. The natural disease progression in adults is characterized by progressive fatty degeneration at the loss of contractile muscle tissue. Previous work on natural history in children measured an increase in contractile CSA of the thigh in one year that, however, was attributed to growth.(36)

The timelines of fatty infiltration differ between muscle groups. This may explain why we observed a more uniform distribution of fat in patients with more disease progression (unimodal or 'dromedary') and bimodal distribution in patients in better condition ('camel') (Figure 1). This distribution may have biomarker value as will be further explained below.

Figure 1 Distribution of fat infiltration across cohorts – adults & children with SMA

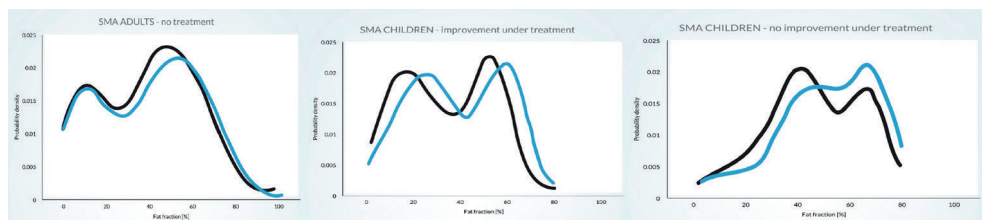


Figure 1 The histogram of fat distribution in adults (left) and treated children (middle and right panel) In adults and in children that improved under treatment (first two panels), we note a bimodal distribution pattern ("camel" like) versus the more uniform pattern ("dromedary") in the last panel in children without improvements on motor scores.

We used the data obtained from treatment-naïve patients as a framework to interpret the changes we observed in children during treatment. This is the best alternative to true, age-matched reference data, as there are little to no longitudinal imaging data of children, while future imaging studies on natural disease progression in treatment-naïve children will become increasingly unlikely. The uniformity of the quantitative imaging protocol of both studies facilitated the comparison of the two cohorts. In children

(**chapter 4**), fat infiltration increase was higher than in adults (+3.1%) during their first year of treatment. In contrast to the situation in adults, this was not at the cost of contractile tissue. We further demonstrated that the rate of fat degeneration differed between muscles. The weakest muscle group, i.e. the quadriceps, showed the greatest increase in fat content whereas the strongest muscle, i.e. the hamstrings, showed less increase of fat infiltration. Interestingly, fatty degeneration was not attenuated by the assumed rescue of motor neurons during nusinersen treatment. Savini et al. also describe progression of fat degeneration during treatment in 3 patients. (37) Despite this ongoing fatty infiltration, we observed (trends towards) motor gains in some children. The children that improved under treatment demonstrated the dichotomy in the distribution of fat content that we observed in adults as well (**chapter 3**). The first peak at low levels of fat (<30%) may indicate a phase in the fatty transformation of muscle when it may still respond to treatment. Also, the two peaks in distribution suggests that fat infiltration may not be a gradual process but could include a tipping-point. The tipping-point concept is further emphasized by a higher yearly increase in fat content of high fat-infiltrated muscles. Based on the observations, this tipping point may lie between 30-40% fat content, although this is not a fixed cut-off value. Rather, we think this indicates a transition from low fat content, a slow phase, to a critical phase that is characterized by faster fatty degeneration. It could be that this transition can be explained by the failure of compensatory mechanisms to prevent further degeneration, such as the recruitment of adjacent motor units during reinnervation. We are the first to notice this pattern and retrospectively also recognize this in datasets of other imaging projects on SMA (unpublished data). We have not seen this specific pattern in Duchenne Muscular Dystrophy.(38) The presence of this bimodal distribution as a specific 'qMRI fingerprint', makes it a possible biomarker for treatment responsiveness that deserves further study. If treatment is indeed more effective on a functional level when a proportion of muscles is still before the tipping point, this could predict treatment success, at least with nusinersen. It would be interesting to investigate whether similar fingerprints can be seen in arm muscles, although this may be more challenging given the limited number of muscle groups. Apart from corroborative studies, it could also be interesting to investigate whether the unimodal or bimodal distribution is a biomarker for success of more systemic (e.g. risdiplam) or combined therapies (e.g. SMN augmentation in combination with anti-myostatin drugs). Finally, from the reimbursement perspective, this biomarker may be promising if regulators would seriously like to pursue 'pay-for-performance' strategies. A uniformly distributed high fat content of thigh muscle could for example be used as a rationale for a significantly reduction of drug prices.

The determination of fat content with DIXON is a robust method and also shows correlation with clinical measures in SMA.(39) More so, fat fraction is consistently sensitive to minor changes in muscle across the projects described in this thesis, whether in terms of treatment-naïve natural disease course or under treatment. Altogether, quantitative imaging with DIXON is a strong candidate biomarker for disease progression and treatment effect. Possibly, fat quantification with DIXON can aid in the timely identification of 'responders' and 'non-responders' to treatment.

Because fat infiltration reflects 'end-stage' disease and does not provide information on the quality of remaining muscle, we also explored other quantitative MR parameters.

Quantification of diffusion in muscle

Diffusion tensor imaging quantifies the diffusion of water molecules. The diffusion of water in tissue is mostly non-isotropic as the mobility of water molecules is hindered by surrounding structures such as nerve sheets, proteins, or cell membranes. The parameter fractional anisotropy (FA) reflects the degree of non-isotropy, approaching 1 when anisotropic and close to 0 when isotropic, as illustrated in Figure 2. Mean diffusivity (MD), radial diffusivity (RD) and axial diffusivity (AD) are all derived directional parameters of diffusion. Together, DTI provides a representation of micro-architecture of a tissue.(40–42)

Figure 2 Diffusion tensor imaging explained

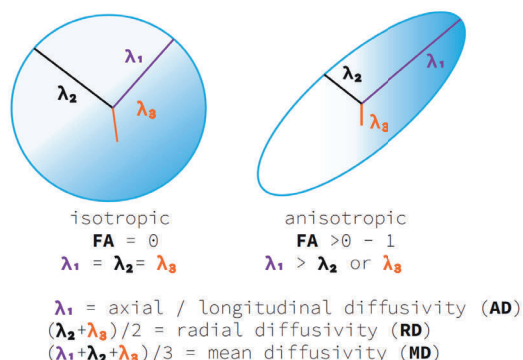


Figure 2 In diffusion tensor imaging, the directionality of diffusion of water molecules is estimated in a three-dimensional model (the tensor). The parameter fractional anisotropy (FA) reflects the degree of non-isotropy, or directional dominance of a region. The FA is close to 0 if diffusion is equal in all directions, such as in a sphere, and is approaching 1 when anisotropic, such as in an ellipsoid. The derived parameters AD, RD and MD are calculated from this tensor model.

In healthy muscle, DTI measures are sensitive enough to detect alterations in muscle already in the 2 days following increased exercise, while no changes on fat-suppressed T2-weighted sequences were noted. (43) This made DTI an interesting application for neuromuscular diseases to capture disease progression. Most of the first studies were done in Duchenne Muscular Dystrophy, in which a strong correlation between DTI values and function was found.(44) DTI had not been applied in SMA when we started this project. We demonstrated that DTI correlates with clinical measures in SMA, which has not been consistently found in, for example, DMD or LGMD.(44,45) More so, we established a similar or even stronger correlation of DTI parameters with clinical scores than we observed for fat fraction, which was the parameter believed to be closest associated with function. This association is even more notable given the small volumes of remaining muscle tissue due to severe fat infiltration in some patients.

Furthermore, we found evidence that the muscle atrophy is reflected by an increased FA and decreased MD. Muscle atrophy is such a characteristic feature of the disease (46) that it is used in the name of the disease. As a marker for muscle microstructure and because of its association with clinical measures(47), DTI seemed promising as measure for disease progression in SMA. However, in our longitudinal study we found no significant changes over the course of one year. This may be in line with the observation that clinical measures remained stable as well, but the fat fraction did increase as an indicator of continuing disease activity. Therefore, we concluded that DTI markers MD and FA were probably not sensitive enough in the setting of slow disease progression in adult patients. It should be noted that clinical outcome measures such as the HFMSE for motor function or MRC sum score of muscle strength are equally insensitive to capture change in a small timeframe in adults in multiple other, smaller cohort studies.(5,9,48,49) However, data from a larger population (approximately 100 patients), i.e. our Dutch cohort study, demonstrates the longitudinal decline of clinical scores and contradicts the hypothesis of relative stability of disease progression.(8) None of the DTI parameters significantly changed within the first year of nusinersen treatment. However, when we looked at DTI values for the three muscle groups separately, we saw significant changes in AD and MD of the hamstrings. It seems like this shift towards normalization of DTI values occurred in the relatively preserved hamstrings which could indicate restoration of microarchitecture in remaining viable muscle tissue. Normalization of DTI values co-occurring with fatty degeneration may seem contradictory. However, similar effects are seen in DMD, i.e. ongoing fat infiltration and muscle hypertrophy, indicate that two distinct pathological processes that can differ between muscle groups.(50) Normalization of DTI

parameters could indicate reversal of atrophy which was not seen in untreated adults and could be a promising effect of treatment.

DTI is therefore still a potential biomarker for disease course, but probably in a younger population with relatively more preserved tissue, or in the monitoring of treatment effects. This could either be either treatment focused on SMN protein level restoration in motor neurons, systemic SMN-augmenting treatment or combinatorial therapy with treatment that targets the muscle specifically, such as with a myostatin-inhibitor. One of the effects seen in mice of this drug combination was the increase in muscle fiber size(51), for which DTI could be sensitive if applied in patients. DTI thus provides multiple measures for aspects of muscle that may change with treatment. DTI is not (yet) specific to determine muscle fiber type, although there has suggestions that higher FA values could be an indication of overrepresentation of type 1 fibers.(52) However, FA elevation is not specific for the presence of type 1 fibers and could be due to other reasons.(41) The determination of fiber type is of particular interest in SMA because research in mice indicated fiber type switching to predominant slow oxidative type 1 fibers in response to muscle atrophy. These changes were restored with an exercise diet.(53) The effects of adaptive changes of fiber type on muscle strength are not clear, contractile property is also determined by the myosin light chain isoforms(54), and observations in mice cannot be generalized to patients. A non-invasive measure of fiber type distribution in patients is particularly interesting to monitor training effects, for example in combination with treatment. MR (phosphor) spectroscopy seems a better alternative to investigate slow- and fast oxidative and glycolytic fibers in muscle, and this has recently been explored in SMA.(55)

Limitations of diffusion tensor imaging

Diffusion tensor imaging reflects local microstructure and anatomy.(56) However, its representation depends on the resolution, which is associated with longer scanning times. Therefore, there is a trade-off between the aimed resolution (ideally, the higher the better), and scanning time (ideally - for the patient, the shorter the better). In our muscle and peripheral nerve studies, the resolution of the DTI sequence was $3 \times 3 \text{ mm}^2$. This was sufficient for muscle imaging, but this was a clear limitation for nerve imaging. In SMA, the nerves are of smaller size due to atrophy. Hence, the resolution covered the course of the nerve roughly, but a higher resolution would have traced it more precisely. Also, when the resolution is less optimal adjusted to size of a round structure such as the nerve, there is the problem with partial volume effects from the outer edges of the squared

voxel. A bigger nerve takes up more volume within a voxel thus eliminating the amount of contaminating signal from the outer corner.⁽⁵⁷⁾ Future studies therefore require a higher resolution for nerve DTI imaging.

Furthermore, DTI is not yet as established as for example T2 or T1- weighted imaging. Compared to the latter, DTI has benefits but also limitations over these more 'anatomical' images. Although promising as technique, it is not known completely how DTI changes represent the microarchitecture of tissue. There can be multiple explanations to a change in a certain parameter/vector, and it is also relevant whether these changes occur in an acute or chronic phase of disease, as has been reviewed by Oudeman et al.⁽⁴²⁾

The association with clinical measures (**chapter 2**), its sensitivity for disease in evolution (**chapter 3&4**) and the characteristics of various tissues (**chapter 2-5**) nevertheless indicate that DTI is a very promising technique to monitor disease course of SMA. Together, these projects provide first benchmarks for future projects.

Quantification of inflammation in muscle

Inflammation as part of muscle pathology is not observed in histopathological studies in SMA, in contrast to muscle diseases like DMD or myositis.^(58–60) This does not rule out that the process of fat replacement could be preceded or followed by minor changes in T2 water signal, which can be quantified by mapping T2 relaxation times in muscle. We found no evidence for relevant T2 changes that accompany fat infiltration across our projects, not in disease course nor in response to treatment. T2 mapping has often been used as meaningful biomarker in other neuromuscular diseases but seems not useful in SMA.

Imaging in neuromuscular disease – correction for confounding

Fat infiltration is the hallmark of most neuromuscular diseases but is in itself a confounding factor in imaging (**chapter 2**). The bias of fat infiltration is due to partial volume effects; fat in fact contains a small proportion of water, such that when estimating the water or fat component in a voxel, this mixed compartment must be removed from the equation. For example, the more fat is present in the voxel, the more the equation must be corrected as to not overestimate the amount of water, since a small part of the water belongs to the fat compartment. The challenge of imaging fat infiltrated muscles in neuromuscular disease because of partial volume effects has been addressed previously.^(61–63) We integrated these recommendations into our studies. For T2 mapping for example, we used an extended phase algorithm that was optimized for the spectrum of fat infiltration above 50%.

Additionally, we used a two-component T2 fat calibration. T2 water will gradually decrease for increasing fat fractions.(62,63) When we simulated this effect and compared this to our data (**chapter 2**), we saw an exact overlay. The decrease of T2 could subsequently be interpreted as an 'artificial' effect rather than a 'true' pathological effect. Similarly, not incorporating the confounding effect of fat would have led to overestimation of T2 that could have been mistaken for evidence for inflammation. A prolonged relaxation time of water in muscle has been found in previous work in SMA, but we believe this is due to not incorporating the partial volume effect of fat.(39) Interestingly, the estimation of fat by EPG is not congruent with fat estimated by DIXON method, and we do not have an explanation for this discrepancy.

Likewise, the far end of the spectrum of fat infiltration pushed the boundaries of the DTI method for it relies on fat suppression. Again, we modeled our outcomes to the confounding effect of fat on DTI parameters that have been described in previous research.(61,64) We then understood that the changes we saw in DTI parameters were not solely due to fat bias and so we interpreted the results from MD and FA as indicators of altered microstructure.

Quantitative imaging of the nerve

Based on other publications on nerve imaging in familial amyloid polyneuropathy(65,66), we explored the feasibility of nerve MRI in SMA. For this purpose, we added a dedicated anatomical sequence (proton density – PD) and retrieved quantitative information on the nerve from the other sequence. The association of both the cross-sectional area (CSA) and of AD with clinical characteristics which we established in cross-sectional analysis made them potential candidates as biomarkers for monitoring treatment effects. When we analyzed CSA and AD changes in relation to treatment effects, only CSA showed significant changes. However, the CSA is in fact a semi-quantitative marker that is also rater dependent. Other putative quantitative markers seem not equipped to track changes during treatment in young children. We don't know whether this is because DTI parameters lack in discrimination between healthy and diseased nerve in SMA, or because DTI parameters are not sensitive enough to change. Due to a lack of reference data on DTI indices of young children, we do not know how DTI properties develop in children that are growing up. This complicates the interpretation of data obtained before and after the start of treatment with nusinersen.

Other candidate neuroimaging biomarkers described in previous research projects (67,68) need to be followed up by longitudinal studies in order to demonstrate sensitivity

for disease progression and/or treatment effects. Further studies on quantitative MR neurography are therefore needed before it can be used as biomarker in SMA.

CLINICAL RECOMMENDATIONS FOR FUTURE MRI STUDIES

We have developed a very short scanning protocol (>> 10 minutes) that was feasible and well-tolerated by all patients and that encompassed a complete set of quantitative measures to evaluate muscle pathology. The short scanning time was especially important to ensure the participation of children. Children older than 6 could participate without problems. From this age, children can express voluntary participation to scanning procedures without sedation. Dedicated care and time are crucial when scanning young children to adequately prepare MR examination. Taking extra care of comfortable positioning and offering them the control over the playlist during the MR scan improves their cooperation. We continuously monitored children for signs of resistance, as discussed prior with the child and parent(s). Young patients with SMA tolerated the MR examination and subsequent clinical testing very well but obviously were accustomed to hospital visits. These children seemed more familiar with clinical procedures and the presence of clinical personnel. In contrast, the 3 children who had to be withdrawn during screening were all afraid of scanning. One had a concomitant phobia of needles, and the other two had recently been diagnosed and their first-ever hospital admittance for treatment was already quite stressing. Participation was too stressful for them. In the end, we included 8 young children brave enough to follow through with multiple scans. We think that older children, e.g. from 10 or 12 years and over, are easier to instruct and have a longer attention span than 6-to-8-year olds.

Image acquisition

In our imaging studies, we have focused on the upper legs of ambulant and non-ambulant patients. One of the reasons for selecting the upper leg for muscle MR studies was that in supine position the legs, in contrast to the arms, are positioned in the middle of the magnetic field of the bore. This reduces inhomogeneities of the magnetic field (Bo-field) that could compromise sensitivity and resolution.

When scanning the legs, a large MR scanner bore is required for patients with severe hip and knee contractures; knee flexion was at times fixed at almost 90 degrees which amounts to a certain vertical height when laying supine. Muscle imaging in patients varying in disease severity provided a complete picture of muscle involvement in SMA (**chapter 2**). In some patients, the extent of fatty degeneration had reached near-total fat

replacement of muscle. Because there was simply too little muscle to examine for follow-up measurements, we excluded these patients for follow-up study. Hence, we excluded 13 patients from the follow-up study on natural disease progression (**chapter 3**). We thus concluded that muscle MRI of lower extremities is limited to young and adolescent patients with type 2 and young to adult patients with type 3 SMA. MRI of the upper extremities could represent a future alternative for other patients, but this requires resolving some logistic and technical issues first, including positioning of the patient (especially those with contractures) and the fact that arms cannot be imaged simultaneously, resulting in prolonged scanning time. Quantitative imaging of the upper arm has been investigated in 13 patients with SMA that had relatively good arm function (MRC score of triceps of ≥ 4). (55) We do not know the feasibility of imaging the upper extremities in patients with more impaired arm function. Also, the upper arm consists of fewer muscles than the upper leg (triceps, biceps and brachialis muscle) as opposed to the 12 muscles present in the thigh that greatly improved statistical power. Nonetheless, quantitative imaging data of the arm will contribute to our knowledge of muscle condition in SMA, because the large majority of patients will lose ambulation and arm function is highly relevant for their quality of life.

Certain contra-indications for 3T MR, such as a rod-length of >30 cm of scoliosis material following scoliosis surgery limited enrollment of patients with SMA type 2 or type 3a. To safeguard patients' airway and oxygenation during the MR examination in supine position, we screened for postural change of $>15\%$ in Forced Vital Capacity (FVC) between sitting and supine position, orthopnea and pronounced swallowing problems. The latter criteria did not result in exclusion of any participants in the study, but the presence of scoliosis material did result in screening-failures of approximately 8 patients. MR imaging is thus not feasible in SMA as outcome measure for all patients.

The exclusion of patients is a clear limitation in a rare disease like SMA. Already, the small number of participants was a major limitation for each of the studies, but particularly for our study in treatment-naïve adults (**chapter 3**).

Post-processing of MR images

The processing of MR images is key to generating data for analysis and each step of the process ultimately determines quality and outcome. The software of the scanner has default settings that are not specific to the quantitative sequences. Therefore, we processed the MR data offline, with a custom toolbox 'QMRI Tools for Mathematica' that was developed specifically for quantification purposes.(69) This open-source toolbox is

publicly accessible, and the published codes provided insight to how the processing steps works. These 'qMRI Tools' have been used in previous studies, providing a reference of uniformly processed data.(70,71) Nonetheless, post-processing consists of a long trajectory with many steps before it delivers final data. Consequently, this requires personnel with expertise and understanding of processing software and codes to process data properly. Before qMRI is generally applicable in clinical practice, post-processing needs to be further automatized and made accessible to those without the in-house expertise.

Segmentation

Manual segmentation was the start of each analysis. This is a labor-intensive part of qMRI. Segmentation is best performed on the DIXON images as the out-of-phase images provide good contrast. The mask created by segmentation on the DIXON images can subsequently be transformed to the image space of other sequences to retrieve their quantitative information for the individual muscles. The use of the DIXON as anatomical reference to draw the region of interest (ROI), i.e. the segmentation, is preferred over drawing ROI's on for example the DTI sequence of a lesser resolution, as has happened in other research projects.(72) Drawbacks of DTI images are that the outline of muscles cannot be easily identified due to the somewhat 'pixelated' images. This increases the risk of including too little (muscle) or too much (of adjacent structures). This could subsequently yield a less accurate segmentation and misinterpretation of results.

Although manual segmentation is very laborious and time-consuming, it is the most precise and preferred method. When muscles are already severely atrophied or even unidentifiable, locating and demarcating the muscle is a challenge. Segmentation of 12 muscles per leg and in 25 slices in a total of 78 muscle scans equals no less than 46.800 segmented muscles. This greatly improved accuracy of data-analysis and an increased statistical power. In contrast to other previous studies on quantitative imaging, we were now able to confirm biomarker relevance of certain imaging parameters. If we had taken another approach, we would have discarded quantitative imaging as a biomarker as has happened repeatedly previously (39,73). For clinical application, we need further innovation that would allow automation of the segmentation process. (Semi-)automated techniques to shorten segmentation time are being explored. The reliability of semi-automated segmentation that requires only minor manual input have since been validated for DIXON and DTI indices.(74,75) For now, this only seems to be feasible when anatomy is preserved, for example in healthy controls or minimally affected patients. Further enhancement of automated techniques is needed to facilitate qMRI use in SMA, as altered anatomy is more the rule than the exception - at least in the thigh.

Alignment of imaging stacks

Another known challenge in longitudinal imaging studies is the correct alignment of stacks of images obtained at different time-points. We developed a method to overcome this, as described in **chapter 3**. Careful planning of your field of view (FOV) is one of the conditions for correct alignment, and figure 4 from **chapter 3** demonstrates the successful result of our attention for this detail. We hope that our methodology can help comparable studies in other neuromuscular diseases in the future.

Quantitative MRI in clinical practice

Notwithstanding, the translation of scientific research to clinical practice does not always require additional years of research. In **chapter 6** we show that we were able to apply the quantitative imaging protocol in our clinical work. In a pre-symptomatic patient, the standard outcome measures for motor function and muscle strength were not adequate to rule out the absence of any symptoms. We therefore explored the usefulness of qMRI to determine when treatment should be started in late onset patients. Although we did not document early qMRI signs of SMA pathology, i.e. fatty infiltration or muscle atrophy, we recorded and quantified recurrent fasciculations with diffusion weighted imaging. This single patient study generated new hypotheses that should be explored in the future.

Future directions

In the near future, we will increasingly care for patients treated with a range of medications, as mono- or combination therapy. We can expect to encounter new phenotypes. MR imaging can be a valuable addition to study pathology and treatment effects at the tissue level. This may provide a valuable new level of insight in the condition of the motor unit. Future studies should improve applicability of qMRI through automation of segmentation and explore feasibility in other muscle groups, for example bulbar, respiratory and arm muscles. Whole body imaging with automated segmentation and quantification may represent the ultimate goal in a field that is rapidly moving towards universal treatment with the concurrent loss of clinical and classification certainties.

MAIN CONCLUSIONS

- A short MR protocol for muscle and peripheral nerve is feasible and informative in SMA and was well-tolerated by patients from 7 years old.
- DIXON and DTI qMRI can be used to quantify muscle pathology specific to SMA
- Quantitative muscle MRI can be used as a biomarker for natural disease progression and for treatment effects
- Fat distribution in the thigh can be uniform or bimodal. Bimodal distribution was associated with trends towards clinical improvement during nusinersen treatment and could be a biomarker for the early identification of responders
- Quantitative MRI of thigh muscle is most informative in young and adolescent patients with SMA type 2 and young to adult patients with SMA type 3
- The value of quantitative MRI to distinguish asymptomatic from pre-symptomatic patients remains uncertain.
- Quantitative MR neurography is in its current format not contributory in monitoring treatment effects in peripheral nerve

REFERENCES

1. Stam M, Haakma W, Kuster L, et al. Magnetic resonance imaging of the cervical spinal cord in spinal muscular atrophy. *NeuroImage Clin.* 2019;doi:10.1016/j.nicl.2019.102002.
2. Wijngaarde CA, Brink RC, De Kort FAS, et al. Natural course of scoliosis and lifetime risk of scoliosis surgery in spinal muscular atrophy. *Neurology.* 2019;doi:10.1212/WNL.0000000000007742.
3. Wadman RI, Wijngaarde CA, Stam M, et al. Muscle strength and motor function throughout life in a cross-sectional cohort of 180 patients with spinal muscular atrophy types 1c–4. *Eur J Neurol.* 2018;25(3):512–518. doi:10.1111/ene.13534.
4. Brogna C, Cristiano L, Verdolotti T, et al. MRI patterns of muscle involvement in type 2 and 3 spinal muscular atrophy patients. *J Neurol.* 2019;doi:10.1007/s00415-019-09646-w.
5. Durmus H, Yilmaz R, Gulsen-Parman Y, et al. Muscle magnetic resonance imaging in spinal muscular atrophy type 3: Selective and progressive involvement. *Muscle and Nerve.* 2017;55(5):651–656. doi:10.1002/mus.25385.
6. Montes J, Dunaway S, Garber CE, Chiriboga CA, De Vivo DC, Rao AK. Leg muscle function and fatigue during walking in spinal muscular atrophy type 3. *Muscle and Nerve.* 2014;doi:10.1002/mus.24081.
7. Armand S, Mercier M, Watelain E, Patte K, Pelissier J, Rivier F. A comparison of gait in spinal muscular atrophy, type II and Duchenne muscular dystrophy. *Gait Posture.* 2005;doi:10.1016/j.gaitpost.2004.04.006.
8. Wijngaarde CA, Stam M, Otto LAM, et al. Muscle strength and motor function in adolescents and adults with spinal muscular atrophy. *Neurology.* 2020;95(14):e1988–e1998. doi:10.1212/WNL.0000000000010540.
9. Piepers S, Van Den Berg LH, Brugman F, et al. A natural history study of late onset spinal muscular atrophy types 3b and 4. *J Neurol.* 2008;doi:10.1007/s00415-008-0929-0.
10. Zerres K, Schöneborn SR. Natural History in Proximal Spinal Muscular Atrophy: Clinical Analysis of 445 Patients and Suggestions for a Modification of Existing Classifications. *Arch Neurol.* 1995;doi:10.1001/archneur.1995.00540290108025.
11. Lamminen AE. Magnetic resonance imaging of primary skeletal muscle diseases: Patterns of distribution and severity of involvement. *Br J Radiol.* 1990;6:483–486. doi:10.1038/ncb0604-483.
12. Quijano-Roy S, Avila-Smirnow D, Carlier RY, et al. Whole body muscle MRI protocol: Pattern recognition in early onset NM disorders. *Neuromuscul Disord.* 2012;22(SUPPL. 2)doi:10.1016/j.nmd.2012.08.003.
13. Ueno T, Yoshioka H, Iwasaki N, Tanaka R, Saida Y. MR findings of spinal muscular atrophy Type II: sibling cases. *Magn Reson Med Sci MRMS an Off J Japan Soc Magn Reson Med.* 2003;2(4):195–198. doi:10.2463/mrms.2.195.
14. Chan WP, Liu GC. MR imaging of primary skeletal muscle diseases in children. *Am J Roentgenol.* 2002;179(4):989–997. doi:10.2214/ajr.179.4.1790989.
15. Inoue M, Ishiyama A, Komaki H, et al. Type-specific selectivity pattern of skeletal muscle images in spinal muscular atrophy. *Neuromuscul Disord.* 2015;25:S194. doi:10.1016/j.nmd.2015.06.042.
16. Purves D, Augustine G, Fitzpatrick D, et al. *Motor neuron-Muscle Relationships.* Neuroscience. 2nd editio. Sinauer Associates; 2001.
17. Mentis GZ, Blivis D, Liu W, et al. Early Functional Impairment of Sensory-Motor Connectivity in a Mouse Model of Spinal Muscular Atrophy. *Neuron.* 2011;doi:10.1016/j.neuron.2010.12.032.

18. Simon CM, Dai Y, Van Alstyne M, et al. Converging Mechanisms of p53 Activation Drive Motor Neuron Degeneration in Spinal Muscular Atrophy. *Cell Rep.* 2017;doi:10.1016/j.celrep.2017.12.003.
19. Sleutjes BTHM, Wijngaarde CA, Wadman RI, et al. Assessment of motor unit loss in patients with spinal muscular atrophy. *Clin Neurophysiol.* 2020;doi:10.1016/j.clinph.2020.01.018.
20. Galea V, Fehlings D, Kirsch S, McComas A. Depletion and sizes of motor units in spinal muscular atrophy. *Muscle and Nerve.* 2001;doi:10.1002/mus.1128.
21. Kariyawasam D, D'silva A, Howells J, et al. Motor unit changes in children with symptomatic spinal muscular atrophy treated with nusinersen. *J Neurol Neurosurg Psychiatry.* 2021;92(1)doi:10.1136/jnnp-2020-324254.
22. Burlet P, Huber C, Bertrand S, et al. The distribution of SMN protein complex in human fetal tissues and its alteration in spinal muscular atrophy. *Hum Mol Genet.* 1998;doi:10.1093/hmg/7.12.1927.
23. Mutsaers CA, Wishart TM, Lamont DJ, et al. Reversible molecular pathology of skeletal muscle in spinal muscular atrophy. *Hum Mol Genet.* 2011;doi:10.1093/hmg/ddr360.
24. Coovert DD, Le TT, McAndrew PE, et al. The survival motor neuron protein in spinal muscular atrophy. *Hum Mol Genet.* 1997;doi:10.1093/hmg/6.8.1205.
25. Groen EJN, Perenthaler E, Courtney NL, et al. Temporal and tissue-specific variability of SMN protein levels in mouse models of spinal muscular atrophy. *Hum Mol Genet.* 2018;27:2851–2862. doi:10.1093/hmg/ddy195.
26. Berciano MT, Castillo-Iglesias MS, Val-Bernal JF, et al. Mislocalization of SMN from the I-band and M-band in human skeletal myofibers in spinal muscular atrophy associates with primary structural alterations of the sarcomere. *Cell Tissue Res.* 2020;doi:10.1007/s00441-020-03236-3.
27. Martínez-Hernández R, Soler-Botija C, Also E, et al. The developmental pattern of myotubes in spinal muscular atrophy indicates prenatal delay of muscle maturation. *J Neuropathol Exp Neurol.* 2009;68(5):474–481. doi:10.1097/NEN.0b013e3181a10ea1.
28. Arnold AS, Gueye M, Guettier-Sigrist S, et al. Reduced expression of nicotinic AChRs in myotubes from spinal muscular atrophy I patients. *Lab Invest.* 2004;doi:10.1038/labinvest.3700163.
29. Ripolone M, Ronchi D, Violano R, et al. Impaired muscle mitochondrial biogenesis and myogenesis in spinal muscular atrophy. *JAMA Neurol.* 2015;doi:10.1001/jamaneurol.2015.0178.
30. Kim JK, Jha NN, Feng Z, et al. Muscle-specific SMN reduction reveals motor neuron-independent disease in spinal muscular atrophy models. *J Clin Invest.* 2020;doi:10.1172/JCI131989.
31. Dixon WT. Simple proton spectroscopic imaging. *Radiology.* 1984;doi:10.1148/radiology.153.1.6089263.
32. Glover GH. Multipoint dixon technique for water and fat proton and susceptibility imaging. *J Magn Reson Imaging.* 1991;doi:10.1002/jmri.1880010504.
33. Ma J. Dixon techniques for water and fat imaging. *J. Magn. Reson. Imaging.* 2008;doi:10.1002/jmri.21492.
34. Kaufmann P, McDermott MP, Darras BT, et al. Observational study of spinal muscular atrophy type 2 and 3: Functional outcomes over 1 year. *Arch Neurol.* 2011;68(6):779–786. doi:10.1001/archneurol.2010.373.
35. Kaufmann P, McDermott MP, Darras BT, et al. Prospective cohort study of spinal muscular atrophy types 2 and 3. *Neurology.* 2012;79(18):1889–1897. doi:10.1212/WNL.0b013e318271f7e4.
36. Mercuri E, Finkel R, Montes J, et al. Patterns of disease progression in type 2 and 3 SMA: Implications for clinical trials. *Neuromuscul Disord.* 2016;26(2):126–131. doi:10.1016/j.nmd.2015.10.006.

37. Savini G, Asteggiano C, Paoletti M, et al. Pilot Study on Quantitative Cervical Cord and Muscular MRI in Spinal Muscular Atrophy: Promising Biomarkers of Disease Evolution and Treatment? *Front Neurol.* 2021;doi:10.3389/fneur.2021.613834.
38. Godi C, Ambrosi A, Nicastro F, et al. Longitudinal MRI quantification of muscle degeneration in Duchenne muscular dystrophy. *Ann Clin Transl Neurol.* 2016;doi:10.1002/acn3.319.
39. Bonati U, Holiga Š, Hellbach N, et al. Longitudinal characterization of biomarkers for spinal muscular atrophy. *Ann Clin Transl Neurol.* 2017;4(5):292–304. doi:10.1002/acn3.406.
40. Chianca V, Albano D, Messina C, et al. Diffusion tensor imaging in the musculoskeletal and peripheral nerve systems: from experimental to clinical applications. *Eur. Radiol. Exp.* 2017. doi:10.1186/s41747-017-0018-1.
41. Froeling M, Nederveen AJ, Nicolay K, Strijkers GJ. DTI of human skeletal muscle: The effects of diffusion encoding parameters, signal-to-noise ratio and T2 on tensor indices and fiber tracts. *NMR Biomed.* 2013;26(11):1339–1352. doi:10.1002/nbm.2959.
42. Oudeman J, Nederveen AJ, Strijkers GJ, Maas M, Luijten PR, Froeling M. Techniques and applications of skeletal muscle diffusion tensor imaging: A review. *J. Magn. Reson. Imaging.* 2016. doi:10.1002/jmri.25016.
43. Froeling M, Oudeman J, Strijkers GJ, et al. Muscle Changes Detected with Diffusion-Tensor Imaging after Long-Distance Running. *Radiology.* 2015;274(2):548–562. doi:10.1148/radiol.14140702.
44. Ponrartana S, Ramos-Platt L, Wren TAL, et al. Effectiveness of diffusion tensor imaging in assessing disease severity in Duchenne muscular dystrophy: preliminary study. *Pediatr Radiol.* 2015;45(4):582–589. doi:10.1007/s00247-014-3187-6.
45. Arrigoni F, De Luca A, Velardo D, et al. Multiparametric quantitative MRI assessment of thigh muscles in limb-girdle muscular dystrophy 2A and 2B. *Muscle and Nerve.* 2018;58:550–558. doi:10.1002/mus.26189.
46. Dubowitz V, Sewry C. *Muscle Biopsy.* 3rd ed. Saunders Elsevier; 2007.
47. Otto LAM, van der Pol W-L, Schlauffke L, et al. Quantitative MRI of skeletal muscle in a cross-sectional cohort of Spinal Muscular Atrophy patients with types 2-3. *NMR Biomed.* 2020;doi:10.1002/nbm.4357.
48. Deymeer F, Serdaroglu P, Parman Y, Poda M. Natural history of SMA IIIb: Muscle strength decreases in a predictable sequence and magnitude. *Neurology.* 2008;71(9):644–649. doi:10.1212/01.wnl.0000324623.89105.c4.
49. Werlauff U, Vissing J, Steffensen BF. Change in muscle strength over time in spinal muscular atrophy types II and III. A long-term follow-up study. *Neuromuscul Disord.* 2012;doi:10.1016/j.nmd.2012.06.352.
50. Wokke BH, van den Bergen JC, Versluis MJ, et al. Quantitative MRI and strength measurements in the assessment of muscle quality in Duchenne muscular dystrophy. *Neuromuscul Disord.* 2014;doi:10.1016/j.nmd.2014.01.015.
51. Zhou H, Meng J, Malerba A, et al. Myostatin inhibition in combination with antisense oligonucleotide therapy improves outcomes in spinal muscular atrophy. *J Cachexia Sarcopenia Muscle.* 2020;doi:10.1002/jcsm.12542.
52. Scheel M, von Roth P, Winkler T, et al. Fiber type characterization in skeletal muscle by diffusion tensor imaging. *NMR Biomed.* 2013;doi:10.1002/nbm.2938.
53. Chali F, Desseille C, Houdebine L, et al. Long-term exercise-specific neuroprotection in spinal muscular atrophy-like mice. *J Physiol.* 2016;doi:10.1113/JP271361.

54. Scott W, Stevens J, Binder-Macleod SA. Human skeletal muscle fiber type classifications. *Phys. Ther.* 2001;doi:10.1093/ptj/81.11.1810.
55. Habelts LE, Bartels B, Asselman F-L, et al. Magnetic resonance spectroscopy reveals mitochondrial dysfunction and muscle remodeling. *Brain.* 2021;in review.
56. Basser PJ, Mattiello J, LeBihan D. MR diffusion tensor spectroscopy and imaging. *Biophys J.* 1994;doi:10.1016/S0006-3495(94)80775-1.
57. Vos SB, Jones DK, Viergever MA, Leemans A. Partial volume effect as a hidden covariate in DTI analyses. *Neuroimage.* 2011;doi:10.1016/j.neuroimage.2011.01.048.
58. Dalakas MC. Polymyositis, dermatomyositis, and inclusion-body myositis. *N. Engl. J. Med.* 1991. doi:10.1056/NEJM199111213252107.
59. McDouall RM, Dunn MJ, Dubowitz V. Nature of the mononuclear infiltrate and the mechanism of muscle damage in juvenile dermatomyositis and Duchenne muscular dystrophy. *J Neurol Sci.* 1990;doi:10.1016/0022-510X(90)90156-H.
60. Mastaglia FL, Walton JN. Histological and histochemical changes in skeletal muscle from cases of chronic juvenile and early adult spinal muscular atrophy (the Kugelberg-Welander syndrome). *J Neurol Sci.* 1971;doi:10.1016/0022-510X(71)90249-8.
61. Williams SE, Heemskerk AM, Welch EB, Li K, Damon BM, Park JH. Quantitative effects of inclusion of fat on muscle diffusion tensor MRI measurements. *J Magn Reson Imaging.* 2013;38(5):1292–1297. doi:10.1002/jmri.24045.
62. Schlaeger S, Weidlich D, Klupp E, et al. Decreased water T2 in fatty infiltrated skeletal muscles of patients with neuromuscular diseases. *NMR Biomed.* John Wiley and Sons Ltd; 2019;32(8) doi:10.1002/nbm.4111.
63. Keene KR, Beenakker JM, Hooijmans MT, et al. T2 relaxation time mapping in healthy and diseased skeletal muscle using extended phase graph algorithms. *Magn Reson Med.* 2020;doi:10.1002/mrm.28290.
64. Hooijmans MT, Damon BM, Froeling M, et al. Evaluation of skeletal muscle DTI in patients with duchenne muscular dystrophy. *NMR Biomed.* 2015;28:1589–1597. doi:10.1002/nbm.3427.
65. Kollmer J, Sahn F, Hegenbart U, et al. Sural nerve injury in familial amyloid polyneuropathy MR neurography vs clinicopathologic tools. *Neurology.* 2017;89(5)doi:10.1212/WNL.0000000000004178.
66. Kollmer JC, Hund E, Hornung B, et al. Mr neurography: In-vivo detection of lower limb nerve injury in hereditary transthyretin familial amyloid polyneuropathy. *J Peripher Nerv Syst.* 2013;18.
67. Kollmer J, Kessler T, Sam G, et al. Magnetization transfer ratio: a quantitative imaging biomarker for 5q spinal muscular atrophy. *Eur J Neurol.* 2020;doi:10.1111/ene.14528.
68. Kollmer J, Hilgenfeld T, Ziegler A, et al. Quantitative MR neurography biomarkers in 5q-linked spinal muscular atrophy. *Neurology.* 2019;doi:10.1212/WNL.0000000000007945.
69. Froeling M. QMRTools: a Mathematica toolbox for quantitative MRI analysis. *J Open Source Softw.* 2019;doi:10.21105/joss.01204.
70. Schlauffke L, Rehmann R, Rohm M, et al. Multicenter evaluation of stability and reproducibility of quantitative MRI measures in healthy calf muscles. *NMR Biomed.* 2019;1–14. doi:10.1002/nbm.4119.
71. Hooijmans MT, Froeling M, Koeks Z, et al. Multi-parametric MR in Becker muscular dystrophy patients. *NMR Biomed.* 2020;33(11)doi:10.1002/nbm.4385.

72. Barp A, Carraro E, Albamonte E, et al. Muscle MRI in two SMA patients on nusinersen treatment: A two years follow-up. *J Neurol Sci.* 2020;doi:10.1016/j.jns.2020.117067.
73. Annoussamy M, Seferian AM, Daron A, et al. Natural history of Type 2 and 3 spinal muscular atrophy: 2year NatHisSMA study. *Ann Clin Transl Neurol.* 2020;(November):1–15. doi:10.1002/acn3.51281.
74. Secondulfo L, Ogier AC, Monte JR, et al. Supervised segmentation framework for evaluation of diffusion tensor imaging indices in skeletal muscle. *NMR Biomed.* 2020;doi:10.1002/nbm.4406.
75. Ogier AC, Heskamp L, Michel CP, et al. A novel segmentation framework dedicated to the follow-up of fat infiltration in individual muscles of patients with neuromuscular disorders. *Magn Reson Med.* 2020;doi:10.1002/mrm.28030.



APPENDICES

Thesis assessment committee

Nederlandse samenvatting

Dankwoord

Curriculum Vitae

List of publications

THESIS ASSESSMENT COMMITTEE

Prof. Dr. M.J.N.L. Benders

Department of Woman & Baby and UMC Utrecht Brain Center
Wilhelmina Children's Hospital, University Medical Center Utrecht
The Netherlands

Prof. Dr. K.P.J. Braun

Department of Pediatric Neurology and UMC Utrecht Brain Center
Wilhelmina Children's Hospital, University Medical Center Utrecht
The Netherlands

Prof. Dr. P.A. de Jong

Department of Radiology
University Medical Center Utrecht
The Netherlands

Prof. Dr. Ir. A.J. Nederveen

Department of Radiology
Amsterdam University Medical Center
The Netherlands

Prof. Dr. J.H. Veldink

Department of Neurology and UMC Utrecht Brain Center
University Medical Center Utrecht
The Netherlands

NEDERLANDSE SAMENVATTING

Spinale musculaire atrofie (SMA) is een progressieve spierziekte die in de meest ernstige vorm de belangrijkste erfelijke oorzaak is van sterfte op de kinderleeftijd. Op de kinderleeftijd openbaart de ziekte zich door toenemende spierzwakte dat maakt dat kinderen bepaalde mijlpalen in de motorische ontwikkeling, zoals omrollen, zitten en lopen, niet behalen of vroeg verliezen. De diagnose wordt gesteld bij een combinatie van symptomen (hypotonie of spierzwakte, ontbreken van reflexen, fasciculaties van de tong, tremor) en bevestigd met een genetische test voor een homozygote deletie van het SMN1 gen. De overerving van SMA is autosomaal recessief; dit betekent dat ouders beiden drager zijn en zelf geen klachten hebben. In zeldzame gevallen veroorzaakt een spontane puntmutatie in combinatie met een heterozygote deletie van het SMN1 gen SMA. Het SMN1 gen is verantwoordelijk voor het aanmaken van een eiwit dat essentieel is voor het functioneren en voortbestaan van de zenuwcellen in het ruggenmerg (motor neuronen) die de spieren aansturen.

SMA kent een klinische subclassificatie, gebaseerd op de leeftijd waarop de klachten zijn ontstaan en de behaalde mijlpalen in motorische ontwikkeling. De meeste ernstige vorm van SMA is type 1 SMA waarbij bij zuigelingen onmiddellijk of binnen maanden na geboorte al ernstige, snel progressieve spierzwakte wordt gezien. Zij zijn zeer slap vanwege het verlies van spierkracht en spierspanning, en ondervinden problemen met de ademhaling, met drinken, zij kunnen zich niet omrollen en verliezen snel het vermogen om ledematen tegen de zwaartekracht op te tillen. Het snelle debuut (<6 maanden) en het onvermogen om zelfstandig te zitten is het criterium voor type 1 SMA. Als er nog voldoende kracht bestaat om het hoofd te bewegen, wordt dit meegenomen in de klinische classificatie (type 1c). De prognose was voor de komst van behandeling voor deze jonge kinderen grimmig waarbij zij zonder ondersteuning binnen 2 jaar kwamen te overlijden. Wanneer de klachten zich na 6 maanden openbaren (maar vóór 18 maanden) wordt gesproken van type 2 SMA. Deze kinderen hebben zich motorisch ontwikkeld tot (zelfstandig) zitten, maar komen door de spierzwakte in met name de bovenbenen niet tot zelfstandig lopen en raken hierdoor rolstoel gebonden. Wanneer kinderen de motorische mijlpaal van zelfstandig lopen (zonder enige ondersteuning) hebben behaald, worden zij geclassificeerd als type 3. Wanneer klachten van spierzwakte pas later op de volwassen leeftijd ontstaan, spreekt men van type 4 SMA. Er is dus een grote variatie in ziekte-ernst die uiteen loopt van baby's die niet kunnen omrollen tot volwassenen met milde klachten, terwijl mensen met SMA hetzelfde genetisch defect delen. Deze verscheidenheid maakt dat eerder in de wetenschappelijke literatuur het ziektebeeld bij baby's, kinderen en

volwassenen vaak als aparte ziekte-entiteiten werden opgevat. De eponiemen 'Werdnig-Hoffman ziekte' en 'Kugelberg-Welander ziekte' waren in gebruik voor wat wij verstaan onder type 1 SMA en respectievelijk type 3 SMA.

In 1995 beschreef groep van professor Judith Melki de genetische oorzaak van SMA; de deletie van het SMN1 gen. Het ontbreken van dit gen wordt deels opgevangen door een zogenaamd 'reserve' gen, het SMN2 gen, waarvan het bestaan uniek is voor mensen. Echter, het SMN2 gen is malfunctionerend en maakt maar kleine hoeveelheden van het SMN (survival motor neuron) eiwit aan, in onvoldoende mate om klachten te voorkomen. Het aantal kopieën van het SMN2 gen varieert tussen 1 tot 5 of meer. Er wordt aangenomen dat hoe meer SMN eiwit er aangemaakt wordt, hoe milder de ziekte verloopt. De ziekte-ernst wordt dus deels gemoduleerd door de hoeveelheid kopieën van het SMN2 gen. Toch verklaart dit niet volledig de verschillen in ziekte-ernst tussen mensen met SMA.

Hoewel de motor neuronen het meest kwetsbaar zijn voor een tekort aan SMN eiwit, is dit eiwit in alle cellen van het lichaam aanwezig en is het betrokken bij veel cellulaire functies. De effecten van een SMN tekort vertalen zich daarom in afwijkingen van andere weefsels en organen, zoals spieren, hart, milt, nieren en bloedvaten. Hoewel veel studies zich aanvankelijk op de motor neuronen hebben gericht, wordt er nu meer onderzoek verricht naar de gevolgen van SMN deficiëntie in andere organen.

De ontwikkeling van het eerste medicijn 20 jaar na de ontdekking van het "SMA-gen" is voor wetenschappelijke begrippen zeer snel. De identificatie van de genetische achtergrond van SMA heeft gemaakt dat er specifieke behandelstrategieën zijn ontwikkeld voor het SMN1 gen en het SMN2 gen. De huidige therapieën zijn erop gericht het SMN eiwit te verhogen (nusinersen/Spinraza en risdiplam/Evrysdi) of door gentherapie het ontbrekende SMN1 gen via een virale vector terug in het lichaam te brengen (onasemnogene abeparvovec/Zolgensma). Maar ook andere behandelstrategieën worden ontwikkeld om symptomen te verlichten, bijvoorbeeld door het verbeteren van de neuromusculaire overgang (pyridostigmine) of het versterken van de spier (myostatine-inhibitor).

De behandelingen voor zeldzame ziekten zijn extreem kostbaar. De kosten voor gentherapie worden op 1,9 miljoen voor een éémalige injectie geschat, Spinraza kost 80.000 euro per injectie en de kosten voor Risdiplam worden op 250.000 euro per jaar geschat, voor levenslange behandeling. Dit heeft geleid tot ethische en beleidsmatige discussies over kosteneffectiviteit en vergoedingen, waarbij in Nederland tot een voorwaardelijke toelating van Spinraza werd besloten waarbij de kosteneffectiviteit moet worden aangetoond voor

de groep patiënten ouder dan 9,5 jaar. Artsen en beleidsmakers worden met de komst van behandeling ook geconfronteerd met dilemma's waarbij het belang van patiënten, de belasting van behandeling en kosteneffectiviteit afgewogen moeten worden.

Om de belasting en risico's van een behandeling te rechtvaardigen is het belangrijk om vroegtijdig het onderscheid te kunnen maken tussen zij die wel en zij die niet of onvoldoende reageren op behandeling. De klinische studies van Spinraza laten namelijk zien dat minder dan de helft van de jonge kinderen tijdens behandeling vooruitgang op motorische schalen. Uit vervolgstudies blijkt dat een vroegtijdige behandeling de beste resultaten geeft. Echter, er moet nog veel meer onderzoek worden verricht naar specifiek welke groepen baat hebben bij Spinraza en wat de lange-termijn effecten van behandeling zijn. Dit geldt voor Spinraza maar ook voor andere, nieuwe geneesmiddelen. Adequate uitkomstmaten voor de beoordeling van een behandeling zijn hiermee onontbeerlijk. Het testen van spierkracht en motorische functie zijn beproefde uitkomstmaten die hun dienst hebben bewezen in de kliniek en in medicijnonderzoek. Echter, in spierkracht kan dagelijkse variatie zitten en met name in oudere patiënten is achteruitgang van spierkracht iets wat subtiel, doch progressief verloopt. Daarom zijn meer uitkomstmaten gewenst die de ziekte preciezer kunnen volgen, het ziekteverloop kunnen meten en die effecten van behandeling kunnen monitoren, ofwel 'biomarkers'. Beeldvorming met MRI is een potentiële kandidaat als zogenaamde biomarker.

MRI (magnetic resonance imaging) wekt met een sterk magneetveld en radiogolven bepaalde signalen in het lichaam op. Deze signalen worden opgevangen en door een computer omgezet in beelden. Elk soort weefsel heeft een uniek signaal waarmee weefsel zich kunnen onderscheiden. Dit proefschrift richt zich op beeldvorming van spieren en zenuwen met MRI.

Met het ten gronde gaan van zenuwcellen in het ruggenmerg (motor neuronen) worden dientengevolge ook de zenuwen aangedaan en daarmee de spieren. Daarbij zijn de spieren zelf ook onderhevig aan een SMN eiwit tekort in het weefsel. Het bestuderen van deze schakels van het motorisch systeem zou nieuwe inzichten in de ziekte en aangrijpingspunten voor behandeling kunnen bieden. Eerdere spier MRI studies hebben gebruikt gemaakt van een visuele schaal om een score te geven aan spieren die door de ziekte aangedaan zijn. In dit proefschrift worden kwantitatieve MRI technieken gebruikt, waarvan wij geloven dat zij preciezer zijn. In andere spierziektes is de meerwaarde van kwantitatieve MRI technieken vastgesteld om het ziekteverloop te bestuderen.

Dit proefschrift heeft daarom twee doelstellingen;

1. Het in kaart brengen van eigenschappen van spier en zenuw met kwantitatieve MRI.
2. Het onderzoeken van de gevoeligheid van kwantitatieve MRI technieken voor het meten van ziektebeloop en het effect van behandeling,

In hoofdstuk 2 beschreven we de karakteristieken van de spieren in het bovenbeen in een grote groep mensen met SMA van verschillende leeftijden, type SMA en ziekteduur. Ter referentie includeerden we mensen zonder SMA van zoveel mogelijk dezelfde leeftijd. Bij SMA worden spieren dunner (spieratrofie) en vervangt vet de spier. Het kwantificeren van vet in een spier geeft aan in welke mate de spier aangedaan is. In gezonde spieren is de vethoeveelheid laag (8%) maar bij de spierziekte SMA bestaat het spiervolume gemiddeld 48% uit vet. Mensen met type 2 hadden meer vervetting van de spieren dan mensen met type 3. We observeerden dat sommige spieren juist een lager vetpercentage hadden, en pas in een laat stadium van de ziekte toenemen in vetpercentage. Dit is eerder waargenomen, maar nog niet verklaard. We hebben geen aanwijzingen gevonden dat er ontsteking van de spieren (inflammatie) speelt bij SMA. Dit is bijvoorbeeld wel het geval bij andere spierziektes, zoals in Duchenne Spierdystrofie. Uit verschillende parameters hebben we aanwijzingen gevonden voor atrofie van de spiercellen (het krimpen van cellen). Spieratrofie is een gekend fenomeen bij SMA (de ziekte heet daarom ook spinale spieratrofie), en dit is te ook zien op spierbiopten. Het vermogen van DTI als beeldtechniek om de microstructuur van de spier te kunnen afleiden is een belangrijke bevinding. Bij het monitoren van het effect van toekomstige behandelingen op de spier heeft een non-invasieve techniek zoals MRI de voorkeur boven bijvoorbeeld het uitvoeren van een spierbiopt.

In hoofdstuk 3 demonstreerden we dat MRI in staat is subklinische ziekteprogressie te meten; in één jaar tijd bleven klinische metingen van spierkracht en motorische functie stabiel, terwijl de vervetting toenam (+1.3%). Er werden geen veranderingen in andere parameters gemeten. Deze longitudinale studie is een waardevolle toevoeging aan de kennis over ziektebeloop in patiënten zonder behandeling. Nu behandeling voorhanden is, zal het niet meer mogelijk zijn om het natuurlijke beloop, zonder medicatie, te bestuderen.

Hoofdstuk 4 beschrijft de veranderingen in de bovenbeenspieren van 8 jonge kinderen tijdens hun eerste jaar van behandeling met nusinersen. Zij werden voor de start van behandeling, na de oplaadfase (bij 2 maanden) en ongeveer rond 1 jaar na start van de

behandeling gescand (na 6de injectie). Vervetting van de beenspieren nam gemiddeld toe met 3,2%. Interessant genoeg vonden we tegelijkertijd aanwijzingen voor het verbeteren van de spierstructuur van de hamstrings, ofwel kniebuigers, onder behandeling. De vervetting van de hamstrings was tevens lager dan andere spiergroepen in een jaar. Dit zijn voorzichtige conclusies over het effect van behandeling op spieren.

Ondanks een toename in vervetting van de spieren in alle kinderen, ging een klein gedeelte van de kinderen vooruit op motorische schalen. Deze kinderen demonstreerden een specifiek patroon van vervetting, waarbij er nog een proportie van spieren bestaat die minder aangedaan is. Het zou kunnen dat dit patroon een aanwijzing vormt voor wie zou reageren op behandeling. Deze waarneming moet door verder onderzoek worden bevestigd. Dit onderzoek draagt bij aan de kennis over de effecten van nusinersen behandeling, en bevestigt MRI als potentiële biomarker.

In hoofdstuk 5 onderzochten we of deze kwantitatieve maten ook bijdragend zijn om behandeling te volgen op het niveau van de zenuw. Uit cross-sectioneel onderzoek in patiënten van verschillende leeftijd zonder behandeling bleken sommige parameters veelbelovend. In de monitoring van een kleine groep behandelde kinderen nam echter alleen de oppervlakte van de zenuw significant toe. Echter, de onderzochte groep was zeer klein wat de power van statistische analyse negatief beïnvloedde. Er is tevens weinig referentie data beschikbaar over MRI maten, zeker op de kinderleeftijd. We concludeerde op basis hiervan dat zenuw-MRI in deze vorm niet bijdragend is als uitkomstmaat. Verder onderzoek is nodig om de biomarker waarde vast te stellen of uit te sluiten in een grotere populatie.

In hoofdstuk 6 werd spier-MRI voor het eerst ingezet in klinische praktijk. In de vorm van een case-report rapporteerden we lichamelijk onderzoek en aanvullend onderzoek bij een jongeman met genetisch vastgestelde SMA, maar zonder klachten van spierzwakte, iets wat zelden voorkomt. MRI-spier liet zien dat de persoon zich in een vroeg stadium van de ziekte bevindt waarbij de spieren geen afwijkingen vertoonden. Echter, we zagen al wel fasciculaties van de spier die kunnen duiden op axonaal verval, wat geïnterpreteerd kan worden als vroeg kenmerk van achteruitgang van zenuwfunctie. MRI-spier kan bijdragend zijn in het vroegtijdig detecteren van uitingen van ziekte. De huidige klinische classificatie van SMA is gebaseerd op de aanwezigheid van spierzwakte, gelieerd aan het debuut van klachten. Nu SMA opgenomen wordt in de hielprikscreening bij geboorte, zullen er meer kinderen gediagnosticeerd worden nog voordat zij überhaupt klachten laten zien. Momenteel geldt het protocol dat in het geval van 4 SMN2 kopieën, wat gerelateerd is aan een later debuut van klachten, een afwachtend beleid wordt gehanteerd. Behandeling

met nusinersen wordt geïnitieerd wanneer er sprake is van klachten. Wellicht zou spier MRI kunnen bijdragen in de afweging rondom de timing van het starten van behandeling.

MRI-spier is hiermee een bewezen biomarker voor ziekte-ernst, ziekteprogressie en behandel effect. Het gebruik van MRI-spier is uiteraard niet gelimiteerd tot toepassing in het bovenbeen en dit proefschrift biedt technische aanbevelingen en referentiewaarden voor verder onderzoek met MRI. Het SMA Expertisecentrum heeft ook andere beeldvormingsstudies verricht die veelbelovend zijn, zoals de toepassing van kwantitatieve MRI voor het cervicale ruggenmerg en MR spectroscopie van de bovenarm tijdens inspanning. Er is tevens een platform opgericht om het effect van medicatie te monitoren met 7T MRI welke gericht is op de korte en lange termijn en voor diverse behandelingen (Spinraza, Risdiplam, pyridogstigmine).

De implementatie van MRI-spier als uitkomstmaat in klinische studies, medicijnstudies en in klinische praktijk zou verder inzicht bieden in de betrokkenheid van spieren in de neuromusculaire ziekte SMA.

SMA Expertisecentrum & klinische database

Het SMA Expertisecentrum is gespecialiseerd in de diagnose, zorg, behandeling en onderzoek van de ziekte SMA - voor kinderen en volwassenen. Zij heeft een database opgericht waarin ruim 400 mensen met SMA geregistreerd zijn. De database bevat klinische data, genetische data, vragenlijsten, medische voorgeschiedenis, motorische testen en laboratorium testen van patiënten. Data van wetenschappelijk onderzoek dat het SMA Expertisecentrum uitvoert, wordt ook in deze beveiligde database opgeslagen. Het is de grootste database van SMA-patiënten uit één centrum.

Het SMA Expertisecentrum is nauw verbonden met het Spieren voor Spieren kindercentrum in het Wilhelmina Kinderziekenhuis, een gespecialiseerd centrum voor spierziekten op de kinderleeftijd, en met de polikliniek Neuromusculaire Ziekten van het UMC Utrecht.

DANKWOORD

"- and every step was an arrival" – Rainer Maria Rilke

Nu ik op het einde van dit traject ben aangekomen, wil ik de mensen bedanken die er al waren, nog zijn, of zij die mijn pad hebben gekruist, waarvan ik een paar in het bijzonder wil noemen:

Prof. van der Pol, beste Ludo, bedankt dat je mij een kans hebt geboden in jullie team. Ik heb veel van je geleerd en heb grote bewondering voor je inzet voor de SMA-gemeenschap. Het was een bijzondere tijd om te hebben meegemaakt door de komst van de eerste medicijnen voor kinderen met SMA en mee te werken aan een nieuw perspectief. Helaas was er door de drukte die zorg en onderzoek brachten niet meer tijd voor bespiegelingen. Je gaf mij raad, bedankt voor je steun en begeleiding tijdens mijn traject. Je zei mij ooit 'nice girls don't get the corner office', ik ga mijn best doen dit ongelijk te bewijzen.

Prof. Hendrikse, beste Jeroen, bedankt voor het gemakkelijke contact, snelle reacties en de uitnodigingen voor de inspirerende schrijfsessies in het Academiegebouw.

Dr. Froeling, beste Martijn, enorm bedankt voor al jouw tijd en hulp bij al mijn vragen, zonder jouw figuren zouden de artikelen half zo interessant ogen. Zonder jouw deskundigheid zouden deze projecten überhaupt niet zijn geslaagd. Ik had nooit verwacht dat ik zo veel enthousiasme voor MRI zou krijgen, al voelde ik me soms nogal de alpha in een beta wereld.

De leden van de promotiecommissie voor hun tijd en bereidheid tot deelname aan dit discours, prof. dr. Benders, prof. dr. Braun, prof. dr. de Jong, prof. dr. Nederveen, prof. dr. Veldink, prof. dr. van Gijn.

Allen van het SMA-team – boss-lady Fay-Lynn met haar onvermoeibare toewijding aan zorg, onderzoek en ons team, Ewout, Camiel, bedankt voor het inwerken, Marloes, die de voorloper was voor deze MRI-projecten, Renske, Inge, Bart, Danny, Laura, Maria, Leandra, Féline, Christa, Angela, Esther, Chantall, Ruben. We hebben samen mooi onderzoek gedaan, het was een fijn team om deelgenoot van te zijn geweest. Zoals Ludo ooit zei, het voelt een beetje als familie. Bedankt voor alles.

De deelnemers aan de onderzoeken en hun families, Suzanne, Lotte en de studenten die hebben meegewerkt aan de studies. Bedankt aan Annemarie en Yt.

Mijn lieve ouders, jullie hebben mij het zelfvertrouwen gegeven om alles aan te durven gaan, en de discipline geleerd om deze ook af te ronden. Pappa heeft mij geleerd mij uit te spreken, en mamma om aandacht te hebben voor de mensen om je heen. De kring van lieve vrienden waarmee ik mij mag omgeven zijn het bewijs van zo'n opvoeding. Pappa was trots op elke stap die ik nam, hij heeft het begin meegemaakt maar niet de voltooiing van dit traject. Mamma heeft trouw alle krantenknipsels over SMA verzameld. Dit proefschrift is opgedragen aan jullie.

Mijn broer Laurens, we flikken het maar toch mooi alle twee, ik ben trots op je

Mijn familie - Sjany en Peter, tante Connie en ome Paul, ome Jos, Kyveli en de (extended) Griekse familie

Al mijn lieve vrienden die er toen voor mij waren, stuk voor stuk bijzondere mensen, wat hebben we al niet meegemaakt met z'n allen, van Maastricht tot Berlijn, Drenthekabinet tot Chateau - liefste Anne, like-mind en paranimf, Emma, Kristel, Barbara, Ruben, Kaj, Justin, Carmen, Liza, Liesbeth
Ik ben blij te zien dat de kring zich blijft uitbreiden, inclusief offspring.

Mijn oudste vriendinnen - Kirsten en Anne-May

Mijn lieve vriendinnen uit de jaarclub - Caro, Myrte, Jennifer, Manon

Iedereen die me thuis heeft laten voelen in Rotterdam - Ayla, voor het jarenlange delen van de dagelijkse kost (letterlijk en figuurlijk), Iris, Julia en Britt, maar ook Kevin, Roel, Amanda

Mijn collega's van het lab - Harold, Kevin, Bram, Henk-Jan, Balint, Janna, Loes, Eva, Diederik, Viyanti, Mark Janssen (niet te verwarren met Marc Jansen), Hannelore, Stephan, Rick, Anne en andere collega's uit het Stratenum, voor alle leuke momenten, het ga jullie goed! Bas, bedankt voor het warme welkom destijds.

Mijn collega's uit het rijtje aan het raam - mede-MRI fanaat Marieke en Ingrid, voor het delen van lief&leed, dagelijkse besommeringen en wetenschappelijk advies. Jeroen, like-mind, de cher van de labmeetings, voor alle high- tot low-brow lol die we gehad hebben en voor het opleuken van alle dagen. Jullie hebben stuk voor stuk mijn tijd op het lab gemaakt.

Bedankt aan alle assistenten van de Neurologie die mij destijds hebben verwelkomd.

Thanks to my MR colleagues Lara and Alberto, I'm glad to have worked with you and to have participated in the traveling legs project.

Roel Haeren, voor je begeleiding in het onderzoek dat destijds mijn enthousiasme voor de wetenschap heeft ontketend.

Vincent, jij gelooft in mij en ik geloof in jou. Ik kijk uit naar ons avontuur in Berlijn!

CURRICULUM VITAE

Louise Otto (31-07-1992, Arnhem, the Netherlands) graduated grammar school (Stedelijk Gymnasium Arnhem) in 2010 after which she started medical school at Maastricht University, the Netherlands where she obtained her degree in 2016.

In 2017 she joined the SMA Center of Expertise of University Medical Center Utrecht, the Netherlands as a research physician and PhD student. The focus of her work is MR imaging; executing multiple imaging studies in children and adults with the neuromuscular disease Spinal Muscular Atrophy (SMA). She combines novel imaging techniques with clinical research; in order to develop tools for clinical practice. She has documented the natural history of SMA with imaging, as well as patients under treatment. As the future will hopefully behold multiple therapeutic options for patients, her work on imaging biomarkers is becoming increasingly important. Her work was acknowledged with several stipends and awards, including SMA Europe's Best Young Researcher Award in 2020.

She currently works as a medical doctor at the department of Internal Medicine / Emergency Care at Maastad Hospital in Rotterdam, where she is based.

In her future career, she wishes to combine scientific research and clinical care.

LIST OF PUBLICATIONS

Louise A.M. Otto, Martijn Froeling, Ruben P.A. van Eijk, Fay-Lynn Asselman, Renske I. Wadman, Inge Cuppen, Jeroen Hendrikse, W. Ludo van der Pol. Quantification of disease progression in spinal muscular atrophy with muscle MRI – a pilot study. *NMR in Biomedicine* 2021; e4473.

Louise A.M. Otto, W. Ludo van der Pol, L. Schlawke, Camiel A. Wijngaarde, Marloes Stam, Renske I. Wadman, Inge Cuppen, Ruben P.A. van Eijk, Fay-Lynn Asselman, Bart Bartels, Danny van der Woude, Jeroen Hendrikse, Martijn Froeling. Quantitative MRI of skeletal muscle in a cross-sectional cohort of Spinal Muscular Atrophy patients types 2-3. *NMR in Biomedicine* 2020; e4357.

Karljin Hakvoort*, **Louise Otto***, Roel Haeren, Govert Hoogland, Olaf Schijns, Hans Vink, Dionne Klein, Marc van Zandvoort, Kim Rijkers. Shedding light on human cerebral lipofuscin: An explorative study on identification and quantification. *Journal of Comparative Neurology* 2021; 529(3): 605-615.

Camiel A. Wijngaarde, Esther S. Veldhoen, Ruben P.A. van Eijk, Marloes Stam, **Louise A.M. Otto**, Fay-Lynn Asselman, Roelie M. Wösten-van Asperen, Erik H.J. Hulzebos, Laura P. Verweij-van den Oudenrijn, Bart Bartels, Inge Cuppen, Renske I. Wadman, Leonard H. van den Berg, Cornelis K. van der Ent & W. Ludo van der Pol. Natural history of lung function in spinal muscular atrophy. *Orphanet Journal of Rare Diseases* 2020; 15: 88.

Camiel A. Wijngaarde, Marloes Stam, **Louise A.M. Otto**, Bart Bartels, Fay-Lynn Asselman, Ruben P.A. van Eijk, Leonard H. van den Berg, H. Stephan Goedee, Renske I. Wadman, W. Ludo van der Pol. Muscle strength and motor function in adolescents and adults with spinal muscular atrophy. *Neurology* 2020; 95(14): e1988-e1998.

Camiel A. Wijngaarde, Marloes Stam, **Louise A.M. Otto**, Ruben P.A. van Eijk, Inge Cuppen, Esther S. Veldhoen, Leonard H. van den Berg, Renske I. Wadman, W. Ludo van der Pol. Population-based analysis of survival in spinal muscular atrophy. *Neurology* 2020; 95(14): e1634-e1644.

Boudewijn T.H.M. Sleutjes, Camiel A. Wijngaarde, Renske I. Wadman, **Louise A.M. Otto**, Fay-Lynn Asselman, Inge Cuppen, Leonard H. van den Berg, W. Ludo van der Pol, H. Stephan Goedee. Assessment of motor unit loss in patients with spinal muscular atrophy. *Clinical Neurophysiology* 2020; 131(6): 1280-1286.

Kevin R. Keene, JanWillem M. Beenakker, Melissa T. Hooijmans, Karin J. Naarding, Erik H. Niks, **Louise A. M. Otto**, W. Ludo van der Pol, Martijn R. Tannemaat, Hermien E. Kan, Martijn Froeling. T2 relaxationtime mapping in healthy and diseased skeletal muscle using extended phase graph algorithms. *Magnetic Resonance in Medicine* 2020; 84(5): 2656-2670.

Lara Schlaffke, Alberto de Luca, **Louise AM Otto**, Robert Rehmann, Marlena Rohm, Jędrzej Burakiewicz, Celine Baligand, Jithsa Monte, Chiel den Harder, Aart Nederveen, Hermien E. Kan, Martijn Froeling. Multi-centric evaluation of stability of quantitative outcome measures in healthy calf muscles. *NMR in Biomedicine* 2019; 32(19): e4119.

Marloes Stam, Wieke Haakma, Lidy Kuster, Martijn Froeling, Marielle E.P. Philippens, Clemens Bos, Alexander Leemans, **Louise A.M. Otto**, Leonard H. van den Berg, Jeroen Hendrikse, W. Ludo van der Pol. Magnetic resonance imaging of the spinal cord in spinal muscular atrophy. *NeuroImage: Clinical* 2019; 24: 102002.

Camiel A. Wijngaarde, Rob C. Brink, Floor A. S. de Kort, Marloes Stam, **Louise A. M. Otto**, Fay-Lynn Asselman, Bart Bartels, Ruben P.A. van Eijk, Marjolein Verhoef, Leonard H. van den Berg, Renske I. Wadman, René M. Castelein, W-Ludo van der Pol. Natural course of scoliosis and lifetime risk of scoliosis surgery in spinal muscular atrophy. *Neurology* 2019; 92(3): e149-e158.

Wadman RI, Wijngaarde CA, Stam M, Bartels B, **Otto LAM**, Lemmink HH, Schoenmakers MAGC, Cuppen I, van den Berg LH, van der Pol WL. Muscle strength and motor function throughout life in a cross-sectional cohort of 180 patients with spinal muscular atrophy types 1c-4. *Eur J Neurol.* 2018; 25(3): 512-518.

Stam M, Wadman RI, Wijngaarde CA, Bartels B, Asselman FL, **Otto LAM**, Goedee HS, Habets LE, de Groot JF, Schoenmakers MAGC, Cuppen I, van den Berg LH, van der Pol WL. Protocol for a phase II, monocentre, double-blind, placebo-controlled, cross-over trial to assess efficacy of pyridostigmine in patients with spinal muscular atrophy types 2-4 (SPACE trial). *BMJ Open* 2018; 8: e019932.

Forthcoming

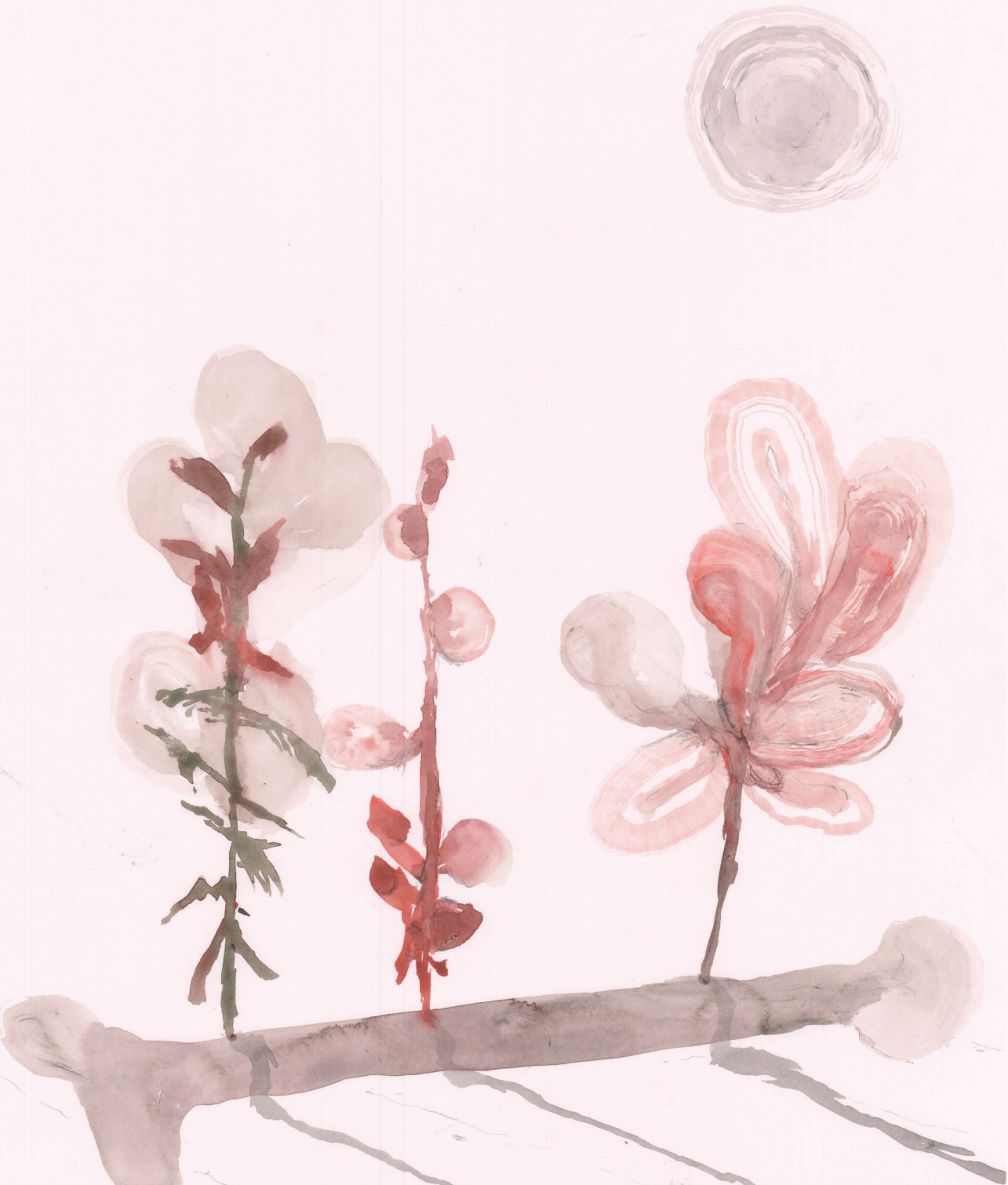
Louise A.M. Otto, M. Froeling, Ruben P.A. van Eijk, Renske I. Wadman, Inge Cuppen, Danny R. van der Woude, Bart Bartels, Fay-Lynn Asselman, J. Hendrikse, W.L. van der Pol. Monitoring nusinersen treatment effects in children with spinal muscular atrophy with quantitative muscle MRI. (submitted)

LAM Otto, M Froeling, RPA van Eijk, F Asselman, I Cuppen, J Hendrikse, WL van der Pol. Quantitative MR neurography of the sciatic nerve in patients with spinal muscular atrophy: a longitudinal study during nusinersen treatment. (submitted)

Louise A.M. Otto, Martijn Froeling, H. Stephan Goedee, MD, PhD, Boudewijn T.H.M. Sleutjes, PhD, Jeroen Hendrikse, W. Ludo van der Pol. Can quantitative MRI detect pre-symptomatic abnormalities in SMA? A case-report. (submitted)

Marloes Stam*, Camiel A. Wijngaarde*, Bart Bartels*, Fay-Lynn Asselman, **Louise A.M. Otto**, Laura E. Habets, Ruben P.A. van Eijk, Bas M. Middelkoop, H. Stephan Goedee, Janke F. de Groot, Kit. C. B. Roes, Marja A.G.C. Schoenmakers, Edward E.S. Nieuwenhuis, Inge Cuppen, Leonard H. van den Berg, Renske I. Wadman#, W. Ludo van der Pol#. Randomised, double-blind, cross-over, phase 2 trial of pyridostigmine versus placebo in spinal muscular atrophy types 2,3 and 4. (submitted)

Esther S Veldhoen; Camiel A Wijngaarde; Erik H.J. Hulzebos; Roelie W Wosten-van Asperen; Renske I Wadman; Ruben P.A. van Eijk; Fay Lynn Asselman; Marloes Stam; **Louise A.M. Otto**; Inge Cuppen; Laura P. Verweij-van den Oudenrijn; Bart Bartels; Michael A Gaytant; Cornelis K van der Ent; W Ludo van der Pol. Natural history of respiratory muscle strength in spinal muscular atrophy: a prospective national cohort study. Orphanet of Journal of Rare Diseases. (in review)



UMC Utrecht



Universiteit Utrecht

ISBN 978-94-6458-075-4